UNCLASSIFIED

## AD NUMBER

**AD460283**

## NEW LIMITATION CHANGE

TO

**Approved for public release, distribution unlimited**

FROM

**Distribution authorized to U.S. Gov't. agencies and their contractors; Administrative/Operational Use; 6 May 1960. Other requests shall be referred to Defense Atomic Support Agency Albuquerque, NM.**

## AUTHORITY

**DNA, ltr, 14 Sep 1995**

THIS PAGE IS UNCLASSIFIED

THIS REPORT HAS BEEN DELIMITED
AND CLEARED FOR PUBLIC RELEASE
UNDER DOD DIRECTIVE 5200.20 AND
NO RESTRICTIONS ARE IMPOSED UPON
ITS USE AND DISCLOSURE.

DISTRIBUTION STATEMENT A

APPROVED FOR PUBLIC RELEASE;
DISTRIBUTION UNLIMITED.

# DISCLAIMER NOTICE

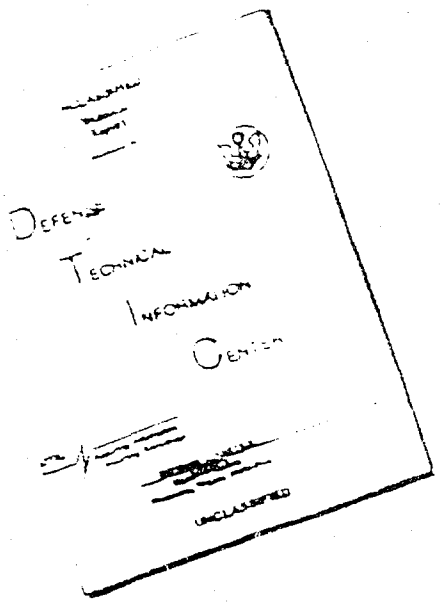


THIS DOCUMENT IS BEST QUALITY AVAILABLE. THE COPY FURNISHED TO DTIC CONTAINED A SIGNIFICANT NUMBER OF PAGES WHICH DO NOT REPRODUCE LEGIBLY.

REPRODUCED FROM
BEST AVAILABLE COPY

UNCLASSIFIED

AD. 460283

DEFENSE DOCUMENTATION CENTER

FOR

SCIENTIFIC AND TECHNICAL INFORMATION

CAMERON STATION ALEXANDRIA, VIRGINIA

UNCLASSIFIED

NOTICE: When government or other drawings, specifications or other data are used for any purpose other than in connection with a definitely related government procurement operation, the U. S. Government thereby incurs no responsibility, nor any obligation whatsoever; and the fact that the Government may have formulated, furnished, or in any way supplied the said drawings, specifications, or other data is not to be regarded by implication or otherwise as in any manner licensing the holder or any other person or corporation, or conveying any rights or permission to manufacture, use or sell any patented invention that may in any way be related thereto.

CONFIDENTIAL

UNCLASSIFIED

WT-1423

This document consists of 132 pages.

No. [illegible] of 160 copies, Series A

# OPERATION PLUMBBOB

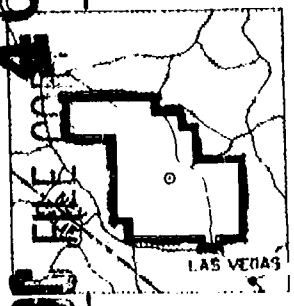


NEVADA TEST SITE

MAY–OCTOBER 1957

TECHNICAL LIBRARY
a/15/9/61
of the
AUG 9 1961
DEFENSE ATOMIC
SUPPORT AGENCY

## Project 3.4

## BLAST EFFECTS ON EXISTING UPSHOT-KNOTHOLE AND TEAPOT STRUCTURES (U)

DDC
RECEIVED
APR 2 1965
DDC-IRA E

Issuance Date: May 6, 1960

Classification (Cancelled) UNCLASSIFIED
DNASA SC-3 memo 30 Nov 1961
by 4/7/64

HEADQUARTERS FIELD COMMAND
DEFENSE ATOMIC SUPPORT AGENCY
SANDIA BASE, ALBUQUERQUE, NEW MEXICO

This material contains information affecting the national defense of the United States within the meaning of the espionage laws, Title 18, U. S. C., Secs. 793 and 794, the transmission or revelation of which in any manner to an unauthorized person is prohibited by law.

CONFIDENTIAL

UNCLASSIFIED

AD No. 460283

DDC FILE COPY

460283

CANCELLED
CONFIDENTIAL

UNCLASSIFIED

WT-1423

OPERATION PLUMBBOB, PROJECT 3.4

# BLAST EFFECTS ON EXISTING UPSHOT-KNOTHOLE AND TEAPOT STRUCTURES


E. H. Bultmann, Jr., Capt., USAF
Eugene Sevin
T. H. Schiffman

Armour Research Foundation
Chicago 16, Illinois

and

Structures Division
Research Directorate
Air Force Special Weapons Center
Kirtland Air Force Base, New Mexico



QUALIFIED REQUESTERS MAY OBTAIN COPIES OF THIS REPORT FROM DDC
NOT FOR PUBLIC RELEASE

This material contains information affecting the national defense of the United States within the meaning of the espionage laws, Title 18, U.S.C., Secs. 793 and 794, the transmission or revelation of which in any manner to an unauthorized person is prohibited by law.


UNCLASSIFIED



CONFIDENTIAL
CANCELLED

# FOREWORD

This report presents the final results of one of the 46 projects comprising the military-effect program of Operation Plumbbob, which included 24 test detonations at the Nevada Test Site in 1957.

For overall Plumbbob military-effects information, the reader is referred to the "Summary Report of the Director, DOD Test Group (Programs 1-9)," ITR-1445, which includes: (1) a description of each detonation, including yield, zero-point location and environment, type of device, ambient atmospheric conditions, etc.; (2) a discussion of project results; (3) a summary of the objectives and results of each project; and (4) a listing of project reports for the military-effect program.

QUALIFIED REQUESTERS MAY OBTAIN COPIES OF THIS REPORT FROM DDC.
NOT FOR PUBLIC RELEASE.

# ABSTRACT

Project 3.4 comprised eight individual tests, seven of which utilized structures remaining from Operations Upshot-Knothole and Teapot. The general objective of the project was to secure blast loading and response data from the behavior of these structures during Operation Plumbbob. In most instances the specific objectives were those of the original test effort. In some cases, however, existing structures were used for new purposes.

The following structures were retested:

1. TP 3.7a-1 and b-1 (full-scale mill buildings)
2. TP 3.8a-1 (reinforced concrete panels)
3. UK 3.8 (underground beams, also tested as TP 3.4)
4. UK 3.7 (underground chamber, modified)
5. UK 3.5ba and bc (roof panel structure, modified)
6. UK 3.29c-1 and c-15 (wall panel structure, modified)
7. In addition to the above, observations were made of a number of existing structures in Frenchman Flat and Area 1 of Yucca Flat for which additional damage was anticipated and which were not included in the test plans of other agencies.

The only completely new items tested were a series of concrete panels whose behavior to close-in thermal radiation was investigated.

The objective of the test utilizing the TP 3.7a-1 and b-1 structures was to determine the blast response of full-scale mill type buildings as a check on the reliability of existing damage prediction schemes, thereby supplementing the results of the original TP 3.7 test. Both the structures collapsed in this test, in accordance with the blast response prediction.

The objective of the test utilizing the TP 3.8a-1 panels was to determine the blast response of fixed-end concrete panels to supplement the findings of the original TP 3.8 test. The panels sustained a slight further permanent deformation.

The objective of the test utilizing the UK 3.8 underground beams was to determine the blast response of these items to supplement the findings of the original test with respect to effective vertical earth pressures and attenuation with depth. The beams sustained appreciable additional deformation in this test. The results obtained showed a marked attenuation of effective vertical earth pressures (i.e., damage) with depth.

The objectives of the test utilizing the modified UK 3.7 structure were to determine the air blast loading in the interior of an underground chamber which is vented to the outside by a relatively large opening, and to determine the response of an underground reinforced-concrete roof slab for the purpose of correlating any damage incurred with existing load and response prediction schemes. The pressure measurements obtained in this structure showed the general precursor shape of the exterior wave and a reduction to 60 percent of the peak overpressure.

The objective of the test utilizing the modified UK 3.5b structure was to determine the air blast loading on a rectangular block in the interior of a partially open building. The data obtained was to be correlated with existing shock tube data on a geometrically similar configuration. The pressure measurements obtained in the empty cell and on the block showed general agreement with shock tube data. The measured peak interior pressures were in excess of the exterior peak pressure by 20 percent.



CONFIDENTIAL

The test utilizing the modified UK 3.29c test cells was to determine the air blast loading behind solid wall panels (corrugated asbestos and unreinforced cinder block) which fail due to the incident shock wave, and to compare this information with existing shock tube data for model wall panels. The pressure measurements obtained showed that the interior pressure wave was essentially unaltered by the failing corrugated asbestos wall, but that it was markedly affected by the failing cinder block wall. In the latter case the interior wave was a compression wave with a rise time of about 93 msec and a peak overpressure nearly 20 percent in excess of freestream.

The objective of the test utilizing the special concrete panels was to determine the comparative behavior of these materials to close-in thermal radiation. Essentially no damage was observed to any of the panels tested. It is concluded from this that even untreated portland-cement concretes can successfully withstand the effects of thermal inputs comparable to that obtained at 700-foot slant range from Shot Priscilla.

The objective of the test utilizing the various existing structures in Frenchman Flat and Area 1 of Yucca Flat was to gain bonus information on the blast response of these structures and also to maintain a permanent record of the existing condition of structures in this area. Numerous structures sustained additional damage.



CONFIDENTIAL

# PREFACE

The work reported herein was performed by the Armour Research Foundation (ARF) under the provision of Air Force Contract AF29(601)-454 (ARF Project K110). This contract was monitored by the Structures Division, SWRS, Headquarters Research Directorate, Air Force Special Weapons Center, Kirtland Air Force Base, New Mexico.

ARF personnel who contributed to this report include: E. V. Gallagher, A. Litvin, K. E. McKee, R. W. Sauer, T. H. Schiffman, and E. Sevin.

AFSWC personnel who were intimately connected with the project were Eric H. Wang, Chief, Structures Division, Capt. R. E. Grubaugh, Lt. E. H. Bultmann, and Lt. D. D. Young.

Special thanks are due project personnel of the original Upshot-Knothole and Teapot tests for their cooperation. Professor G. K. Sinnamon of the University of Illinois, who was associated with Upshot-Knothole Projects 3.7 and 3.8 and Teapot Project 3.7 was particularly helpful. The assistance and cooperation of LCDR J. F. Clarke, Director of Program 3, is also acknowledged.

# CONTENTS


FOREWORD . . . . . 4

ABSTRACT . . . . . 5

PREFACE . . . . . 7

CHAPTER 1 INTRODUCTION . . . . . 15

1.1 Objectives . . . . . 15
1.1.1 Response of Drag Type Buildings, TP 3.7a-1, b-1 . . . . . 15
1.1.2 Response of Reinforced Concrete Panels, TP 3.8 a-1 . . . . . 15
1.1.3 Response of Underground Structural Elements, UK 3.8 (also tested as TP 3.4) . . . . . 15
1.1.4 Interior Loading and Response of Underground Structures in the Precursor Region, UK 3.7 (modified) . . . . . 15
1.1.5 Blast Loading on Interior Obstacles, UK 3.5 ba, bc (modified) . . 15
1.1.6 Blast Loading Behind Failing Walls, UK 3.29 c-1, c-15 (modified) . . . . . 17
1.1.7 Resistance of Concrete to Thermal Radiation (new construction) . . 17
1.1.8 Miscellaneous Structures . . . . . 17
1.2 Background . . . . . 17

CHAPTER 2 RESPONSE OF DRAG TYPE BUILDINGS . . . . . 18

2.1 Procedure . . . . . 18
2.1.1 Test Structures . . . . . 18
2.1.2 Instrumentation . . . . . 20
2.2 Results . . . . . 20
2.2.1 Visual Examination . . . . . 20
2.2.2 Air Pressure Records . . . . . 23
2.2.3 Displacement Records . . . . . 24
2.2.4 Survey Measurements . . . . . 24
2.3 Discussion . . . . . 24
2.4 Conclusions . . . . . 27

CHAPTER 3 RESPONSE OF CONCRETE PANELS . . . . . 28

3.1 Procedure . . . . . 28
3.1.1 Test Structures . . . . . 28
3.1.2 Instrumentation . . . . . 31

3.2 Results . . . . . 31
3.2.1 Air Pressure Data . . . . . 32
3.2.2 Mechanical Scratch Gages . . . . . 32
3.3 Discussion . . . . . 32

CHAPTER 4 RESPONSE OF UNDERGROUND STRUCTURAL ELEMENTS . . . . 34

4.1 Procedure . . . . . 34
4.1.1 Test Structures . . . . . 34
4.1.2 Instrumentation . . . . . 38
4.2 Results . . . . . 38
4.2.1 Visual Examination . . . . . 38
4.2.2 Air Pressure Data . . . . . 38
4.2.3 Survey Measurements . . . . . 43
4.2.4 Mechanical Gages . . . . . 43
4.3 Discussion . . . . . 45
4.4 Conclusions . . . . . 46

CHAPTER 5 INTERIOR LOADING AND RESPONSE OF UNDERGROUND STRUCTURES . . . . . 47

5.1 Procedure . . . . . 47
5.1.1 Test Structures . . . . . 47
5.1.2 Instrumentation . . . . . 47
5.2 Results . . . . . 49
5.3 Discussion . . . . . 49
5.3.1 Interior Loading . . . . . 49
5.3.2 Structure Damage . . . . . 57
5.4 Conclusions . . . . . 57

CHAPTER 6 BLAST LOADING ON INTERIOR OBSTACLES . . . . . 58

6.1 Procedure . . . . . 58
6.1.1 Test Structures . . . . . 58
6.1.2 Instrumentation . . . . . 58
6.2 Results . . . . . 59
6.2.1 Free-Stream Overpressure . . . . . 59
6.2.2 Linearized Pressure-Time Curves . . . . . 63
6.2.3 Comparison with Shock-Tube Data . . . . . 63
6.3 Discussion . . . . . 63
6.3.1 Pressures in the Empty Cell . . . . . 63
6.3.2 Pressures on the Interior Block . . . . . 65
6.4 Conclusions . . . . . 65

CHAPTER 7 BLAST LOADING BEHIND FAILING WALLS . . . . . 69

7.1 Procedure . . . . . 69
7.1.1 Test Structures . . . . . 69
7.1.2 Instrumentation . . . . . 71
7.2 Results . . . . . 71
7.3 Discussion . . . . . 73
7.3.1 Pressure Records . . . . . 73
7.3.2 Correlation with Shock Tube Tests . . . . . 73
7.4 Conclusions . . . . . 76
7.5 Recommendations . . . . . 76



CONFIDENTIAL

CHAPTER 8 RESISTANCE OF CONCRETE TO THERMAL RADIATION . . . . . 77

8.1 Procedure . . . . . 78
8.1.1 Test Items . . . . . 78
8.1.2 Instrumentation . . . . . 78
8.2 Results . . . . . 78
8.3 Discussion . . . . . 81
8.4 Conclusions . . . . . 82
8.5 Recommendations . . . . . 82

CHAPTER 9 MISCELLANEOUS STRUCTURES . . . . . 83

9.1 Procedure . . . . . 83
9.1.1 Test Structures . . . . . 83
9.1.2 Instrumentation . . . . . 84
9.2 Results . . . . . 84
9.2.1 UK 3.4, 3.4a, b, c, and e Truss Sections—Description . . . . . 84
9.2.2 UK 3.5c Structure—Description . . . . . 86
9.2.3 UK 3.11a and b Structures—Description . . . . . 86
9.2.4 UK 3.12a Structure—Description . . . . . 87
9.2.5 UK 3.13b Structure—Description . . . . . 87
9.2.6 UK 3.14 Structure—Description . . . . . 88
9.2.7 UK 3.15 Structure—Description . . . . . 89
9.2.8 UK 3.16a, b, c, Structures—Description . . . . . 89
9.2.9 UK 3.29a, b, c, and d Structures—Description . . . . . 90
9.2.10 TP 31.1a-2 Structure—Description . . . . . 90
9.2.11 TP 31.1b-2 Structure—Description . . . . . 90
9.2.12 TP 31.1c-2 Structure—Description . . . . . 95
9.2.13 TP 31.1e-1 Structure—Description . . . . . 95
9.2.14 TP 31.1e-2 Structure—Description . . . . . 96
9.2.15 TP 31.1f-1 Structure—Description . . . . . 96
9.2.16 TP 31.1b-2 Structure—Description . . . . . 96
9.2.17 TP 31.2e-1 Structure—Description . . . . . 96
9.2.18 TP 34.1-h, i, j, k, l, m Structures—Description . . . . . 96

REFERENCES . . . . . 128

FIGURES

1.1 Site plan of project 3.4 structures in Frenchman Flat . . . . . 16
2.1 TP 3.7a-1 structure, half-end elevation . . . . . 19
2.2 TP 3.7b-1 structure, half-end elevation . . . . . 19
2.3 Pretest, TP 3.7a-1 structure, side view, facing south . . . . . 21
2.4 Pretest, TP 3.7b-1 structure, front view, facing west . . . . . 21
2.5 Pretest, TP 3 7b-1 structure, side view, facing south . . . . . 22
2.6 Posttest, TP 3.7a-1 structure, front side view, facing northwest . . . . 22
2.7 Posttest, TP 3.7b-1 structure, front side view, facing northwest . . . . 22
2.8 Posttest, TP 3.7b-1 structure, view of north end column footing, facing southwest . . . . . 23
2.9 Free-field pressure-time records, TP 3.7a-1 structure (3,600-foot ground range) . . . . . 25
2.10 Free-field pressure-time records, TP 3.7b-1 structure (5,000-foot ground range) . . . . . 26
3.1 Details of TP 3.8a-1 test panels . . . . . 29
3.2 Details of TP 3.8a-1 supporting structure . . . . . 30
3.3 Pretest, TP 3.8a-1, rear side view of test panels, facing southwest . . . . 31



CONFIDENTIAL

3.4 Details and typical installation of scratch gages on 38a-1 panel and UK 3.8 beams . . . . . 32
3.5 Pretest, TP 3.8a-1, interior view of scratch gage on Panel A . . . . 33
3.6 Estimated surface overpressure versus time variation at 3,500-foot ground range . . . . . 33
4.1 Details of typical UK 3.8 test structure . . . . . 35
4.2 Details of typical UK 3.8 test beams . . . . . 37
4.3 Typical arrangement of test beams in roof of UK 3.8 structure . . . . 37
4.4 Pretest, interior view of scratch deflection gage in UK 3.8 structure . . 39
4.5 Posttest, UK 3.8a, front side view of earth cover, facing northwest . . . 39
4.6 Posttest, UK 3.8a, front side view of collapsed section, facing west . . . 39
4.7 Posttest, UK 3.8a, interior view of cell facing north . . . . . 40
4.8 Posttest, UK 3.8a, damaged test beams . . . . . 40
4.9 Posttest, UK 3.8a, damage to beam P3 . . . . . 40
4.10 Estimated surface overpressure versus time variation at 900-foot ground range . . . . . 41
4.11 Location of survey points on UK 3.8 test beams . . . . . 41
4.12 Variation in center displacement of UK 3.8 test beams along length of structure . . . . . 42
5.1 Details of UK 3.7 test chamber and location of pressure gages . . . . 48
5.2 Pretest, UK 3.7, view of entranceway steps, facing east . . . . . 49
5.3 Posttest, UK 3.7, view of entranceway steps, facing east . . . . . 50
5.4 Pretest, UK 3.7, view of entranceway partition wall, facing west . . . 51
5.5 Posttest, UK 3.7, view of entranceway partition wall, facing west . . . 51
5.6 Crack pattern on roof of UK 3.7 structure . . . . . 52
5.7 Observed pressure variation in entranceway (gage P1) . . . . . 53
5.8 Comparison of pressure variations . . . . . 53
5.9 Wave diagram . . . . . 55
6.1 Pretest, UK 3.5b structure, front side view, facing northwest . . . . 59
6.2 Pretest, UK 3.5bc cell, interior front view of 2-foot cubicle, facing west . . 59
6.3 Location of pressure gages in UK 3.5ba and bc test cells . . . . . 60
6.4 Pressure-time records of various gages . . . . . 61
6.5 Pressure-time record of gage P4 at center of floor in empty cell . . . 62
6.6 Free-stream static pressure record of Gage P6 . . . . . 62
6.7 Diffraction phase pressure-time records of various gages . . . . . 64
6.8 Comparison of linearized pressure-time data at various gage locations . . 66
6.9 Inside initial and maximum pressure ratios versus percent openings . . 67
7.1 Pretest, UK 3.29c-1, front view of transite wall, facing west . . . . 70
7.2 Pretest, UK 3.29c-15, front view of cinder block wall, facing west . . . 70
7.3 Pretest, UK 3.29c typical installation of pressure gage . . . . . 70
7.4 Posttest, UK 3.29c-1, front view of test cell, facing west . . . . . 71
7.5 Posttest, UK 3.29c-15, front view of test cell, facing west . . . . . 71
7.6 Overpressure versus time variation behind cinder block panel . . . . 72
7.7 Predicted static resistance function for cinder block panel . . . . . 74
8.1 Pretest view of concrete panels at 60-foot ground range, facing ground zero . . . . . 79
8.2 Posttest view of concrete panels at 60-foot ground range, facing ground zero . . . . . 79
8.3 Pretest view of concrete panels at 300-foot ground range, facing ground zero . . . . . 80
8.4 Posttest view of concrete panels at 300-foot ground range, facing ground zero . . . . . 80
8.5 Posttest view of damaged concrete panels at 300-foot ground range, facing ground zero . . . . . 81
9.1 Pretest, UK 3.4a, b, and c structures, front side view, facing southwest . . 98



CONFIDENTIAL

9.2 Posttest, UK 3.4a structure, side view, facing south . . . . . 98
9.3 Posttest, UK 3.4b foundation, front side view, facing southwest . . . . 98
9.4 Posttest, UK 3.4c structure, rear view, facing east . . . . . 99
9.5 Preshot, UK 3.4e beam, front side view, facing northwest . . . . . 99
9.6 Posttest, UK 3.4e beam, front side view, facing southwest . . . . 99
9.7 Pretest, UK 3.5c structure, front view, facing west . . . . . 99
9.8 Posttest, UK 3.5c structure, front view, facing west . . . . . 99
9.9 Posttest, UK 3.5c structure, rear view, facing east . . . . . 99
9.10 Pretest, UK 3.11a structure, front side view, facing southwest . . . . 100
9.11 Posttest, UK 3.11a structure, front side view, facing southwest . . . 100
9.12 Pretest, UK 3.11a structure, interior of roof, facing southwest . . . . 100
9.13 Posttest, UK 3.11a structure, interior of roof, facing south . . . . 100
9.14 Pretest, UK 3.11b structure, front side view, facing southwest . . . . 100
9.15 Posttest, UK 3.11b structure, front side view, facing southwest . . . 100
9.16 Posttest, UK 3.12a structure, rear side view, facing southeast . . . . 101
9.17 Pretest, UK 3.12a structure, interior of roof, facing west . . . . . 101
9.18 Posttest, UK 3.12a structure, interior of roof, facing west . . . . 101
9.19 Posttest, UK 3.13b structure, front view, facing west . . . . . 101
9.20 Pretest, UK 3.14 structure, facing northeast . . . . . 101
9.21 Pretest, UK 3.14 structure, interior side view, facing southeast . . . 101
9.22 Posttest, UK 3.14 structure, rear side view, facing northeast . . . . 102
9.23 Pretest, UK 3.15 structure, front side view, facing southwest . . . . 102
9.24 Posttest, UK 3.15 structure, front side view, facing southwest . . . . 102
9.25 Pretest, UK 3.15 structure, interior side view, facing southeast . . . 102
9.26 Posttest, UK 3.15 structure, interior side view, facing southeast . . . 102
9.27 Posttest, UK 3.16c, front side view, facing southwest . . . . . 102
9.28 Location of survey points on roof of UK 3.12a structure . . . . . 103
9.29 Pretest, UK 3.29a-16, rear panel (22-gage corrugated metal) . . . . 103
9.30 Posttest, UK 3.29a-16, rear panels (22-gage corrugated metal) . . . 103
9.31 Pretest, UK 3.29b-10, front panel (4-inch brick and 8-inch block) . . . 104
9.32 Posttest, UK 3.29b-10, front panel (4-inch brick and 8-inch block) . . . 104
9.33 Pretest, UK 3.29b-15, rear panel (4-inch brick and 8-inch block) . . . 105
9.34 Posttest, UK 3.29b-15, rear panel (4-inch brick and 8-inch block) . . . 105
9.35 Pretest, UK 3.29d-11, front panel (4-inch brick and 8-inch block) . . . 106
9.36 Posttest, UK 3.29d-11, front panel (4-inch brick and 8-inch block) . . . 106
9.37 Pretest, UK 3.29d-1, rear panel (4-inch brick and 8-inch block) . . . 107
9.38 Posttest, UK 3.29d-1, rear panel (4-inch brick and 8-inch block) . . . 107
9.39 Pretest, TP 31.1a-2, side view of building, facing southeast . . . . 108
9.40 Posttest, TP 31.1a-2, side view of building, facing southeast . . . . 108
9.41 Pretest, TP 31.1a-2, side view of building, facing northwest . . . . 109
9.42 Posttest, TP 31.1a-2, side view of building, facing northwest . . . . 109
9.43 Posttest, TP 31.1a-2, second floor interior . . . . . 110
9.44 Pretest, TP 31.1b-2, side view of building, facing southeast . . . . 110
9.45 Posttest, TP 31.1b-2, side view of building, facing southeast . . . . 111
9.46 Pretest, TP 31.1b-2, side view of building, facing northwest . . . . 111
9.47 Posttest, TP 31.1b-2, side view of building, facing northwest . . . . 112
9.48 Posttest, TP 31.1b-2, interior of second story . . . . . 112
9.49 Posttest, TP 31.1b-2, interior of second story . . . . . 113
9.50 Pretest, TP 31.1c-2, side view of building, facing southwest . . . . 113
9.51 Pretest, TP 31.1c-2, side view of building, facing northeast . . . . 114
9.52 Posttest, TP 31.1c-2, side view of building, facing northeast . . . . 114
9.53 Posttest, TP 31.1c-2, interior of building . . . . . 115
9.54 Posttest, TP 31.1e-1, side view of building, facing southwest . . . . 115
9.55 Posttest TP 31.1e-1, side view of building, facing northeast . . . . 116
9.56 Pretest, TP 31.1e-1, interior of living room, facing northwest . . . . 116



CONFIDENTIAL

9.57 Posttest, TP 31.1e-1, interior of living room, facing northwest . . . . 117
9.58 Posttest, TP 31.1e-1, interior of ceiling, facing northwest . . . . 117
9.59 Pretest, TP 31.1f-1, side view of building, facing southwest . . . . 118
9.60 Posttest, TP 31.1f-1, side view of building, facing southwest . . . . 118
9.61 Posttest, TP 31.1f-1, front view of building, facing south . . . . 119
9.62 Pretest, TP 31.1f-1, side view of building, facing northeast . . . . 120
9.63 Posttest, TP 31.1f-1, side view of building, facing northeast . . . . 120
9.64 Pretest, TP 31.1f-1, interior of living room, facing northwest . . . . 121
9.65 Posttest, TP 31.1f-1, interior of living room, facing northwest . . . . 121
9.66 Pretest, TP 31.2e-1, side view of building, facing southeast . . . . 122
9.67 Pretest, TP 31.2e-1, side view of building, facing northwest . . . . 123
9.68 Pretest, TP 31.2e-1, interior of building, facing north . . . . . 123
9.69 Posttest, TP 31.2e-1, side view of building, facing northeast . . . . 124
9.70 Pretest, TP 34.1k, side view of shelter, facing southeast . . . . . 125
9.71 Pretest, TP 34.1i, side view of shelter, facing southeast . . . . . 126
9.72 Pretest, TP 34.1j, side view of shelter, facing southeast . . . . . 127

TABLES

2.1 Summary of Peak Pressure Data . . . . . 24
2.2 Summary of Experimental and Predicted Response of TP 3.7 Structures . . 27
3.1 Center Deflection of TP 3.8a-1 Panels . . . . . 31
4.1 Dimensions and Properties of Test Beams . . . . . 36
4.2 Location of Survey Points on Test Beams in UK 3.8b and c Cells . . . 43
4.3 Results of Level Survey of UK 3.8b Test Beams (4-foot earth cover) . . 44
4.4 Results of Level Survey of UK 3.8c Test Beams (8-foot earth cover) . . 44
4.5 Average Center Deflections of UK 3.8 Test Beams . . . . . 45
4.6 Maximum and Permanent Strain Measurements from Deforest Mechanical Strain Gages . . . . . 45
9.1 Summary of Loading and Damage to UK Structures in Frenchman Flat . . 84
9.2 Summary of Loading and Damage to FCDA Structures in Yucca Flat . . . 85
9.3 Results of Pretest and Posttest Survey of UK 3.12a Roof . . . . . 88
9.4 Midspan Deflections of UK 3.14 Wall Panels . . . . . 89
9.5 Summary of Damage to UK 3.29a Wall Panels . . . . . 91
9.6 Summary of Damage to UK 3.29b Wall Panels . . . . . 92
9.7 Summary of Damage to UK 3.29c Wall Panels . . . . . 93
9.8 Summary of Damage to UK 3.29d Wall Panels . . . . . 94



CONFIDENTIAL

# Chapter 1

# INTRODUCTION

## 1.1 OBJECTIVES

The general objective of Project 3.4 was to secure blast loading and response data from the behavior, during Operation Plumbbob, of structures remaining from previous test operations. More specifically, the objective was to record the blast effect on structures of Operations Upshot-Knothole and Teapot caused by Shot Priscilla in Frenchman Flat and to record the blast effects on certain existing structures in Area 1 of Yucca Flat caused by Shot Galileo. The Frenchman Flat structures were of primary interest because many of these had sustained only minor damage in previous tests. Additional damage of interest to these structures was expected, because Shot Priscilla was to be of larger yield than previous shots in Frenchman Flat.

Project 3.4 comprised eight individual tests, seven of which utilized existing Upshot-Knothole (UK) and Teapot (TP) structures. The specific objectives of the individual tests, and the structures utilized, are listed below. The reader is referred to the references listed at the end of this report for a more detailed discussion of the objectives, plan, and description of each of the original test efforts.

1.1.1 Response of Drag Type Buildings, TP 3.7 a-1, b-1. The objective of this test was to determine the blast response of two full-scale mill-type buildings as a check on the reliability of existing damage-prediction schemes for such structures to supplement the findings of Project 3.7 of Operation Teapot and Project 3.1 of Operation Redwing (Reference 1).

1.1.2 Response of Reinforced Concrete Panels, TP 3.8 a-1. The objective of this test was to determine the blast response of two fixed-end concrete panels to supplement the findings of the original TP 3.8 test (Reference 2).

1.1.3 Response of Underground Structural Elements, UK 3.8 (also tested as TP 3.4). The objective of this test was to determine the blast response of underground beam elements to supplement the findings of the original UK 3.8 and TP 3.4 tests (References 3 and 4).

1.1.4 Interior Loading and Response of Underground Structures in the Precursor Region, UK 3.7 (modified). The objectives of this test were to determine air-blast loading in the interior of an underground chamber vented to the outside by a relatively large opening, and the response of the UK 3.7 structure for use in correlating any damage observed with existing schemes for load and response prediction (Reference 5).

1.1.5 Blast Loading on Interior Obstacles, UK 3.5 ba, bc (modified). The objective of this test was to determine the air-blast loading on a rectangular obstacle in the interior of a partially open building and to correlate the data with existing shock-tube data on a geometrically similar configuration.

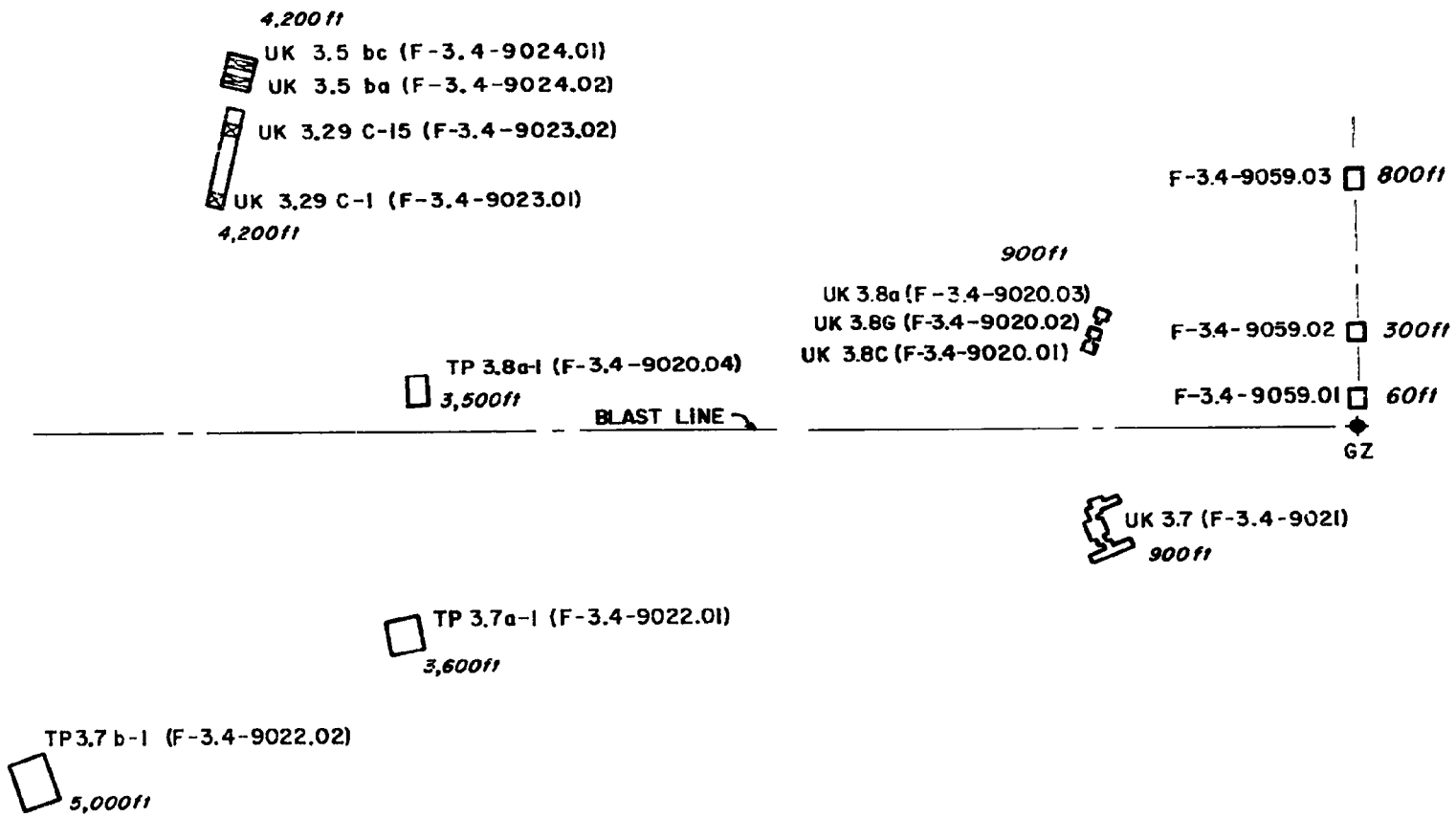


Figure 1.1 Site plan of Project 3.4 structures in Frenchman Flat.



CONFIDENTIAL

1.1.6 Blast Loading Behind Failing Walls, UK 3.29 c-1, c-15 (modified). The objective of this test was to determine the air-blast loading behind solid wall panels that fail because of the incident shock wave and to compare this information with existing shock-tube data utilizing model wall panels.

1.1.7 Resistance of Concrete to Thermal Radiation (new construction). The objective of this test was to determine the effects of thermal radiation on various types of concrete surfaces. Both refractory concretes and portland-cement concretes with special coatings were tested.

1.1.8 Miscellaneous Structures. The objective of this test was to record the before and after conditions of all existing items at the test site for which additional damage might be anticipated and which were not included in the test plans of other agencies. In this manner, it was hoped to gain bonus information on the blast response of structures and to maintain a permanent record of the existing condition of structures at the test site.

## 1.2 BACKGROUND

In the past, existing structures have been treated on an individual basis by the agency involved in the original test. In many instances, useful information could be derived from these structures although they would not warrant additional effort on an individual basis. The Nevada Test Site (NTS) is now sufficiently populated with various test structures so that a considerable amount of data can be obtained at relatively low cost by partially restoring and instrumenting these structures or by simply observing their condition before and after a new shot. In certain instances, slight modifications of existing structures, with appropriate instrumentation, can provide data which differ substantially from that sought in the original test.

With these aims in mind, the following UK and TP structures in Frenchman Flat were selected for retesting: (1) TP 3.7 a-1 and b-1 (mill buildings), (2) TP 3.8 a-1 (concrete panels), (3) UK 3.7 (underground chamber), (4) UK 3.8 (underground beams, also tested as TP 3.4), (5) UK 3.5 ba and bc (roof paneled structure), and (6) UK 3.29 c-1 and c-15 (wall panels).

The data obtained from the first four test structures were intended primarily to supplement the findings of the original test efforts, and the data obtained have been made available to the interested agencies. The remaining two structures were utilized for new purposes. The test dealing with thermal effects on concrete surfaces represented the only effort which had no connection with previous tests.

Additional background, test results, and discussion for each of the eight tests are presented in subsequent chapters of this report. Detailed analyses of results are limited to test objectives essentially original to this program. Only modest analyses are presented where the data obtained simply supplement previous test results; it is left to the originating agency to utilize these data as desired. However, it is intended that this report be as self-contained as practical.

A site plan of structures for Project 3.4 in Frenchman Flat is shown in Figure 1.1. The operation Plumbbob designations are indicated in Figure 1.1, but the original structure designations are retained throughout this report.



CONFIDENTIAL

# Chapter 2

# RESPONSE OF DRAG TYPE BUILDINGS

The principal objective of the test utilizing the TP 3.7 structures was to check the reliability of existing damage-prediction schemes on drag type buildings. This was to be accomplished by comparing the observed behavior of these structures with posttest predictions based on existing blast-load and response schemes. It is emphasized that the intent was not to test the reliability of either the load-prediction method or the response scheme independently, but rather to check the validity of the composite analysis. Furthermore, it was believed that the emphasis should have been on the reliability of the conclusions resulting from the analysis (i.e., conclusions as to negligible, light, or severe damage, or collapse of the structure) rather than on close quantitative correlation with the displacement behavior at arbitrary points of the structure. The latter result was preferred, of course, but in view of the present status of knowledge, it seemed unrealistic to base a test on this expectation alone. The results of the TP 3.7 experiment seem to support this view (Reference 1).

Based on the post-Teapot damage-prediction scheme utilizing the pre-Plumbbob pressure predictions (Reference 6), collapse of the TP 3.7 a-1 structure (at 3,600 feet) should have impended, and the TP 3.7 b-1 structure (at 5,000 feet) should have sustained large permanent displacements. Thus, it appeared reasonable to expect useful information from the present test effort.

## 2.1 PROCEDURE

2.1.1 Test Structures. This test utilized two of the existing TP 3.7 structures which were originally designed to represent two types of single-story, steel-framed, industrial buildings (Reference 1). One of the structures, TP 3.7 a-1 at 3,600 feet ground range (Plumbbob designation: F-3.4-9022.01), had corrugated asbestos roofing and siding, while the other structure, TP 3.7 b-1 at 5,000 feet ground range (Plumbbob designation: F-3.4-9022.02), had similar roofing, but was covered with reinforced-concrete siding with a window opening equal in area to approximately 30 percent of the nominal wall area. The test structures are shown schematically in Figures 2.1 and 2.2, which are representative of the as-built condition.

The following discussion of the test structures is taken from Reference 1 and pertains to the as-built condition of the buildings:

> The test structures of both types were assumed to be interior bays of a multiple-bay building having a span of 40 ft, a bay length of 20 ft, and a height to the bottom chord of the roof truss of approximately 20 ft. Interior bays were chosen for study to avoid the complications which would be introduced by the stiffening effects of end walls and cross-bracing in end frames. The span of 40 ft was used in order to keep the cost of the structures as low as practicable, though a span of 60 or 70 ft would have been more nearly representative of the types of structures which are of interest.

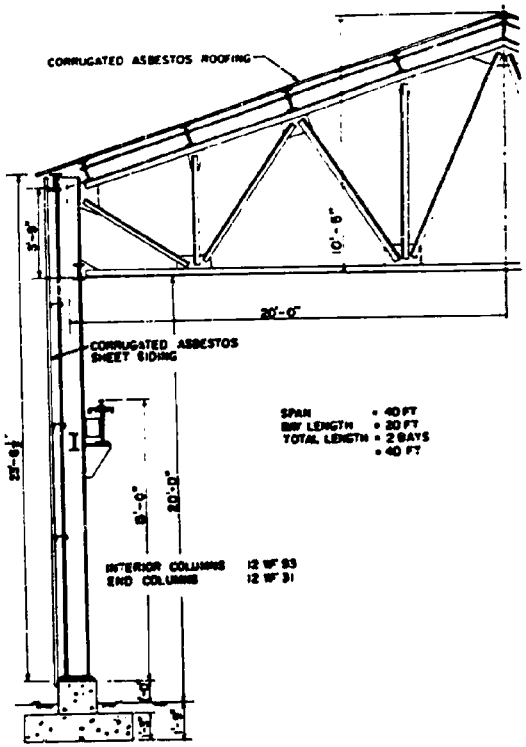


Figure 2.1 TP 3.7 a-1 structure, half-end elevation.

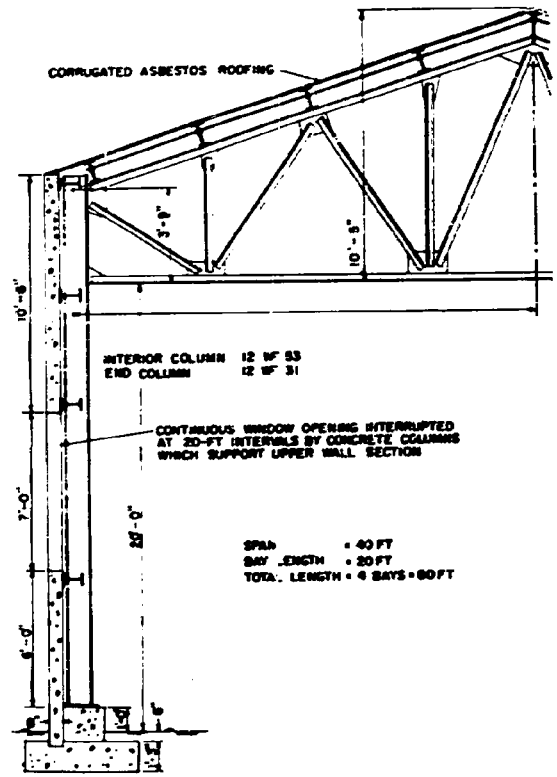


Figure 2.2 TP 3.7 b-1 structure, half-end elevation.



CONFIDENTIAL

The roof structure (in both buildings) was a Warren truss, the end post of which was formed by the column. In order that the probability of failure in the columns rather than in the truss might be increased, the structures were designed for a span of 60 ft. In fabrication, the center 20 ft of the truss was left out....

Structure 3.7-a had a length of only two bays. The columns in the end frames were reduced in size relative to the center columns in proportion to their respective contributory drag areas in order that all three frames in the building would deflect equally under blast, thereby behaving in a manner typical of a long multiple-bay building of the same kind when subjected to a similar blast. In structure 3.7-b four bays were used. This was done in order that the behavior under blast of the center frame might still typify the action of a long multiple-bay structure even though the ends of the test structure were open....

The column base connection used might be considered by some to be a slight departure from common design practice. A connection which would act essentially as a hinge was specified, rather than a fixed connection which might have been more reasonable for a crane supporting column such as this. The hinged base was chosen because its action could be controlled and defined. If a fixed base had been called for, the uncertainties as to the actual degree of fixity present under high load and the possible rotation of the footing itself would make analysis virtually impossible.

As a result of the Operation Teapot test, the asbestos coverings on both structures were destroyed, some members were bent, and the sway bracing was loosened. Permanent deflections at the top of the columns of approximately 14.7 and 2.5 inches were recorded for structures TP 3.7 a-1 and b-1, respectively.

For the present test, both structures were rehabilitated to the extent of repairing broken connections and tightening anchor bolts and sway bracing. No attempt was made to straighten bent members or to replace damaged roof and wall covering. Preshot photographs of these structures are shown in Figures 2.3, 2.4, and 2.5.

2.1.2 Instrumentation. The only on-structure instrumentation consisted of one BRL self-recording displacement-time gage per structure, located so as to determine the deflection at the top of the front center column relative to the footing. This duplicated one of the measurements obtained in the original TP 3.7 test. Permanent deflections of the structures were to be determined by means of before and after field survey measurements. Still photography was also employed.

Free-field blast measurements were obtained by means of a BRL self-recording q gage located adjacent to each structure at a height of 10 feet aboveground.

## 2.2 RESULTS

2.2.1 Visual Examination. The three TP 3.7 structures which were standing prior to the test collapsed. Only two (a-1 and b-1) were of particular interest to Project 3.4. The third structure (b-2) had been partially pulled over, following the Operation Teapot test. A description of the failure of all three structures is given below.

The TP 3.7 a-1 structure collapsed in a direction away from ground zero (Figure 2.6). All the column-to-foundation connections held, although two appeared to be on the verge of failing. All surfaces facing ground zero were charred and severely pitted. End column-to-truss connections on the ground zero side remained secure; the failure occurred by separation of the column flange from the web combined with a tension failure of the column web and one flange. The interior column truss connection at the lower chord failed by a combination of angle tearing and bolt failure. The upper chord members tore away from the column connections. All the roof purlins were bowed to some extent. The bowing of the roof purlins on the ground zero side was more pronounced; they had approximately a 1-foot center displacement in a plane parallel to the ground. The lesser displacement of the purlins on the lee side of the roof was probably indicative of a reduced blast loading because of shielding from the upstream members. There was some lateral bending of the crane rail beam on the lee side of the structure. This may have been because the tie rods in the bottom plane of the roof trusses transmitted a portion of the weight of the structure to the crane rail beam approximately at mid-span as the structure collapsed. All columns on the lee side of the structure buckled in the vicinity of the lower chord-to-column connection.

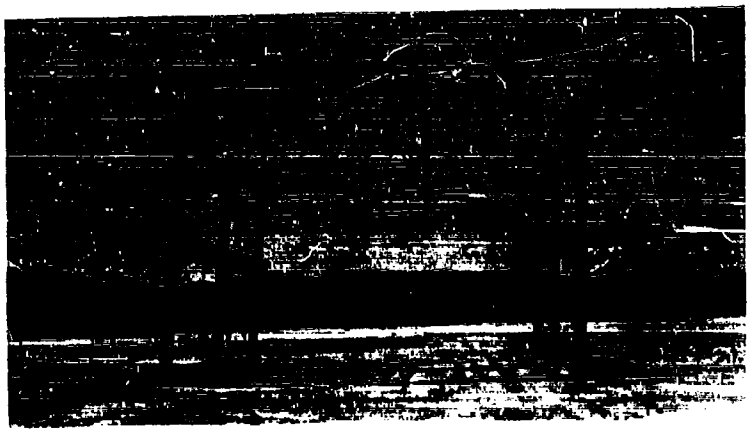

Figure 2.3 Pretest, TP 3.7 a-1 structure, side view, facing south.

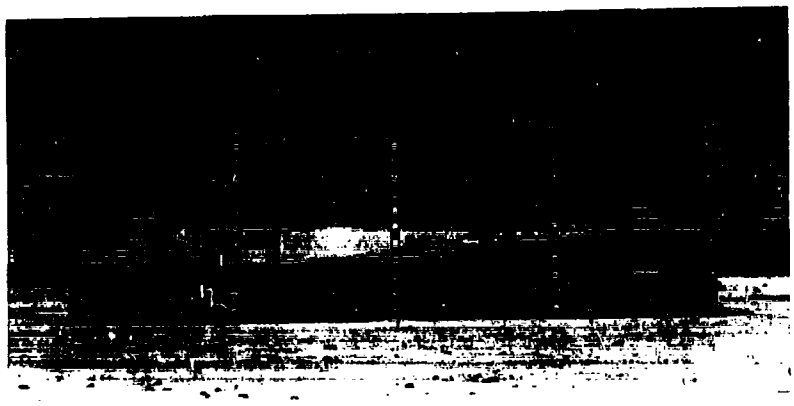

Figure 2.4 Pretest, TP 3.7 b-1 structure, front view, facing west.



CONFIDENTIAL

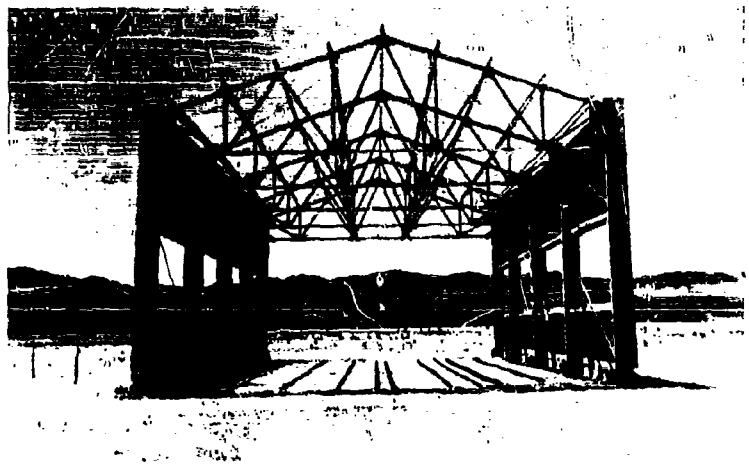

Figure 2.5 Pretest, TP 3.7 b-1 structure, side view, facing south.

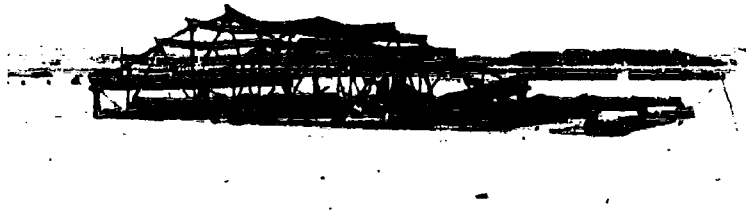

Figure 2.6 Posttest, TP 3.7 a-1 structure, front side view, facing northwest.

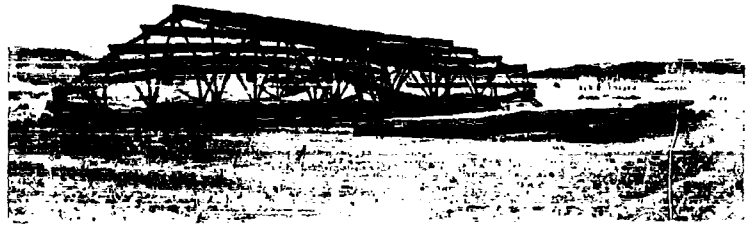

Figure 2.7 Posttest, TP 3.7 b-1 structure, front side view, facing northwest.

The TP 3.7b-1 structure collapsed in a direction away from ground zero (Figure 2.7). The end bents of the structure failed on the lee side by plastic buckling of the columns. All the truss-to-column connections on the ground zero side pulled away from the columns; the failure occurred in the truss-chord portion of the connection. In the interior bents the upper chord-to-column connections on the lee side failed by a combination of angle tearing and bolt failure. The lower chord-to-column connections on the lee side failed by buckling of the column flanges and tearing of the truss chord at the ends of the gusset plates. The lower chord-to-column connections on the ground zero side failed either in the connecting angle or in the bolts. The hinged column bases on the ground zero side appeared to be on the verge of failure. All these connections on the interior columns on the lee side failed because the anchor bolts for the restraining angles pulled out of the foundation. Both the end footings on the lee side of the structure were pulled out of the ground (Figure 2.8). There was pronounced bowing of the roof purlins on the ground zero side of the structure. The purlins on the lee side were not as severely bowed, as was the case for the a-1 structure described previously. The top girts on the rear reinforced-concrete wall were pulled loose from the wall for about 8 feet from each end of the structure. This separation was due to failure of the wall anchors. Cracks in the wall were mainly confined to the vicinity of the columns. The bottom sides of the walls could not be inspected. It is probable that most of the damage to the wall, as well as to the frame itself, occurred upon impact of the structure with the ground.

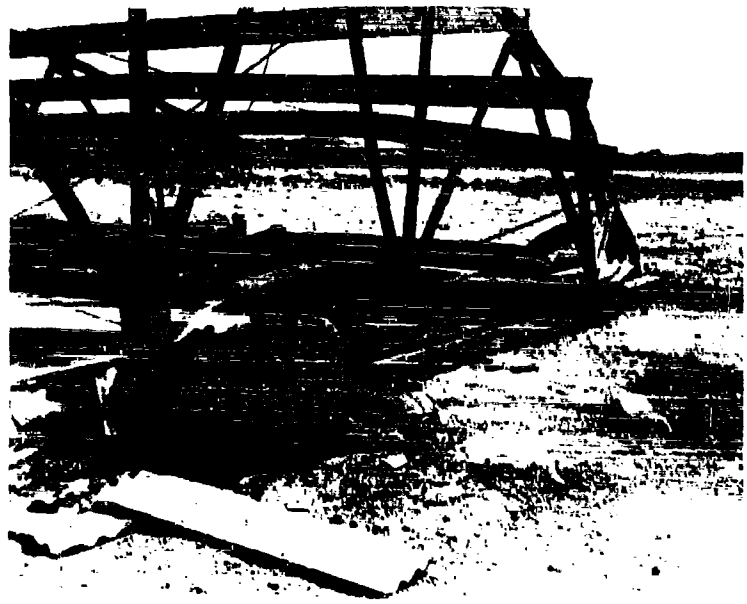

Figure 2.8 Posttest, TP 3.7 b-1 structure, view of north end column footing, facing southwest.

The TP 3.7b-2 structure also collapsed in a direction away from ground zero and in a fashion almost identical to that of the b-1 structure (Figure 2.7). The major differences were: (1) only one end footing on the lee side of the structure was pulled up, the other end column failed at the base connection; (2) the hinged column bases on the ground zero side were all intact; (3) there was less bowing of the roof purlins but, as before, there was an indication that the leeward purlins received less loading; and (4) the wall panels were less severely cracked.

2.2.2 Air Pressure Records. The self-recording q gages adjacent to the TP 3.7a-1 structure (3,600-foot ground range) and the TP 3.7b-1 structure (5,000-foot ground range) each pro-



CONFIDENTIAL

vided what appeared to be good free field records. The traces of overpressure and dynamic pressure versus time are shown in Figures 2.9 and 2.10. These curves were constructed by joining the BRL linearized data points with line segments. As is evident from these figures, the TP 3.7a-1 structure was in the precursor region, whereas the TP 3.7b-1 structure was in a reasonably clean Mach region.

TABLE 2.1 SUMMARY OF PEAK PRESSURE DATA

| Structure and Distance to Ground Zero, feet | 3.7a-1<br>3,600 | 3.7b-1<br>5,000 | 3.7b-2<br>5,750 |
|---|---|---|---|
| Peak overpressure, psi: | | | |
| Structure* | 10.5 | 5.7 | - |
| Blast line† | 9.0 | 5.7 | 3.6‡ |
| Teapot* | 6.6 | 3.4 | 2.7 |
| Peak dynamic pressure, psi: | | | |
| Structure* | 4.5 | 2.5 | - |
| Blast line† | 3.0 | 0.6 | - |
| Teapot* | 1.2 | 0.2 | 0.1 |

*Measured at 10-foot elevation.
†Measured at 3-foot elevation.
‡Extrapolated from blast-line data.

Peak pressure data from the earlier TP 3.7 test are compared in Table 2.1 with the present results, obtained by smoothing the data of Figures 2.9 and 2.10. The peak pressures of 13.2 psi and 7.3 psi shown in the figures are considered to be spurious. The differences noted between blast-line data and data from the self-recording gages adjacent to the structures may be explained in terms of differences in the type, placement, and elevation of the gages, and also, possibly, may be due to lack of radial symmetry of the blast. (Figure 1.1 shows the position of the structures relative to the main blast line.) Of these, the effect of elevation was probably the most significant. Inasmuch as there was no indication of malfunction in the self-recording gages, there is no reason to discount this data, and, in fact, it is probably to be accepted in preference to the blast-line data.

2.2.3 Displacement Records. The self-recording displacement gages mounted on the TP 3.7a-1 and b-1 structures provided no usable records. Indications were that the gage wire went slack prior to or at shock arrival. This is attributed to the fact that the wires stretched as a result of thermal heating and became detached from the gage spool.

2.2.4 Survey Measurements. Pretest survey measurements were made to establish the deflection at the top of each column of the TP 3.7a-1, b-1, and b-2 structures relative to the base. Since there was no point in performing a posttest survey, and since the pretest survey agreed essentially with the posttest survey reported in Reference 1, the results of the pretest survey are not reported here.

## 2.3 DISCUSSION

The test structures sustained significantly higher blast loads than they experienced in the original Operation Teapot test. A comparison of predicted and measured deflection of the TP 3.7a-1 and b-1 structures is shown in Table 2.2. The predicted values were prepared by TP 3.7 project personnel (University of Illinois) from the loading data obtained in the present test.

The data of Table 2.2 represent experimentally determined upper and lower bounds of the collapse pressure for the two types of structures and also show the extent to which these bounds confirmed the blast loading and response prediction schemes employed. This confirmation is believed to be reasonably good, especially for the semi-drag type of structure typified by TP 3.7b-1. In view of the limited instrumentation employed and the extreme damage sustained by



CONFIDENTIAL

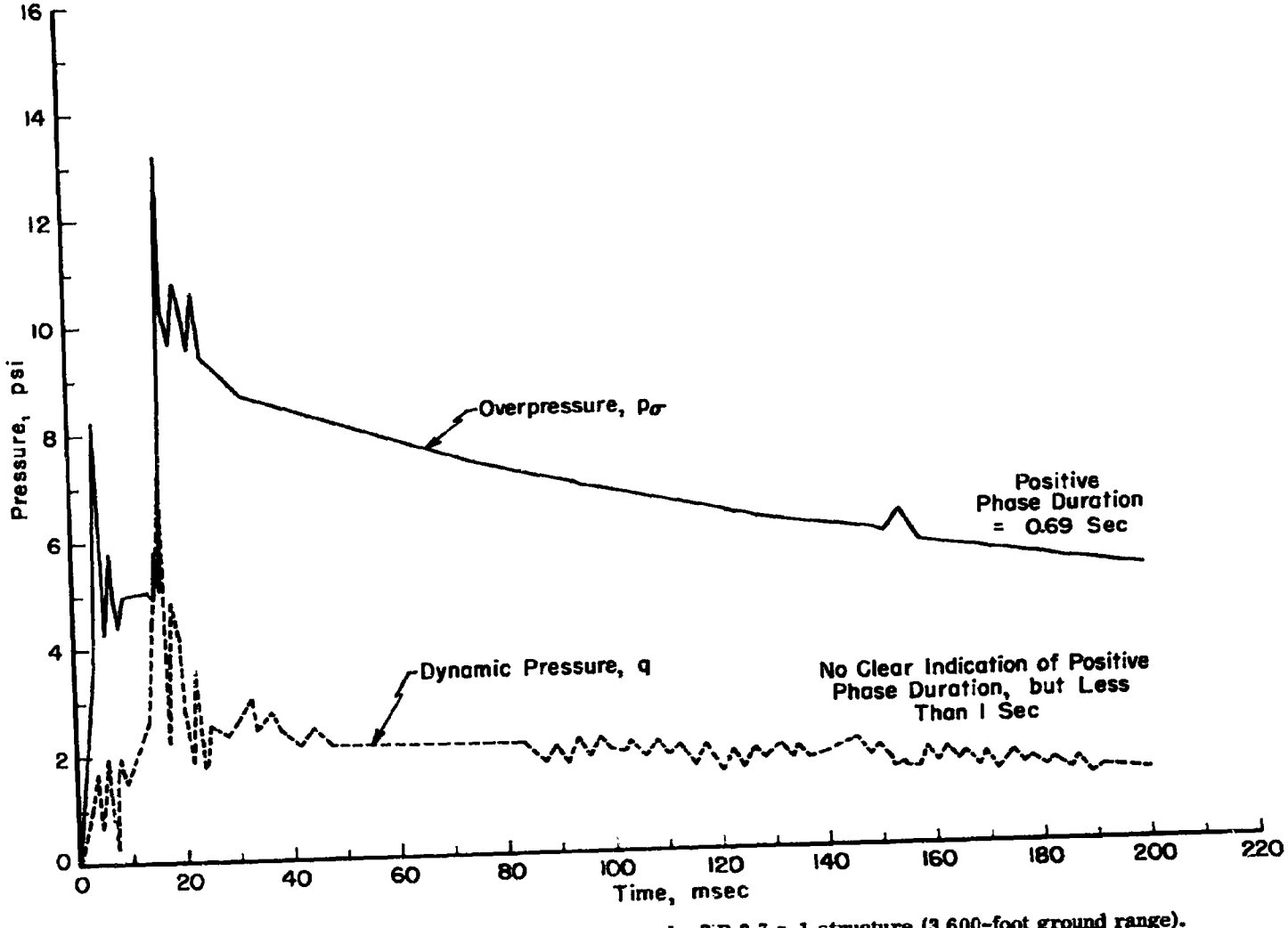


Figure 2.9 Free-field pressure-time records, TP 3.7 a-1 structure (3,600-foot ground range).



CONFIDENTIAL

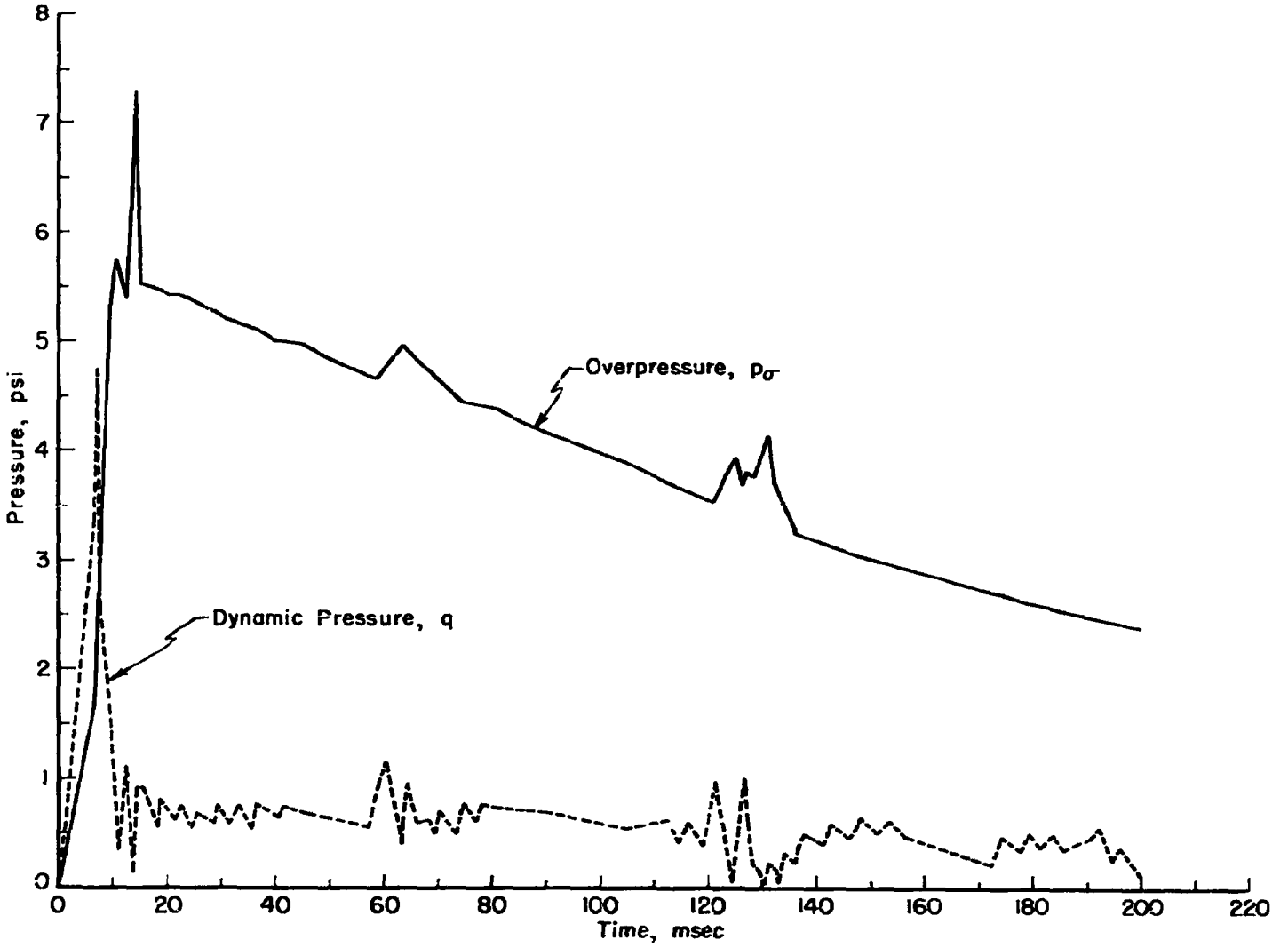


Figure 2.10 Free-field pressure-time records, TP 3.7 b-1 structure (5,000-foot ground range).



CONFIDENTIAL

TABLE 2.2 SUMMARY OF EXPERIMENTAL AND PREDICTED RESPONSE OF TP 3.7 STRUCTURES

| | Experimental Limits of Collapse Pressure | | Predicted Limits of Collapse Pressure | |
|---|---|---|---|---|
| TP 3.7a-1 Drag type structure | Lower* | Upper† | Lower | Upper |
| Peak dynamic pressure, psi | 1.2 | 4.5 | 1.2 | 1.7 |
| Displacement at top of columns, inches | 14.7 | collapse | 35 | collapse |
| TP 3.7b-1 Semi-drag type structure | Lower* | Upper‡ | Lower | Upper |
| Peak dynamic pressure, psi | 0.2 | 2.5 | 0.6 | 0.7 |
| Displacement at top of columns, inches | 2.5 | collapse | 60 | collapse |

*Teapot test, Mach region, 10 ft elevation.
†Plumbbob test, precursor region, 10 ft elevation.
‡Plumbbob test, Mach region, 10 ft elevation.

the test structures, it is felt that more detailed information regarding the behavior of these structures cannot be inferred from the data obtained.

## 2.4 CONCLUSIONS

Collapse of the TP 3.7a-1 drag type structure was shown to be bounded experimentally between peak dynamic pressures of 1.2 psi and 4.5 psi, (overpressures of 6.6 psi and 10.5 psi, respectively). The adequacy of these bounds was compromised somewhat by the fact that the lower bound pressure (Teapot) was for a Mach loading condition while the upper bound pressure (Plumbbob) was for a precursor loading condition. Also, there was about a 20 percent variation between peak overpressures measured at the structure and on the blast line in both tests (Table 2.1). The pressures given above correspond to the widest experimental spread.

Collapse of the TP 3.7b-1 semi-drag type structure was bounded experimentally between peak overpressures of 3.4 and 5.7 psi, with both pressures corresponding to Mach region loads. (The TP 3.7b-2 structure, presently identical to b-1, collapsed at an estimated overpressure of 3.6 psi (Table 2.1). However, this pressure was not accepted as an upper bound in view of the pretest condition of the b-2 structure (Section 2.2.1).) The associated peak dynamic pressures were 0.2 and 2.5 psi, respectively.

The collapse pressures for test structures as predicted by methods developed for the original TP 3.7 test fell within the above bounds. For the conditions of Shot Priscilla, these pressures were about 8.3 psi and 5.5 psi for the TP 3.7a-1 and b-1 structures, respectively.



CONFIDENTIAL

# Chapter 3

# RESPONSE OF CONCRETE PANELS

In Project 3.8 of Operation Teapot the Bureau of Yards and Docks conducted a well-conceived test on the blast response of two types of reinforced concrete panels (Reference 2). However, the test was not as successful as it might otherwise have been, because the panels sustained only small deflections.

Based on pre-Plumbbob pressure predictions (Reference 6), the farther of the two identical test structures (TP 3.8a-2 at 4,850 feet) would have been in a lower overpressure region than was the closer structure (TP 3.8a-1 at 3,500 feet) in Operation Teapot. Thus, the present test was concerned only with the latter structure. Response instrumentation for this test was limited to the measurement of maximum and permanent mid-span displacements of the panels. While this instrumentation was considerably less elaborate than that provided in Operation Teapot, it was felt that sufficient information could be obtained in this manner to satisfy most of the objectives of the original program that dealt with the adequacy of existing methods of response analysis.

## 3.1 PROCEDURE

3.1.1 Test Structures. This test utilized two reinforced-concrete panels originally tested in TP 3.8a-1A and 1B at 3,500-foot ground range; (Operation Plumbbob designation: F-3, 4-9020). The panels, one of which was solid (Panel A) and the other ribbed (Panel B), measured 20 by 5 feet. Schematic drawings of the test panels and supporting foundation are shown in Figures 3.1 and 3.2. The following discussion of the test structures, taken from Reference 2, pertains to the as-built condition of the panels:

> The panels were supported as fixed-end members on the foundation structure. The negative reinforcing steel extended 17 inches from the end of the panels and was welded to plates anchored to the foundation steel. Since the purpose of the foundation was to develop the full yield moment of the panel, it was necessary that the support ends be massive and heavily reinforced.
>
> The panels were set in Hydrostone on the foundation support to provide an even bearing surface. A ¾-inch gap between the end of the panel and the abutment of the end wall of the foundation was packed with Embeco grout. Neoprene wipers were placed along the edges of the panels to prevent excessive infiltration of pressure to the underside of the panel....

Permanent mid-span deflections of approximately 0.3 and 0.7 inch were recorded for the solid and ribbed panels, respectively, during the Operation Teapot test. No attempt was made to rehabilitate or modify these panels for the present test, other than to plug a pressure gage opening in Panel A and to renew the edge seal around both panels. A preshot photograph of the panels and test cell is shown in Figure 3.3.

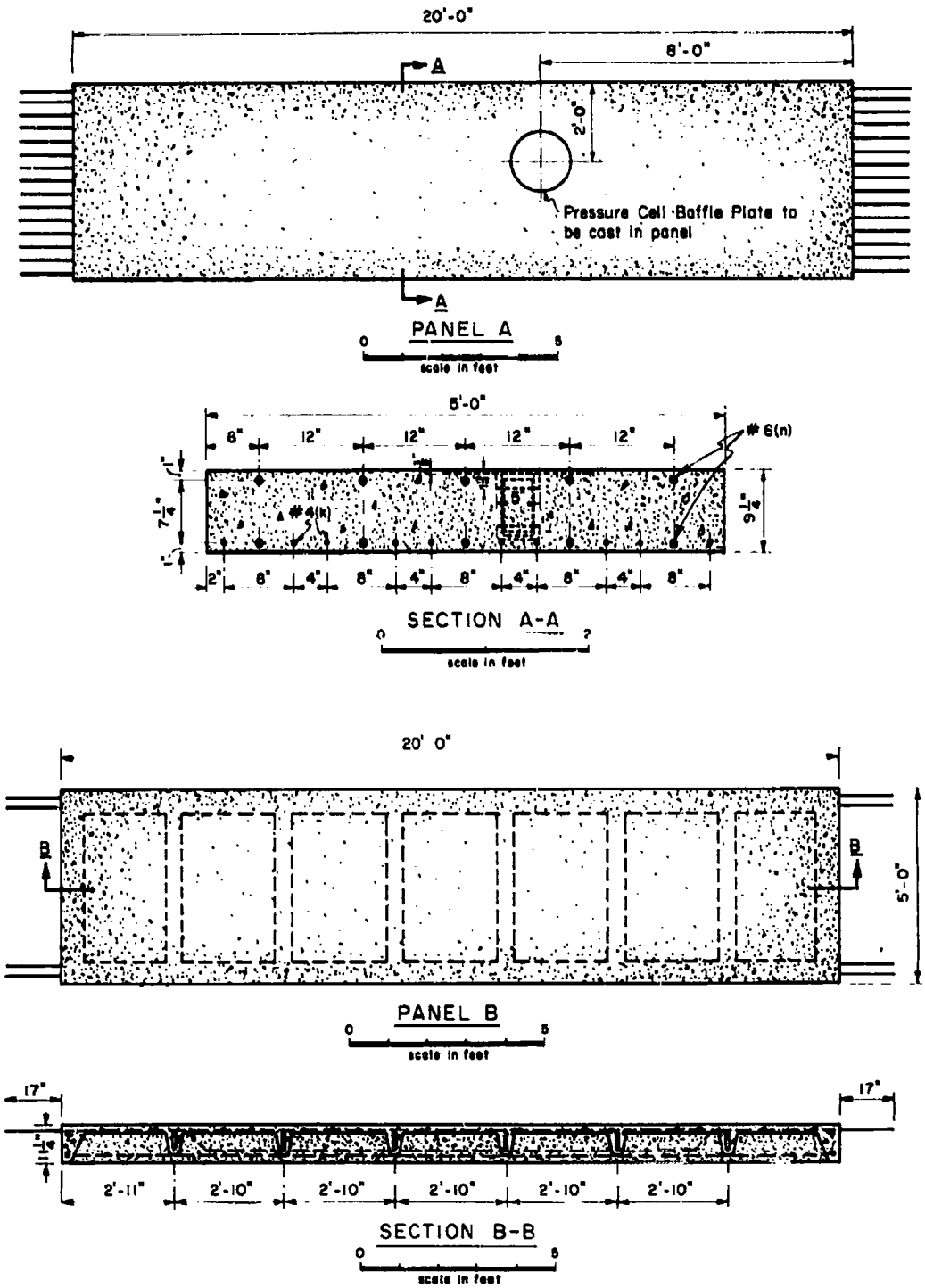


Figure 3.1 Details of TP 3.8 a-1 test panels.



CONFIDENTIAL

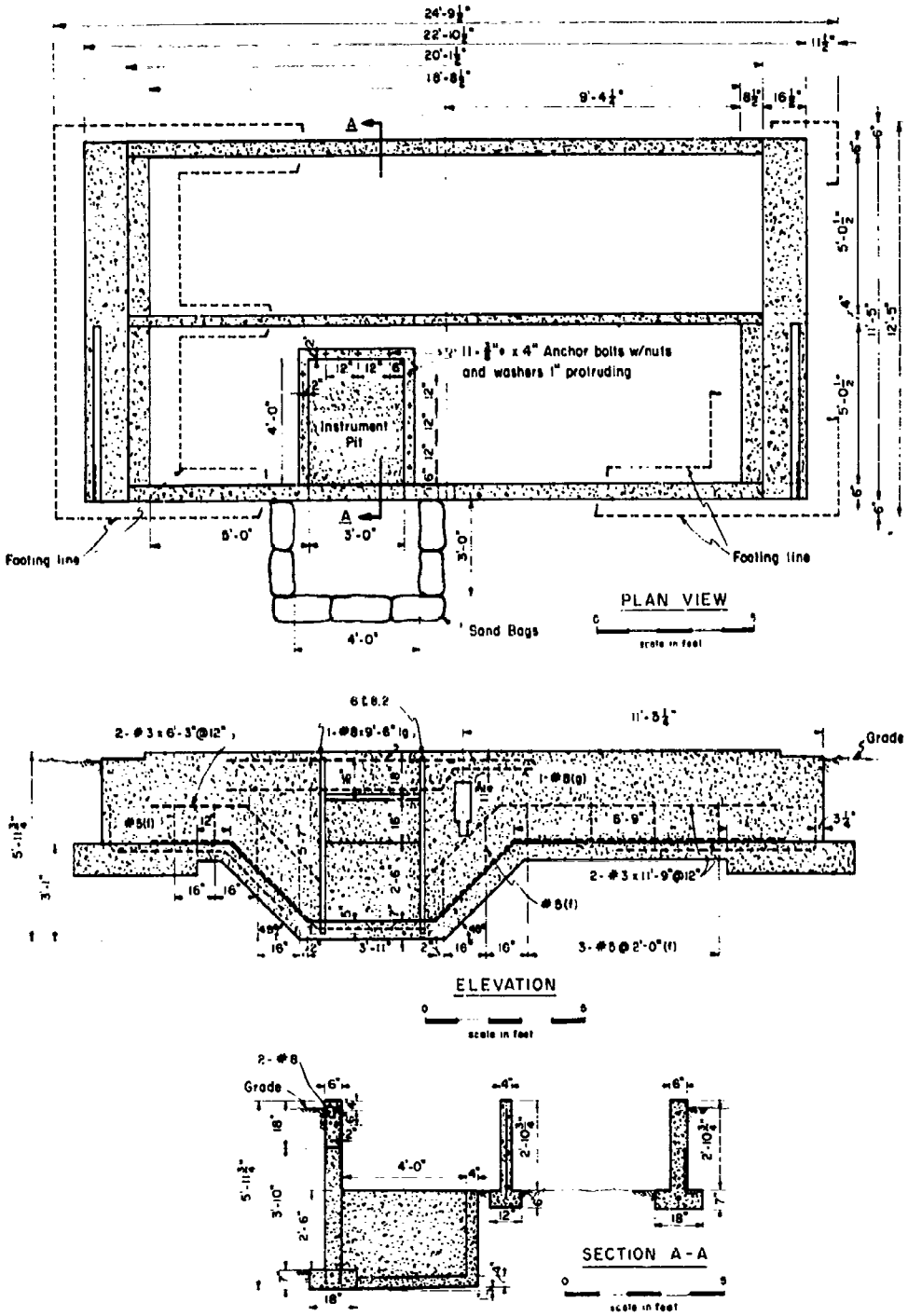


Figure 3.2 Details of TP 3.8 a-1 supporting structure.



CONFIDENTIAL

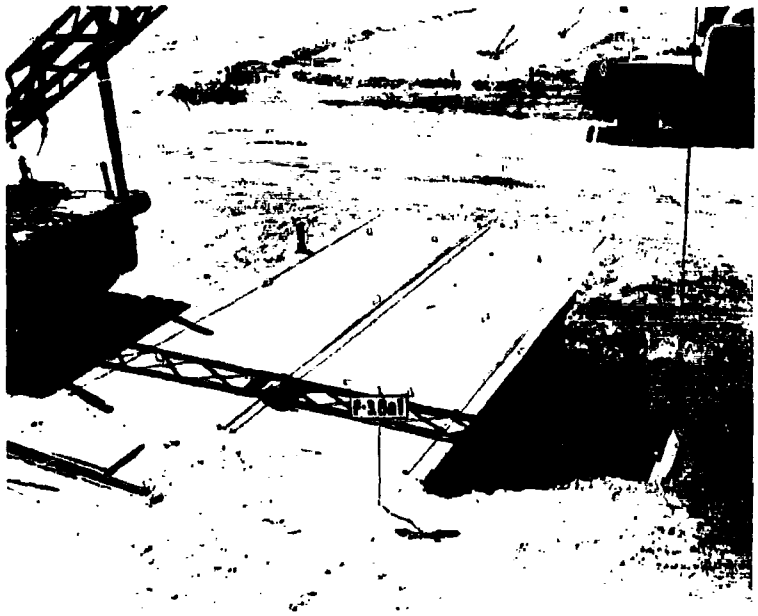

Figure 3.3 Pretest, TP 3.8 a-1, rear side view of test panels, facing southeast.

3.1.2 Instrumentation. The only on-structure instrumentation consisted of one mechanical scratch gage located at mid-span of each panel. Details of the gage, which was designed to record both maximum and permanent panel displacements, are shown schematically in Figure 3.4. A photograph of the gage installation is shown in Figure 3.5. Detailed visual inspection and photographic coverage were also provided.

Free-field blast measurements were obtained from nearby blast-line gages.

## 3.2 RESULTS

A pretest inspection of the TP 3.8a-1 beams disclosed a few hairline cracks on the top and bottom surfaces of both panels. The cracks were more pronounced on the ribbed Panel B. The post-Teapot condition of the panels is documented in Reference 2.

The posttest inspection of the panels showed a slight extension of the crack pattern throughout the structure. While permanent set occurred in both panels, they were not excessively cracked, nor did the supporting structure appear to be damaged. The neoprene seals were partially lifted from the panels.

TABLE 3.1 CENTER DEFLECTION OF TP 3.8a-1 PANELS

| | Maximum Deflection | | Permanent Deflection | |
|---|---|---|---|---|
| Panel | Plumbbob* | Teapot | Plumbbob* | Teapot |
| (A) Solid | 1.28 | 1.3 | 0.34 | 0.34 |
| (B) Ribbed | 1.68 | 1.92 | 0.59 | 0.74 |

*Measured relative to Teapot permanent deflection.



CONFIDENTIAL

3.2.1 Air Pressure Data. Figure 3.6 shows the estimated free-stream overpressure versus time variation on the ground surface at the 3,500-foot location of the TP 3.8a-1 structure. This data was obtained from the nearby blast-line pressure gages at Stations 12B and 12P3. The record shows a typical precursor form having a peak pressure of 9 psi and a positive duration of about 0.8 second. The pressure wave incident on these panels in the Teapot test was of essentially the same form but had a peak of 6.6 psi.

3.2.2 Mechanical Scratch Gages. The mechanical scratch gages provided clear records of both maximum and permanent deflection of the two panels. The data is shown in Table 3.1, and is believed accurate within ±0.02 inch. The corresponding Teapot data taken from Reference 2 is also shown in Table 3.1.

## 3.3 DISCUSSION

The response of the solid panel (A) was almost identical to that recorded in the Teapot test, both with respect to maximum and permanent deflections (Table 3.1). The response of the ribbed Panel (B) was somewhat less than that recorded previously. Of course, the present data represents deflections in excess of the permanent deflection sustained during the Teapot test.

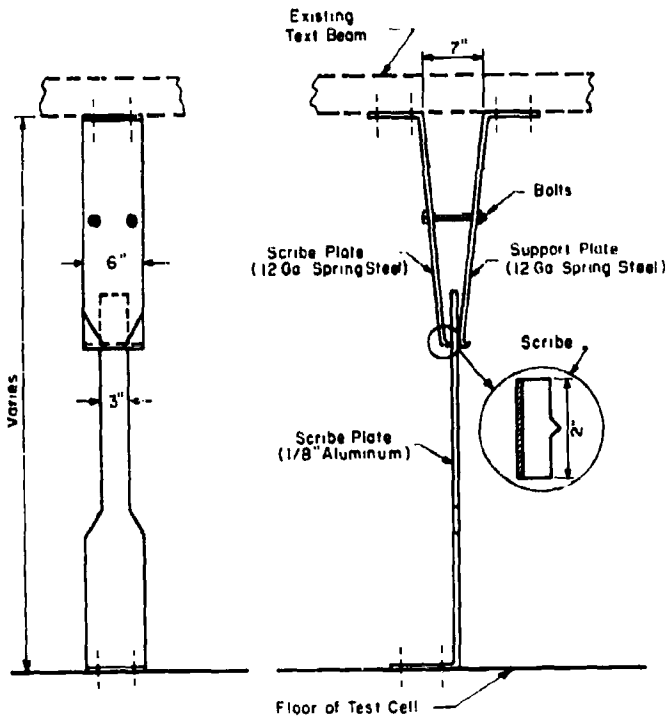


Figure 3.4 Details and typical installation of scratch gages on TP 3.8 a-1 panel and UK 3.8 beams.

No measurements were made of pressure infiltration under the panels. It is reported in Reference 2 that during the Teapot test the pressure under the panels gradually increased to 0.8 psi at maximum deflection and subsequently reached a peak value of 2 psi. Inasmuch as the same means of sealing the panels was employed in the present test and the damage to the seals appeared much the same, it is reasonable to assume that the interior pressures reached at least the level indicated above.

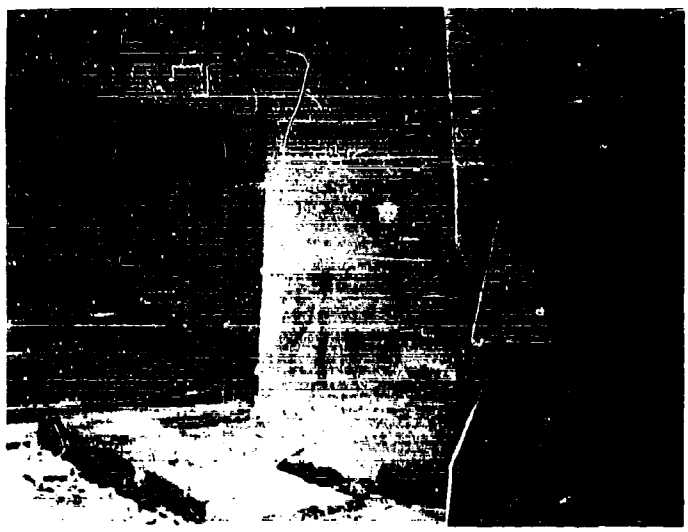

Figure 3.5 Pretest, TP 3.8 a-1, interior view of scratch gage on panel A.

The data obtained were made available to the project personnel engaged in the original TP 3.8 test. They were somewhat skeptical as to the desirability of reworking the TP 3.8 response analysis for the present loading in view of the uncertainty regarding the interior pressures. Also, they are currently engaged in constructing a laboratory device for simulating blast loads on prototype-size reinforced-concrete panels (Reference 7) so that the need for additional data on the TP 3.8 panels is not felt to be acute. For these reasons, no analysis of the data obtained was performed.

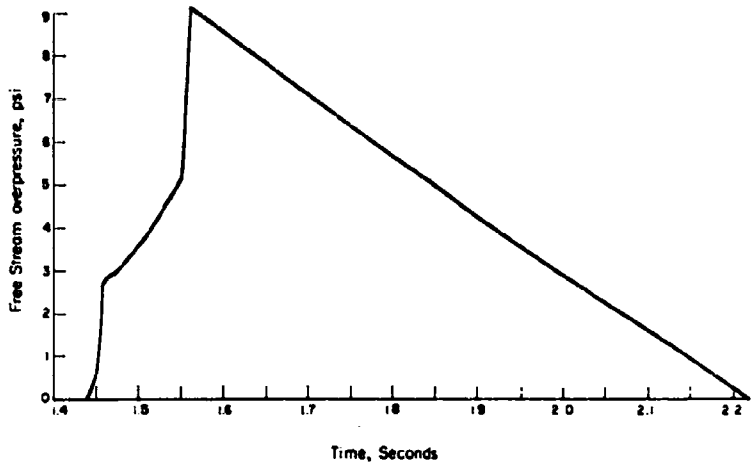


Figure 3.6 Estimated surface overpressure versus time variation at 3,500-foot ground range.



CONFIDENTIAL

# Chapter 4

# RESPONSE OF UNDERGROUND STRUCTURAL ELEMENTS

Project 3.8 of Operation Upshot-Knothole was a well-conceived experiment that fell short of expectations simply because the level of structural damage incurred was far less than desired (Reference 3). The same structures were retested during Operation Teapot as Project 3.4 with essentially the same results (Reference 4). Following that test, the items were all intact and, for the most part, had sustained only negligible permanent deformation. While some useful information had been gained, data were completely lacking in the range of structural action approaching collapse.

This situation, of course, was recognized by the project personnel involved, and, at the conclusion of the TP 3.4 test, it was recommended that these items be retested under more severe loading conditions (Reference 4). In particular, it was felt that valuable information could be obtained by subjecting the structures to pressure levels of the order of 100 psi to 150 psi. Since the pre-Plumbbob pressure predictions indicated a probable pressure level of 130 psi (Reference 6), it seemed worthwhile to retest the structures.

## 4.1 PROCEDURE

4.1.1 Test Structures. This test utilized the existing UK 3.8 structures (References 3 and 4). These consisted of three reinforced-concrete test chambers, the roofs of which contained 10 beam strips of varying mass and stiffness. Beams of three different flexibilities were tested. These were designated as elastic or E-beams, intermediate or M-beams, and plastic, or P-beams.

The test chambers were at a ground range of 900 feet and buried under 1 foot (UK 3.8a, Plumbbob designation: F-3.4-9020.03) 4 foot (UK 3.8b, Plumbbob designation: F-3.4-9020.02) and 8 feet (UK 3.8c, Plumbbob designation: F-3.4-9020.01) of earth cover. The following discussion of the test structures is taken from Reference 3, and pertains to the as-built condition of the chambers and test beams:

> Access to each structure was provided through a vertical shaft extending to a horizontal passage leading into the one end of each structure. The structure having a 1-foot depth of cover had its own access way. For the other two structures a common shaft located between the structures was provided with access to both through separate passageways.
>
> Each of the concrete test chambers was identical in design, with overall outside dimensions of 10 feet-2 inches by 21 feet-2 inches in plan, and 8 feet-3 inches in depth.... [A sketch of a typical structure is shown in Figure 4.1]. The side walls of the chambers were 19 inches thick, the end walls 15 inches thick, and the floors 12 inches thick....
>
> All concrete walls had vertical and horizontal reinforcement in both the inner and the outer faces. All the walls were designed for large pressures, so that under the expected conditions the deflections of the walls and of the floor slab would be negligible. Equivalent static loads for the design of the

base slab were taken as 40 psi, and for the walls 60 psi. For these static load design pressures, the allowable stresses were taken as 1.33 times the normal value or 26,700 psi for the reinforcing steel, and 1.5 times the normal value or about 2,000 psi for concrete.

The percentage of reinforcing steel in the base slab and end walls are approximately 0.65 to 0.75 percent in each direction in each face, and for the side walls 0.5 to 1.0 percent in each direction in each face, with the lower percentages of steel in the directions and regions where the flexural stresses were considered to be the smallest.

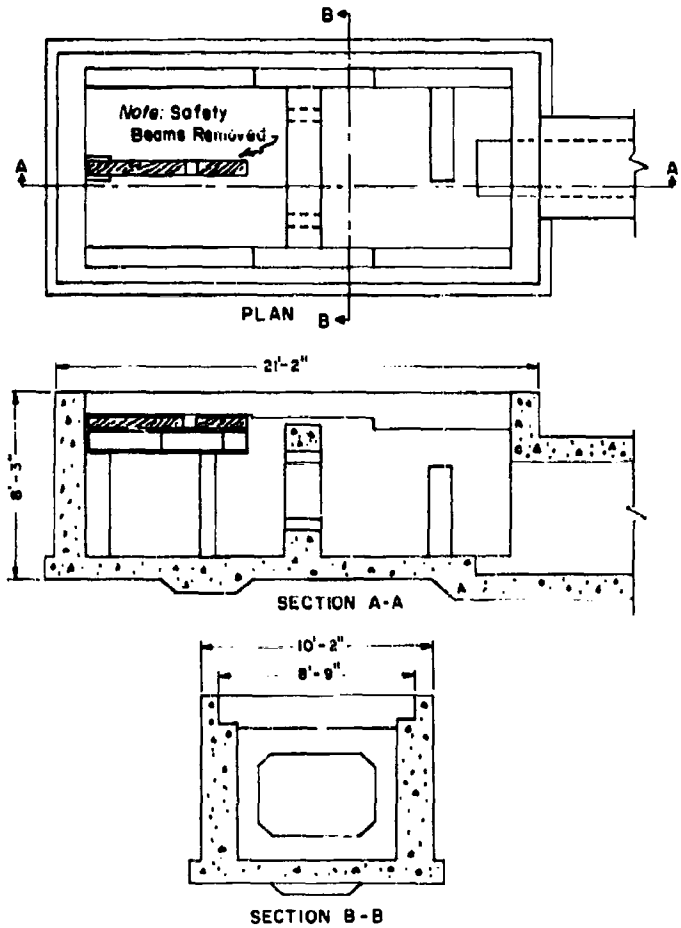


Figure 4.1 Details of typical UK 3.8 test structure.

The base slab, the end walls and the side walls were investigated for critical shearing stresses and were found to be adequate without any special provisions for shear.

Each of the 10 beam strips for the roof of each test chamber was composed of two closely spaced I-sections attached by welding to a common cover plate ½ inch thick. For the plastic beam strips, the I-sections were made by welding two 7-inch channels back-to-back.... [The details of the design of the test beams are shown schematically in Figure 4.2. Pertinent physical properties of the beams are summarized in Table 4.1. Additional details can be found in References 3 and 4. The arrangement of the test beams in the roof of the structures is shown in Figure 4.3.]

To provide the desired conditions of nearly free rotation at the ends of the beam strips, the ends were supported on shoes made of T-sections cut from rolled I-beams .... the beam strips were practically free to rotate at their ends but received sufficient restraint against longitudinal movement to prevent collapse at the ends.



CONFIDENTIAL

TABLE 4.1 DIMENSIONS AND PROPERTIES OF TEST BEAMS

| Quantity | Beam Type | | | |
|---|---|---|---|---|
| | | | Plastic (P) | |
| | Elastic (E) | Intermediate (M) | Original | Modified* |
| Rolled section used, each side | 15 I 50 | 8 I 23 two | 7 [ 9.8 two | 7 [ 9.8 |
| Width of ½ inch plate, (inch) | 23.25 | 20.25 | 21.25 | 21.25 |
| Total width supported, (inch) | 24 | 21 | 22 | 22 |
| Total moment of inertia, $(inch)^4$ | 1462 | 232.8 | 162.0 | 134.2 |
| Distance to neutral axis, (inch) | | | | |
| Top flange | 5.79 | 2.67 | 2.19 | 1.95 |
| Bottom flange | 9.71 | 5.83 | 5.31 | 5.55 |
| Max. stress, 100-psi load, (ksi) | 18.4† | 60.6† | 83.1† | 104.9† |
| Max. defl., 100-psi load, (inch) | | | | |
| Neglecting shear | 0.0605 | 0.333 | 0.501 | 0.557 |
| Including shear | 0.0752 | 0.365 | 0.541 | 0.601 |
| Equiv. dead load, (psi) | | | | |
| 1-ft cover | 1.3 | 1.1 | 1.1 | 1.1 |
| 4-ft cover | 3.6 | 3.4 | 3.4 | 3.4 |
| 8-ft cover | 6.7 | 6.5 | 6.5 | 6.5 |
| Dead load stress, (ksi) | | | | |
| 1-ft cover | 0.23 | 0.7 | 0.9 | 1.1 |
| 4-ft cover | 0.66 | 2.1 | 2.8 | 3.6 |
| 8-ft cover | 1.23 | 4.0 | 5.4 | 6.8 |
| Dead load deflection, (inch) | | | | |
| 1-ft cover | 0.0009 | 0.0040 | 0.0058 | 0.0064 |
| 4-ft cover | 0.0027 | 0.0125 | 0.0184 | 0.0204 |
| 8-ft cover | 0.0051 | 0.0238 | 0.0352 | 0.0391 |
| Fundamental period T, (msec) | | | | |
| Steel section only | 5 | 9 | 11 | 12 |
| 1-ft cover | 9 | 18 | 21 | 23 |
| 4-ft cover | 15 | 32 | 39 | 41 |
| 8-ft cover | 21 | 44 | 53 | 56 |

*Only Beams P2, P3, and P4 were modified.

†Assumes linear elastic action.



CONFIDENTIAL

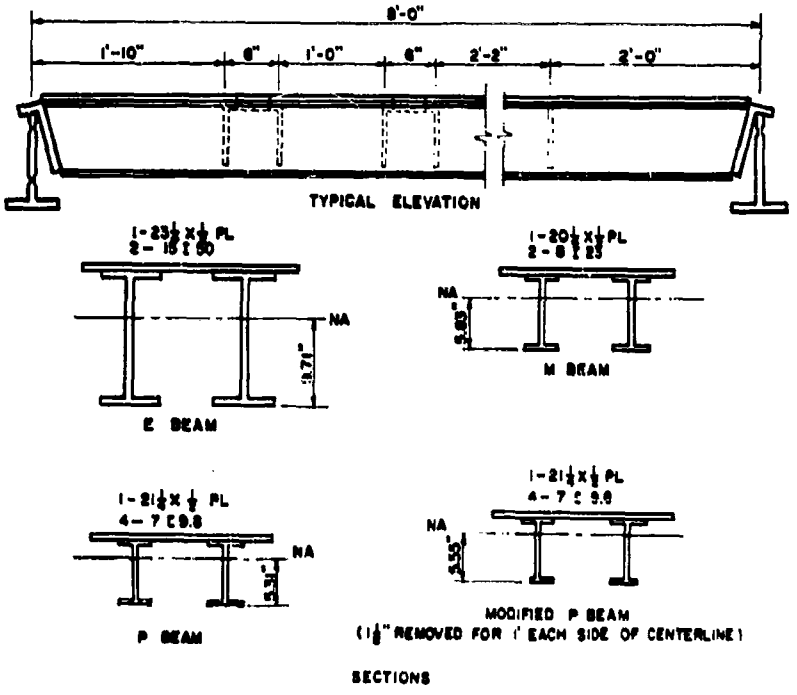


Figure 4.2 Details of typical UK 3.8 test beams.

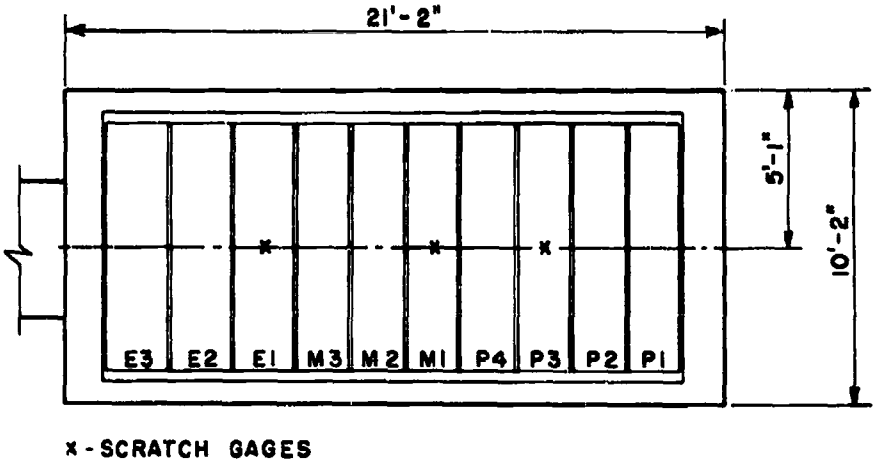


Figure 4.3 Typical arrangement of test beams in roof of UK 3.8 structure.



CONFIDENTIAL

A ¾-inch opening between the cover plates of adjacent beam strips was provided to permit them to deflect independently .... To prevent the infiltration of the backfill through the openings, a canvas cover was looped between the beam strips and placed over the entire roof .... filler strips were used to bridge the narrow gap between the beam strips .... the larger gap at the ends of the beam strips, between these ends and the parapet wall, is bridged by a similar strip ....

The beam strips sustained only minor permanent deformations as a result of previous tests, and no attempt was made to modify their post-Teapot condition. (After the UK 3.8 test it was found that steel of unexpectedly high yield stress had been used in the fabrication of the plastic beams. In an effort to further reduce the strength of these beams prior to the TP 3.4 test, the central portion of the bottom flanges was cut away on all P2, P3, and P4 beams (Figure 4.2).) However, the safety support beam, originally intended to limit the deflection of the plastic beams (Figure 4.1) was removed from each chamber to permit installation of the mechanical scratch gages.

A detailed discussion of the soil conditions around and over the structures at the time of the Upshot-Knothole test is contained in Reference 3. Data on density and unconfined compressive strength were obtained on undisturbed samples and were again obtained as part of the Operation Teapot test. No additional data of this type was obtained during the present test.

The earth cover over the 3.8a structure appeared to be shifted somewhat as a result of the Teapot test. However, no modification of earth cover was attempted.

4.1.2 Instrumentation. On-structure instrumentation consisted of mechanical scratch gages located at mid-span of three beams per cell and a DeForest mechanical strain gage located at mid-span of all beams not otherwise gaged. (This type of gage is described in detail in Reference 8.) In addition, a pretest and posttest level survey of the beams was conducted. The mechanical scratch gages were designed to measure both maximum and permanent deflections (Figures 3.4 and 4.4). They were located on beams E1, M1, and P3 in each cell (Figure 4.3). The level survey measurements followed the procedures established in the original UK 3.8 test.

## 4.2 RESULTS

4.2.1 Visual Examination. Visual inspection of the UK 3.8 structures showed that the response of the test items was generally much more pronounced than that of previous tests. There was a noticeable shifting of the soil above the UK 3.8a structure (Figure 4.5). Beam P3 had collapsed, permitting the soil to partially fill the chamber (Figures 4.6 and 4.7). The mechanical scratch gage attached to beam P3 was badly twisted, as were the other two gages in the cell. Damage to these gages was apparently caused by the entering blast wave. While only Beam P3 was severed from its supports, all the P and M beams showed permanent set, and some beams had appreciable twist. The beam supports were bent, indicating a translation of the beam away from ground zero. The test structure itself was not visibly damaged. Figures 4.8 and 4.9 show the nature of the damage sustained by the UK 3.8a beams. These photographs were taken after the beams were mistakenly removed from the structure.

Examination of the soil over the UK 3.8b and c structures did not suggest any shifting, nor was there any indication of damage to the structures themselves. However, inspection of the scratch gages in these cells indicated that some permanent displacement of the beams had occurred.

4.2.2 Air Pressure Data. Figure 4.10 shows the estimated air pressure versus time variation on the ground surface at the 900-foot location of the UK 3.8 structures. This data was obtained by interpolating among the records of free stream pressure obtained at stations 5B (850-foot ground range) and 6B (1,050-foot ground range) under Project 1.3. The resulting curve shows a typical precursor form having a peak pressure of 160 psi and a positive duration of about 0.25 second. It is to be noted that the loading experienced by these structures in the Teapot test was of essentially the same wave form but had a peak value of 96 psi. The pre-Plumbbob predictions at this location indicated a peak pressure of 130 psi (Reference 6).

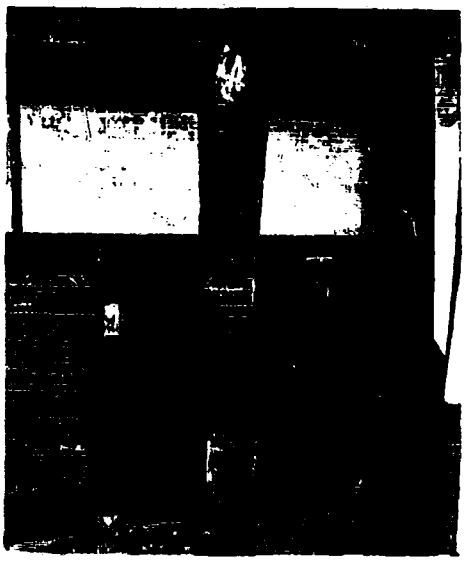

Figure 4.4 Pretest, interior view of scratch deflection gage in UK 3.8 a structure.

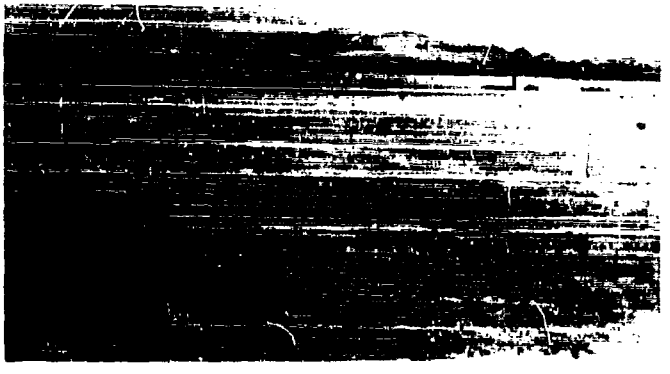

Figure 4.5 Posttest, UK 3.8 a, front side view of earth cover, facing northwest.

Figure 4.6 Posttest, UK 3.8 a, front view of collapsed section, facing west.



CONFIDENTIAL

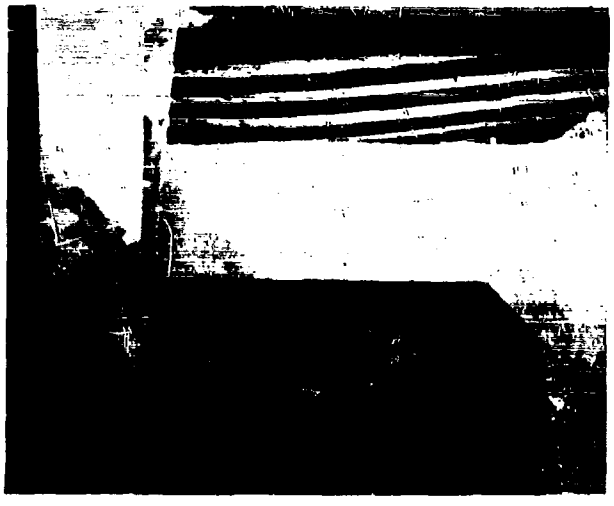

Figure 4.7 Posttest, UK 3.8a, interior view of cell, facing north.

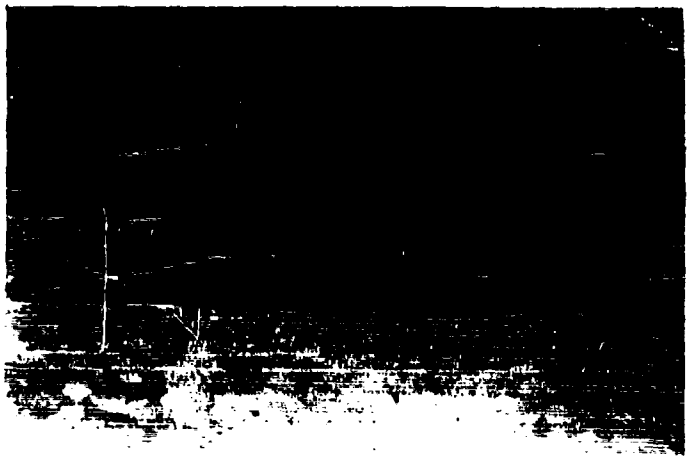

Figure 4.8 Posttest, UK 3.8a, damaged test beams.

Figure 4.9 Posttest, UK 3.8a, damage to Beam P3.



CONFIDENTIAL

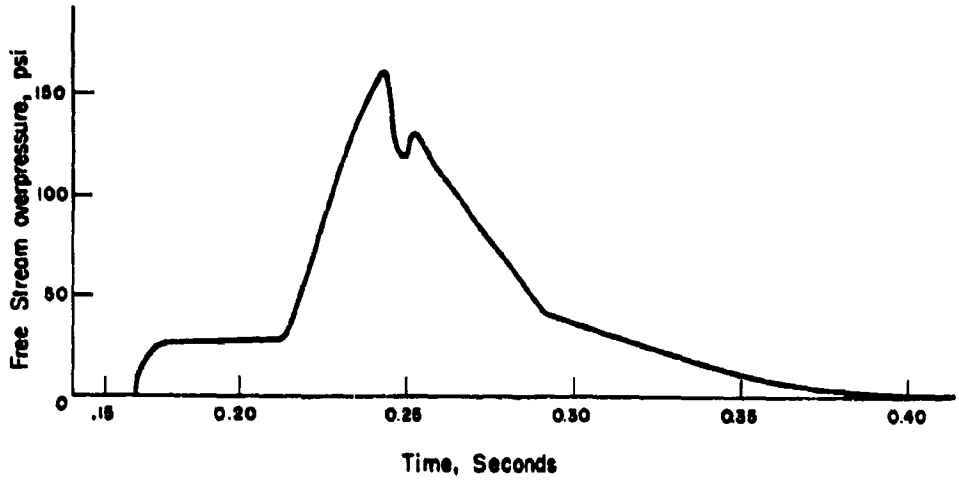


Figure 4.10 Estimated surface overpressure versus time variation at 900-foot ground range.

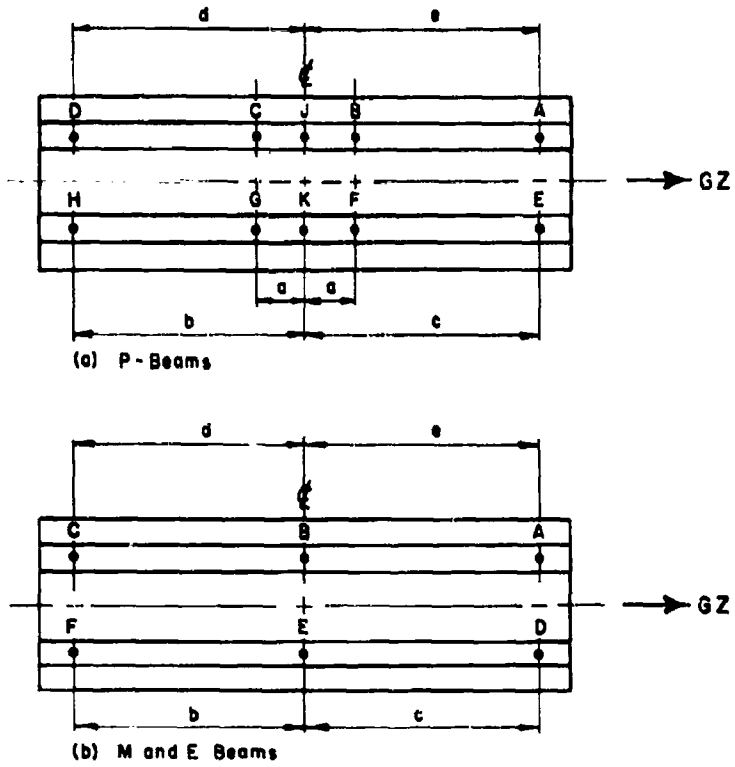


Figure 4.11 Location of survey points on UK 3.8 test beams.



CONFIDENTIAL

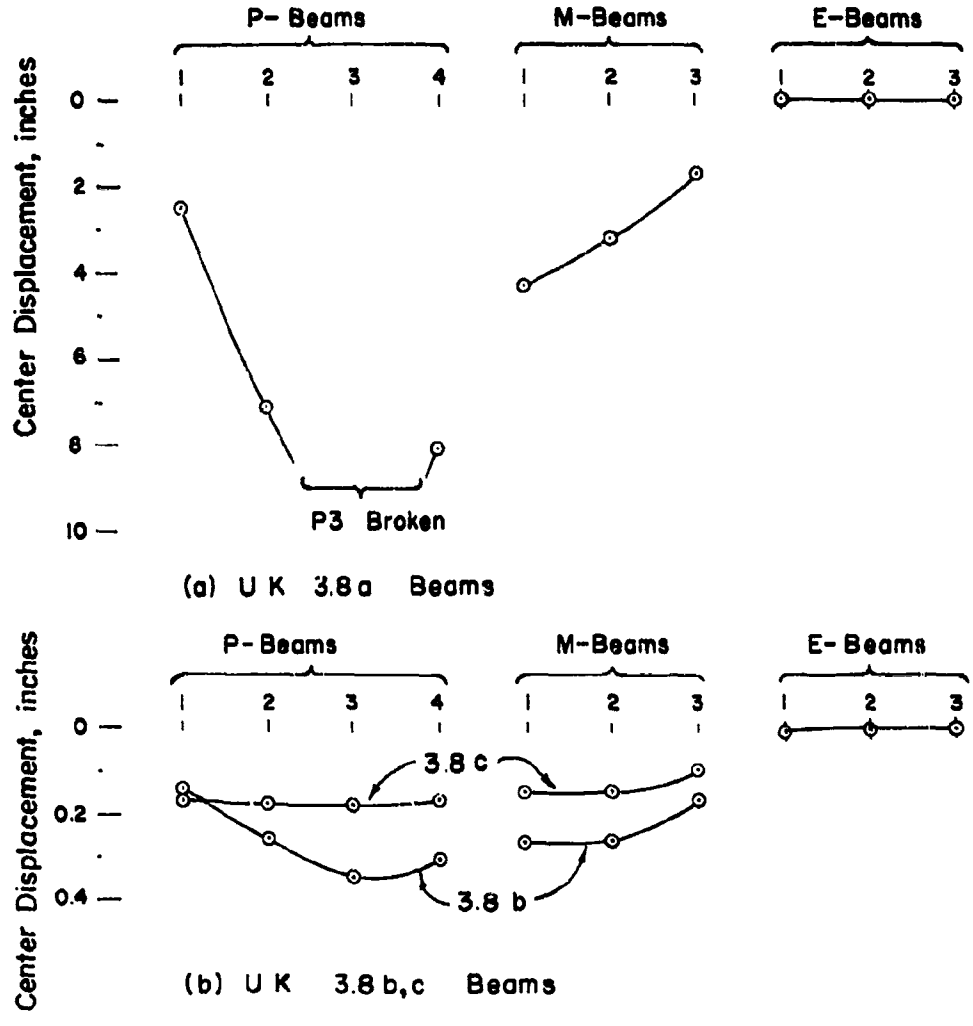


Figure 4.12 Variation in center displacement of UK 3.8 test beams along length of structure.



CONFIDENTIAL

4.2.3 Survey Measurements. Pretest and posttest elevations of various points on all test beams in the UK 3.8b and c structures (i.e., under 4 and 8 feet of earth cover, respectively) were established relative to a bench mark located on a side wall of the cells. A pretest survey was conducted for the beams in the UK 3.8a structure, but they were inadvertently removed after the test before the level survey could be performed. The permanent displacement of these beams, therefore, was measured relative to a string line stretched over the span.

Figure 4.11 and Table 4.2 show the location of points on the test beams for which elevations were determined. The data obtained is summarized in Tables 4.3 and 4.4. It is estimated that the survey results are accurate to within ±0.02 inch. Inspection of these results indicated that the beam supports underwent some permanent displacement. This was most noticeable in the case of the E beams. It also appeared that some twist took place in the P and M beams.

TABLE 4.2 LOCATION OF SURVEY POINTS ON TEST BEAMS IN UK 3.8b AND c CELLS

| Test Beam* | Dimension, inches | | | | |
|---|---|---|---|---|---|
| | a | b | c | d | e |
| 4P1 | 9 | 40½ | 40½ | 40⅜ | 40½ |
| 4P2 | 8 | 40½ | 40½ | 40½ | 40½ |
| 4P3 | 7 | 40½ | 40½ | 40½ | 40½ |
| 4P4 | 6 | 40½ | 40½ | 40½ | 40½ |
| 4M1 | - | 40 | 40½ | 40⅛ | 40½ |
| 4M2 | - | 40¼ | 40¼ | 40¼ | 40¼ |
| 4M3 | - | 40¼ | 40⅜ | 40⅜ | 40¼ |
| 4E1 | - | 41⅛ | 41⅛ | 41⅛ | 40 |
| 4E2 | - | 41⅛ | 41 | 41 | 41 |
| 4E3 | - | 41⅜ | 41 | 41¼ | 41 |
| 8P1 | 9 | 40⅝ | 40⅝ | 40⅝ | 40½ |
| 8P2 | 8 | 40⅝ | 40½ | 40¾ | 40½ |
| 8P3 | 6 | 41⅜ | 39¾ | 41 | 40 |
| 8P4 | 5 | 40⅜ | 40⅝ | 40½ | 40¾ |
| 8M1 | - | 39⅞ | 40¾ | 39¾ | 40⅝ |
| 8M2 | - | 40⅜ | 40⅜ | 40⅜ | 40⅜ |
| 8M3 | - | 40¼ | 40⅜ | 40¼ | 40¼ |
| 8E1 | - | 41⅜ | 41 | 41⅜ | 41 |
| 8E2 | - | 41⅛ | 41⅛ | 41⅛ | 41⅛ |
| 8E3 | - | 41 | 41¼ | 41 | 41¼ |

*The prefix, 4, designates beams under 4-foot cover, UK 3.8b.
The prefix, 8, designates beams under 8-foot cover, UK 3.8c.

Table 4.5 summarizes the average permanent center displacement of the beams, corrected for the motion of the end supports. The data were obtained by averaging the center displacement of each flange and subtracting from this value the average of the displacement of the end points on each flange. The permanent deflections of the UK 3.8a beams, as determined by a string line measurement, are also listed in Table 4.5.

The data of Table 4.5 show a significant variation in the behavior of presumably identical beams along the length of the structure. Furthermore, this variation appears to depend on the depth of earth cover. This is clearly shown in the plot of Figure 4.12.

4.2.4 Mechanical Gages. The mechanical scratch gages gave clear records of maximum and permanent center deflections for the three beams gaged in the UK 3.8b and c cells. The permanent deflection agreed with the survey results within 0.02 inch in all but one instance. The scratch gage on the 4P3 beam recorded a permanent deflection which was 0.04 inch less than that obtained in the survey. With this one exception, the agreement was considered to be



CONFIDENTIAL

TABLE 4.3 RESULTS OF LEVEL SURVEY OF UK 3.8b TEST BEAMS (4-FOOT EARTH COVER)

| Point | Perm. Defl., inch | Point | Perm. Defl., inch | Point | Perm. Defl., inch | Point | Perm. Defl., inch |
|---|---|---|---|---|---|---|---|
| 4P1 A | 0.06 | 4P3 A | 0.12 | 4M1 A | 0.08 | 4E1 A | 0.01 |
| B | 0.10 | B | 0.44 | B | 0.37 | B | 0.08 |
| C | 0.11 | C | 0.45 | C | 0.11 | C | 0.14 |
| D | 0.07 | D | 0.13 | D | 0.09 | D | 0.01 |
| E | 0.07 | E | 0.11 | E | 0.37 | E | 0.06 |
| F | 0.19 | F | 0.43 | F | 0.11 | F | 0.10 |
| G | 0.21 | G | 0.47 | | | | |
| H | 0.29 | H | 0.13 | 4M2 A | No. read. | 4E2 A | −0.01* |
| J | No. read. | J | 0.47 | B | No. read. | B | 0.02 |
| K | 0.21 | K | 0.48 | C | No. read. | C | 0.03 |
| 4P2 A | 0.10 | 4P4 A | 0.08 | D | 0.06 | D | −0.01* |
| B | 0.33 | B | 0.41 | E | 0.34 | E | 0.01 |
| C | 0.34 | C | 0.42 | F | 0.09 | F | 0.03 |
| D | 0.12 | D | 0.12 | 4M3 A | 0.05 | 4E3 A | 0.00 |
| E | 0.11 | E | 0.10 | B | 0.21 | B | 0.00 |
| F | 0.37 | F | 0.39 | C | 0.08 | C | 0.01 |
| G | 0.38 | G | 0.41 | D | 0.03 | D | −0.01* |
| H | 0.13 | H | 0.15 | E | 0.19 | E | 0.00 |
| J | 0.36 | J | 0.43 | F | 0.06 | F | 0.02 |
| K | 0.39 | K | 0.42 | | | | |

*Upward displacement.

TABLE 4.4 RESULTS OF LEVEL SURVEY OF UK 3.8c TEST BEAMS (8-FOOT EARTH COVER)

| Point | Perm. Defl., inch | Point | Perm. Defl., inch | Point | Perm. Defl., inch | Point | Perm. Defl., inch |
|---|---|---|---|---|---|---|---|
| 8P1 A | −0.02* | 8P3 A | 0.00 | 8M1 A | 0.02 | 8E1 A | 0.01 |
| B | 0.14 | B | 0.19 | B | 0.16 | B | 0.06 |
| C | 0.14 | C | 0.19 | C | 0.02 | C | 0.06 |
| D | 0.00 | D | 0.01 | D | 0.03 | D | 0.02 |
| E | −0.01 | E | 0.01 | E | 0.18 | E | 0.02 |
| F | 0.14 | F | 0.20 | F | 0.01 | F | 0.06 |
| G | 0.17 | G | 0.22 | | | | |
| H | 0.01 | H | 0.02 | 8M2 A | No. read. | 8E2 A | 0.10 |
| J | No. read. | J | 0.19 | B | No. read. | B | 0.10 |
| K | 0.17 | K | 0.19 | C | No. read. | C | 0.11 |
| 8P2 A | 0.00 | 8P4 A | 0.01 | D | 0.03 | D | 0.10 |
| B | 0.17 | B | 0.19 | E | 0.18 | E | 0.11 |
| C | 0.18 | C | 0.19 | F | 0.03 | F | 0.09 |
| D | 0.01 | D | 0.07 | 8M3 A | 0.03 | 8E3 A | 0.11 |
| E | 0.00 | E | 0.02 | B | 0.13 | B | 0.10 |
| F | 0.17 | F | 0.19 | C | 0.02 | C | 0.11 |
| G | 0.17 | G | 0.19 | D | 0.02 | D | 0.11 |
| H | 0.01 | H | 0.02 | E | 0.11 | E | 0.11 |
| J | 0.19 | J | 0.19 | F | 0.02 | F | 0.10 |
| K | 0.19 | K | 0.19 | | | | |

*Upward displacement.



CONFIDENTIAL

TABLE 4.5 AVERAGE CENTER DEFLECTIONS OF UK 3.8 TEST BEAMS

| Test Beam | UK 3.8a Max.* Defl., inch | UK 3.8a Max.† Defl., inch | UK 3.8b Max. Defl., inch | UK 3.8b Perm. Defl., inch | UK 3.8c Max. Defl., inch | UK 3.8c Perm. Defl., inch |
|---|---|---|---|---|---|---|
| P1 | | 2.44 | | 0.14 | | 0.17 |
| P2 | | 7.13 | | 0.26 | | 0.18 |
| P3 | | Broken | 0.93 | 0.35 | 0.68 | 0.18 |
| P4 | | 8.06 | | 0.31 | | 0.17 |
| M1 | 4.5 | 4.38 | 0.73 | 0.27 | 0.55 | 0.15 |
| M2 | | 3.25 | | 0.27 | | 0.15 |
| M3 | | 1.75 | | 0.17 | | 0.10 |
| E1 | 0.25 | < 0.06 | 0.28 | 0.01 | 0.21 | 0.00 |
| E2 | | < 0.06 | | 0.00 | | 0.00 |
| E3 | | < 0.06 | | 0.00 | | 0.00 |

*Obtained from damaged scratch gages.
†Measured from string line on top plate of beams.

entirely adequate, considering the fact that the scratch gage records were measured with a scale. The one discrepancy was probably caused by an error in establishing either the pretest or posttest base line on the gage and this would have been the only beam so affected. The maximum displacements obtained for beams P3, M1, and E1 are listed in Table 4.5.

TABLE 4.6 MAXIMUM AND PERMANENT STRAIN MEASUREMENTS FROM DEFOREST MECHANICAL STRAIN GAGES

| Test Beam | Maximum Strain | Permanent Strain |
|---|---|---|
| 1P2 | 0.0685* | -† |
| 1P4 | 0.0635 | -† |
| 4P4 | 0.0095 | 0.005 |
| 4M2 | 0.0032 | 0 |
| 8P4 | 0.0032 | 0.0017 |

*Trace off edge of plate.
†Trace did not return.

The P3 beam was collapsed (Figure 4.9) and the entering blast damaged the three scratch gages inside the structure. It was possible to gain some estimate of the maximum displacement recorded by two of these gages. These results are also shown in Table 4.5.

Interpretable records were obtained from only a few of the 21 DeForest mechanical strain gages. The data obtained are listed in Table 4.6. Inasmuch as all strains exceeded the elastic range, it was not considered feasible to convert this data to mid-span deflections.

## 4.3 DISCUSSION

The results of this test were made available to personnel engaged in the two previous tests. It was the concensus of opinion that, while the data could well serve to further the findings of the earlier tests, this would require extended analysis. Such an effort could not be undertaken within the scope of the present program; therefore, no quantitative interpretation of results is offered. Certain qualitative observations, however, were clear.

On the basis of the measured beam response, there seemed to be no doubt that, in the type of soil encountered, there was a significant attenuation of effective vertical earth pressures



CONFIDENTIAL

within the first few feet of depth. (Effective vertical earth pressure refers to the damage producing agent, not to the free-field pressure. In other words, the test results show a significant attenuation damage with depth.) If anything, the opposite conclusion was reached in the original UK 3.8 test (Reference 3) and apparently reaffirmed in the TP 3.4 test (Reference 4).

Another conclusion reached in earlier tests was to the effect that the beams behaved as though loaded with the vertical forces acting on the earth's surface immediately overhead. In view of the significant variation in response of presumably identical beams in the same structure (Figure 4.12), it does not seem reasonable to assign only a passive role to the soil in regard to the transmission of vertical pressure.

It is believed that the present test effort was extremely worthwhile and that the data gathered represented a significant addition to the limited empirical information relating to the blast response of underground structures. Certainly, any general theory of shock transmission in soil and the response of buried structures must adequately explain the results of this test.

## 4.4 CONCLUSIONS

Inasmuch as no quantitative interpretation of the data obtained was attempted, no definite conclusions can be formulated. However, it does seem that the conclusions reached in earlier tests relating to the lack of attenuation with depth of effective vertical earth pressures and the response of the test beams to these loads needs to be re-evaluated in light of the present test data.

# Chapter 5

# INTERIOR LOADING AND RESPONSE OF UNDERGROUND STRUCTURES

Retesting of the UK 3.7 underground structure was recommended as a means of obtaining loads in the interior of underground chambers located in the precursor region. In the original UK 3.7 test, the blast entered the main chamber of the structure through relatively small roof vents, and the rate of filling was sufficiently slow so that the filling process could be characterized in terms of a single nondimensional time variable (Reference 5). In the present test the filling rate was increased substantially by allowing the blast wave to enter through the main entranceway. For a short-rise-time precursor wave, this was expected to lead to multiple reflections in the interior of the chamber. The test results were to be correlated with existing loading information and, eventually, with the results of proposed shock tube tests on plenum chambers. It was expected that the data would be useful in estimating the loads on equipment stored in underground chambers. Depending upon the response of the structure itself, it was hoped to correlate any additional damage with existing loading and response schemes.

## 5.1 PROCEDURE

5.1.1 Test Structures. This test utilized one portion of the existing UK 3.7 underground structure at 900 feet ground range (Plumbbob designation: F-3.4-9021). This structure was divided into two main chambers, each individually vented to the outside through the roof and closed at the entranceways by means of blast-resistant doors (Reference 5). The north chamber, which was essentially undamaged during prior tests, was modified by the sealing of the roof vents and removal of the blast door, thus permitting the blast wave to enter through a considerably larger opening than previously. Figure 5.1 shows plan and section views of the north test chamber and entranceway. The south portion of the structure was severely damaged during Operation Teapot and was not included in the test. Preshot photographs of the test chamber and entranceway are shown in Figures 5.2 and 5.4.

5.1.2 Instrumentation. On-structure instrumentation consisted of two BRL self-recording pressure gages mounted flush with the floor of the chamber, gages P1 and P2 (Figure 5.1). A self-recording q gage was installed by Project 33.2 on a line midway between the floor gages, and is designated as gage P3 in Figure 5.1. The q gage was elevated 3 feet above the floor and oriented toward the entranceway. Free-field measurements were obtained from nearby blast-line gages.

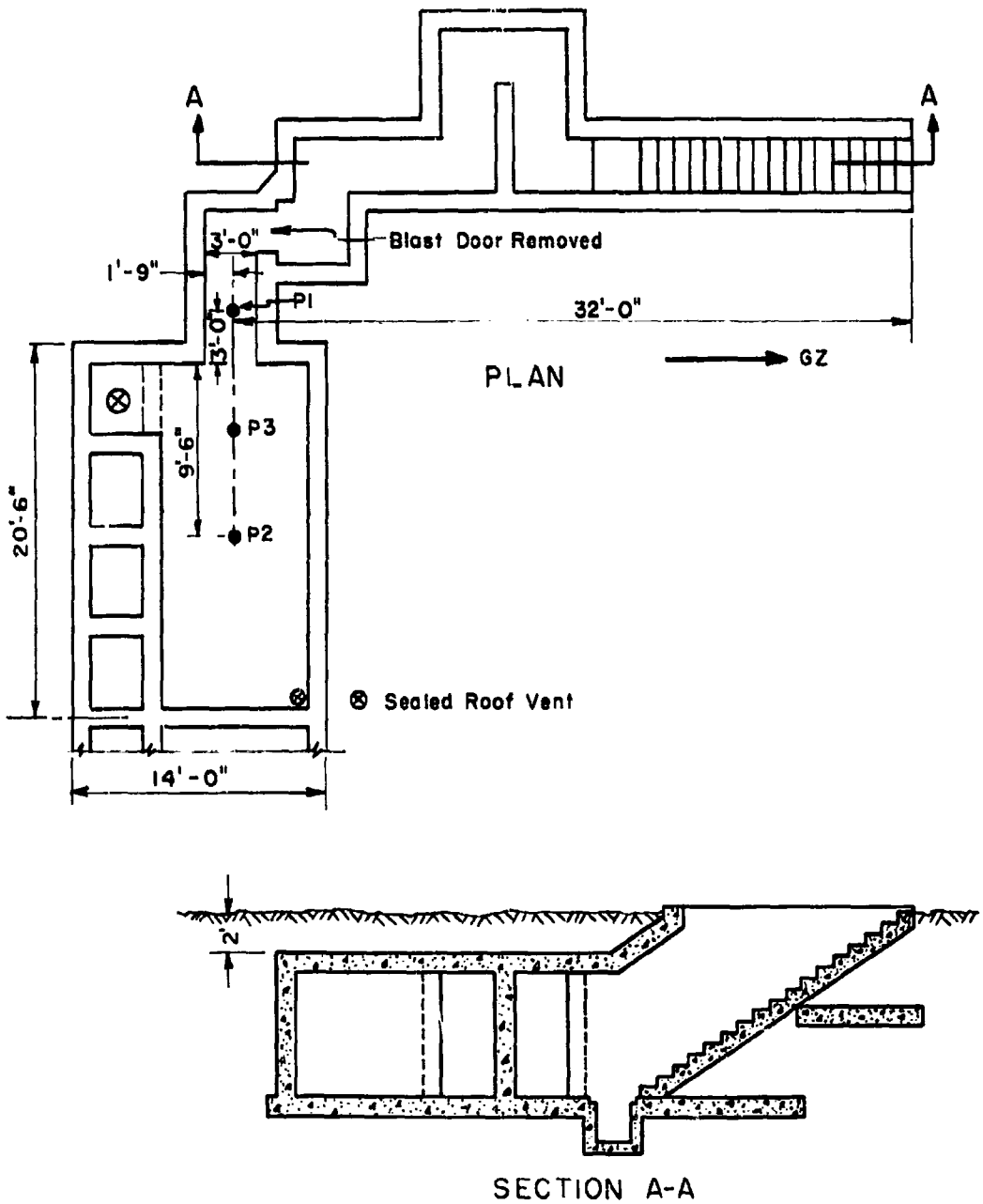


Figure 5.1 Details of UK 3.7 test chamber and location of pressure gages.



CONFIDENTIAL

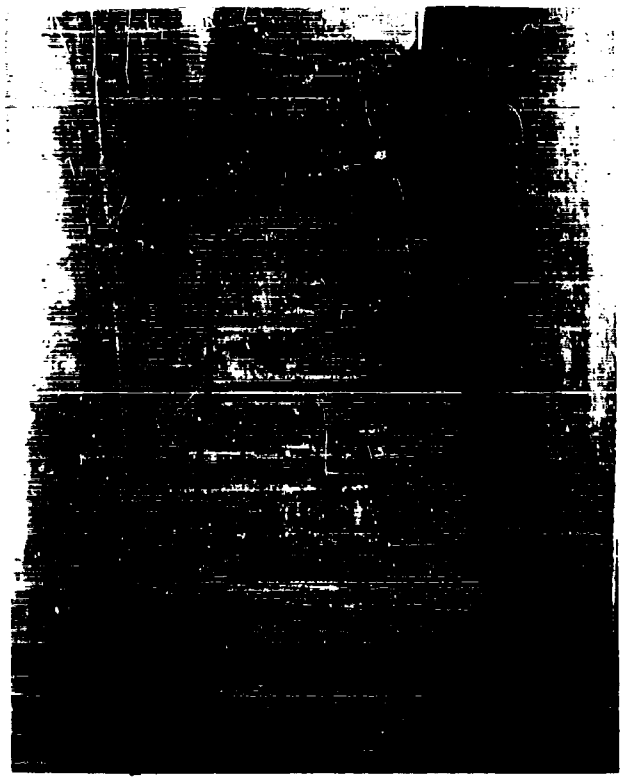

Figure 5.2 Pretest, UK 3.7, view of entranceway steps, facing east.

## 5.2 RESULTS

The test structure was located in an estimated 150 psi overpressure region. (The free-field pressure variation is discussed in Section 4.2.2 and shown in Figure 4.10.) There was no significant damage to the north section of the structure. Such additional damage as occurred was confined mainly to the entranceway. In some places, existing cracks in the stair wall, retaining walls, and entranceway partition walls were enlarged by as much as several inches (Figures 5.3 and 5.5). The roof of the main chamber underwent a slight permanent deformation as evidenced by the crack pattern shown in Figure 5.6. There was no debris on the floor of the main chamber.

Only the entranceway gage (P1) provided a complete record. (It was erroneously stated in the Interim Test Report (ITR-1423) that gage P2 had provided a useable record.) The two other gages failed to initiate and recorded only the following peak pressures: Gage P2—65.2 psi peak overpressure; Gage P3—73.4 psi peak overpressure and 3.1 psi peak dynamic pressure.

## 5.3 DISCUSSION

5.3.1 Interior Loading. The loading or pressure variation on the interior of the UK 3.7 underground structure is determined analytically in the following paragraphs and compared with the pressure variation (see $P_{1m}$ of Figure 5.8) measured in the entrance tunnel or passage during Shot Priscilla. The loading was determined using both a quasi-steady and nonsteady flow



CONFIDENTIAL

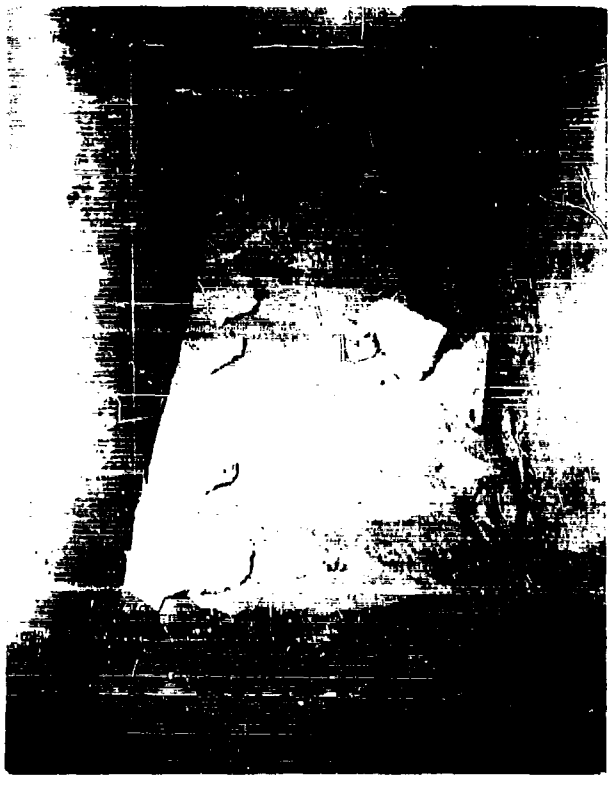

Figure 5.3 Posttest, UK 3.7, view of entranceway steps, facing east.

analysis. To render any such analysis tractable, it is necessary to make a number of assumptions or simplifications which, by their very nature, tend to eliminate some effects which may be observed in the field record. On the other hand, in attempting to compare the field record and the predicted loadings, one must always evaluate or estimate the validity of the observed pressure variation. It is not uncommon in full-scale loading tests to obtain erratic and meaningless pressure records. As previously stated, only one out of three pressure-time gages functioned well enough to yield a pressure-time record. The outside free-stream static-pressure variation at the structure location was obtained by interpolation from two adjacent measurements. The structure geometry, although quite complex, is accurately known, at least for loading purposes.

The validity of the interpolated free-stream static pressure and the pressure $P_{1m}$ observed with gage P1 in the entrance tunnel is assumed and will be discussed in more detail in the conclusion section of this chapter. However, the validity or usefulness of the peak pressure observed from the two pressure gages (P2 and P3) which failed to initiate is considered highly questionable. This conclusion was arrived at, in part, because, in general, the type of gages which were used exhibited mechanical ringing or oscillations, the amplitude of which was due to the intensity of the excitation as well as to the characteristics of the gage itself, and also because it was impossible to estimate with any degree of confidence the amplitude of these oscillations. The values of the peak pressures given in Section 5.2 should be reduced by some unknown amount to determine the mean peak pressure which existed at the pertinent position, assuming, of course, that the gages performed satisfactorily in all other respects. As an example, for Gage P1 the observed peak pressure was 75.4 psig, whereas the mean peak pressure

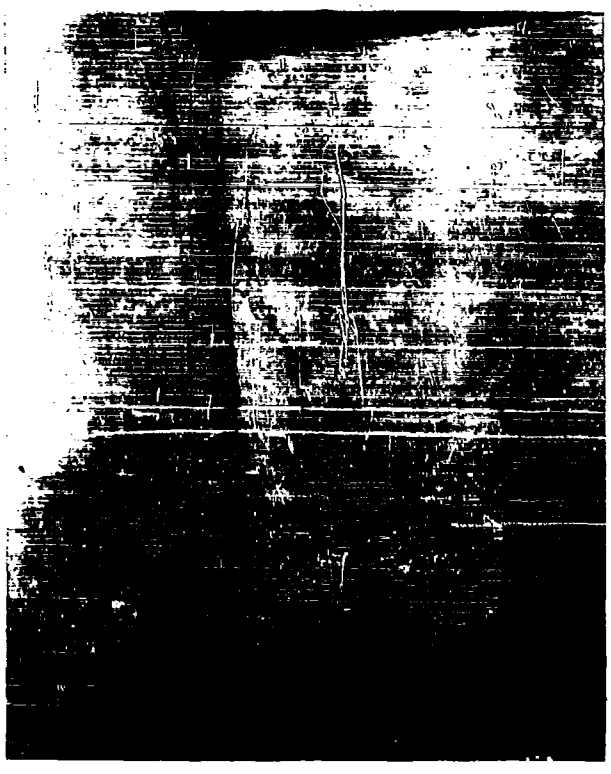

Figure 5.4 Pretest, UK 3.7, view of entranceway partition wall, facing west.

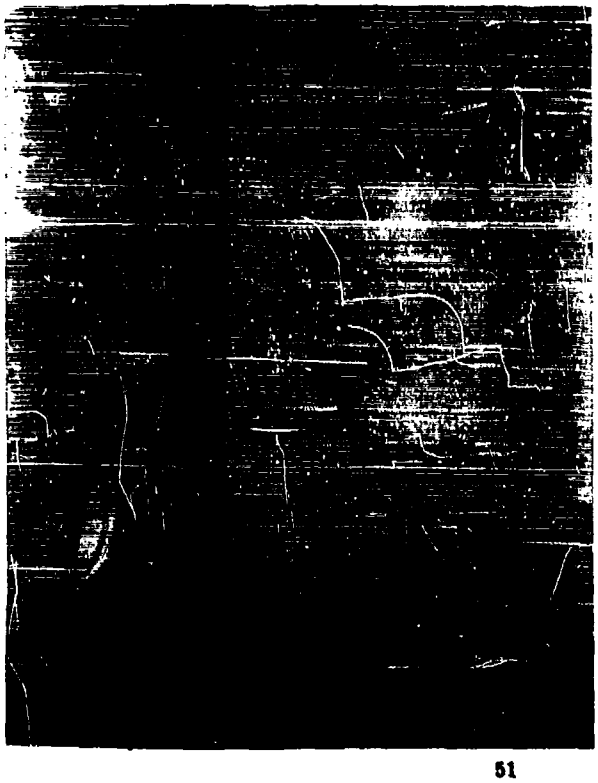

Figure 5.5 Posttest, UK 3.7, view of entranceway partition wall, facing west.



CONFIDENTIAL

was approximately 65 psig (Figure 5.7). This gage then exhibited an overshoot of more than 10 percent. This overshoot could be due either to spurious pressure signals in the air or to the mechanical characteristics of the gage itself, or to both. It is believed that the overshoot was due largely to the latter cause. In any event, the overshoot was of little practical value since the blast analyst was generally interested in average or distributed loadings.

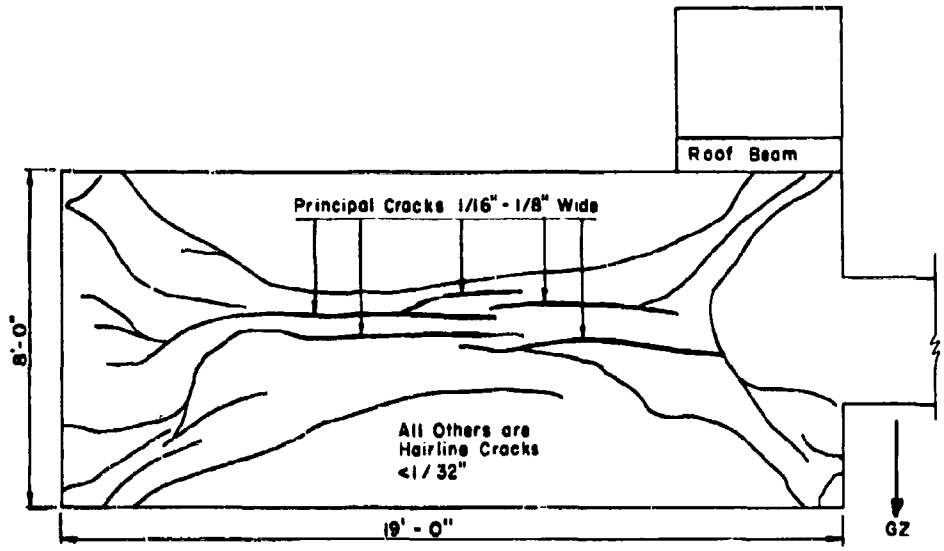


Figure 5.6 Crack pattern on roof of UK 3.7 structure.

The simplest type of analysis which can be applied to the prediction of the pressure variation with time in the shelter is based upon the assumption that the most significant parameter is the instantaneous pressure difference between the outside free-stream pressure and the pressure in the shelter chamber. Thus, the following three steady-state equations are pertinent and must be solved simultaneously (Reference 9):

$$W(t) = \frac{Ak\,P_0}{c_0}\sqrt{\left[\frac{2}{k+1}\right]^{\frac{k+1}{k-1}} \cdot \frac{P_s(t)}{P_0}^{\frac{k+1}{k}}} \quad \text{if } \frac{P_s(t)}{P_i(t)} \geq 1.89$$

and

$$W(t) = \frac{Ak\,P_0}{c_0} \cdot \left[\frac{P_s(t)}{P_0}\right]^{\frac{k+1}{2k}} \sqrt{\frac{\left[\left(\frac{P_s(t)}{P_i(t)}\right)^{\frac{k-1}{k}} - 1\right]\frac{2}{k-1}}{\left[\frac{P_s(t)}{P_i(t)}\right]^{\frac{k+1}{2k}}}} \quad \text{if } \frac{P_s(t)}{P_i(t)} \leq 1.89$$

and

$$W(t) = \frac{\rho_0 V}{k}\,\frac{[P_i(t)]^{\frac{1-k}{k}}}{P_0^{1/k}} \cdot \frac{d}{dt}\,[P_i(t)]$$



CONFIDENTIAL

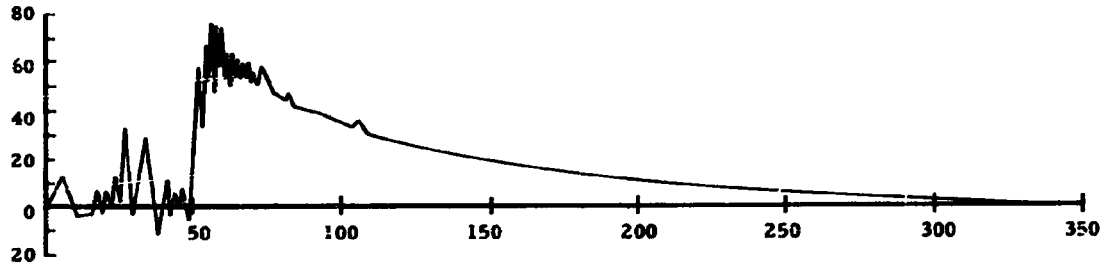


Figure 5.7 Observed pressure variation in entranceway (gage P1).

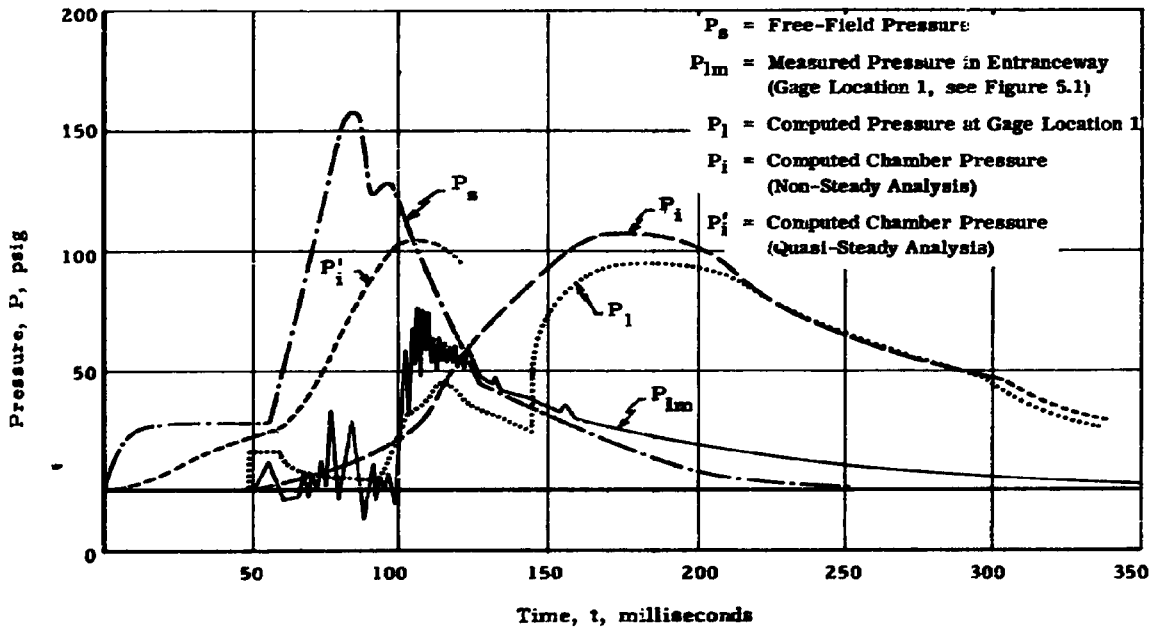


Figure 5.8 Comparison of pressure variations.



CONFIDENTIAL

where: $P_s(t)$ = static pressure outside chamber
$P_i(t)$ = pressure in chamber
$W(t)$ = mass flow
$A$ = flow area at entranceway
$V$ = volume of chamber
$P_0$ = ambient pressure
$\rho_0$ = ambient density
$c_0$ = ambient sound velocity
$k$ = ratio of specific heats (= 1.4 for air)
$t$ = time

In the above equations, all entropy changes in the gas are neglected, and it is assumed that the dynamic energy of the outside blast wave does not contribute to the pressure build-up in the shelter.

The result of this analysis is presented in Figure 5.8 as $P_i'$ and indicates that the maximum pressure in the chamber is in excess of 100 psig. The pressure level within the entrance tunnel would, neglecting local effects, be within the limits of $P_s$ and $P_i'$ at any instant of time. Thus, since Gage P1 was only 3 feet from the chamber, the observed pressure record $P_{1m}$ should be compared with the predicted pressure variation in the chamber $P_i'$. Since the analysis does not account for the finite length of the entrance tunnel nor the finite propagation time of any disturbance (such as a sound wave), the observed pressure record $P_{1m}$ must be translated forward in time (approximately 47 msec) in Fig. 5.8. If this is done, then one will note that for a time of approximately 50 msec the observed pressure, $P_{1m}$, is greater than both the free-field static pressure, $P_s$, and the computed chamber pressure. Such an observation is inconsistent with the original assumptions. Thus, one must conclude that for the values of the parameters of this test, a steady-state analysis is not adequate, at least if comparisons of pressure observations within the entranceway are to be made. Also, the prediction of the pressure variation in the chamber itself is not correct, although it may be a reasonable approximation if an appropriate time shift is made. That is, the form $P_i'$ may be reasonable, and, in particular, the maximum values of $P_i'$ may be nearly correct.

Because of the above results, a non-steady-state analysis was made. Such an analysis is possible only if the problem can be reduced to a one-dimensional non-steady problem. The most important parameter in addition to the outside pressure is the finite length of the entrance tunnel. The problem was idealized as that of a chamber connected to the surface by a straight constant-area channel. The flow in the channel was analyzed by the method of characteristics in which the boundary conditions at the surface and at the chamber end were defined as follows: The free-field static pressure at the entrance was assumed to be the pressure just outside the channel at the tunnel end. In other words, it was assumed that the dynamic pressure did not contribute to the flow into the tunnel or chamber. If the flow direction were from the outside into the tunnel, the pressure just inside the channel was related to the free-field pressure by the appropriate energy equation. If the flow were outward from the tunnel, then the pressure just inside the tunnel must have equaled the free-field pressure, provided of course that the flow was not sonic at that point.

If the flow were sonic, the pressure in the channel could have been increased over the outside pressure. The boundary condition at the end of the channel was handled in a similar manner, except that the chamber pressure was determined by integrating the change in mass in the chamber (which was determined from the flow passing through the channel boundary at the chamber end) and computing the pressure, assuming that air was a perfect gas and that the flow process in the chamber was isentropic.

The details of the method of characteristics are well known and will not be given here (References 9 and 10). To make the analysis tractable, the flow field was assumed to be isentropic. This was a reasonable assumption, since, in general, the strengths of the various shock waves appearing in the flow field were not great. The effects of the various bends in the tunnel were assumed to contribute only in that during the early phases of the flow multiple reflection of relatively weak strength would exist and that these signals would appear as oscillatory sig-



CONFIDENTIAL

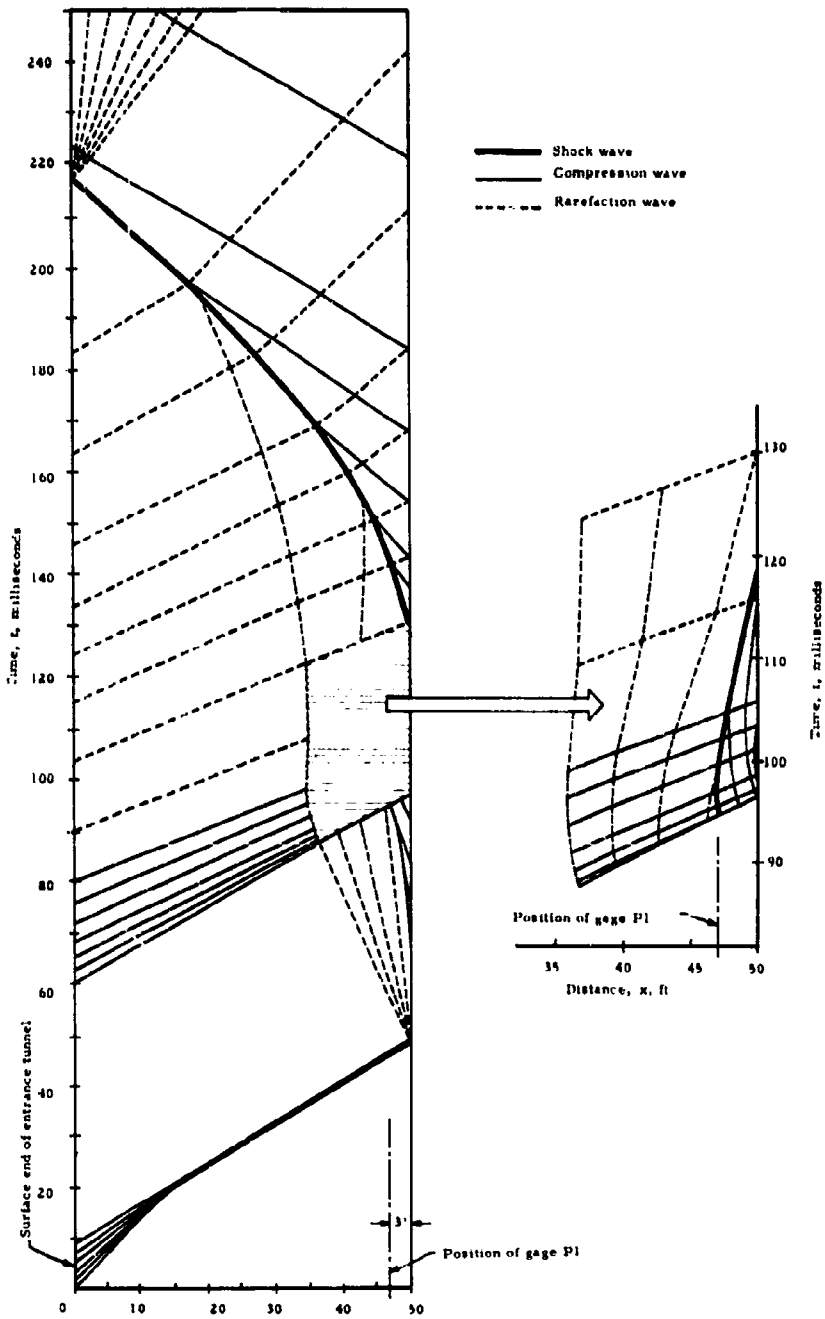


**Figure 5.9 Wave diagram.**



CONFIDENTIAL

nals of a few msec period superimposed upon the results of this analysis. Therefore, the validity of a model composed of a straight channel should have been reasonably good. Perhaps the most important simplification used in the analysis was the assumption of a constant-area channel. Actually, the entrance tunnel had a slight, perhaps 10 percent, constriction in it, where a blast door had originally been installed. This constriction was significant, since it was quite possible for the flow to become choked (i.e., sonic) at this point and thereby reduce the mass entering the chamber. A more elaborate and hence more time-consuming analysis could be made which would consider the area restriction; however, in view of the sketchy field observations which were obtained, the elaborate analysis was abandoned in favor of the simpler analysis.

Figure 5.9 presents a wave diagram of the solution of the problem at hand. A compression wave enters the tunnel and coalesces into a shock wave (about 8 psi) approximately 20 feet from the entrance. Actually, as this compression or shock wave interacts with bends in the tunnel, reflected signals will be sent back toward the entrance; these are neglected. As the shock wave reaches the chamber end of the tunnel, it expands out into the chamber, decreasing in strength to perhaps 1 psi or less. Thus, the side walls, floor, and ceiling of the chamber are exposed to a small pressure pulse. The shock wave reflects from the back wall of the chamber (to perhaps 2 psi or less) and then bounces back and forth in the chamber. After approximately 10 to 20 msec, the shock has decayed down to a sound signal. It is possible to obtain higher pressures locally and for short periods of time in such regions as corners. The average pressure in the room during the first ten msec, after the shock wave enters the chamber, increases to only 1 or 2 psi.

The passage of the shock wave into the chamber results in the generation of a centered rarefaction wave (representing a decrease in pressure) at the chamber end. This wave propagates up the channel toward the surface end. The flow at the chamber end is sonic, and the pressure is greater than that in the chamber. The chamber pressure increases as the air flows into the chamber. At a time t = 70 msec, the chamber pressure equals the pressure in the chamber end and a compression wave (representing an increase in pressure) is initiated and moves toward the surface end. The first compression wave is followed by several more, as the pressure in the chamber continues to increase and the compression wave coalesces into a weak shock wave. At about this same time, a large compression wave enters the tunnel from the surface end and the flow into the tunnel becomes supersonic. Thus, the centered rarefaction wave and the trailing shock wave interact with the compression wave and are swept back toward the chamber. The shock wave is actually swept out of the tunnel and into the chamber, so that for approximately 10 msec a standing (slowly moving) network of shock waves exists in the chamber near the channel. The shock waves are probably confined to a region which extends 2 to 3 feet into the chamber from the tunnel end.

After the compression wave enters the tunnel, a system of rarefaction wave enters, and the flow velocity and pressure drop in the entrance portion of the tunnel. When the head of this rarefaction system reaches the chamber end of the tunnel, the standing shock system reforms and moves back into the tunnel and propagates toward the surface end. This shock wave catches up to the original centered rarefaction wave before it reaches the surface end of the tunnel.

The pressure in the chamber has been increasing steadily and does not begin to level off until t = 130 msec (when the outside pressure decay is felt at the chamber end of the tunnel). At t = 170 msec, the air stops flowing into the chamber and the peak chamber pressure is reached. The flow out of the chamber is quite small at first, so that the chamber pressure falls slowly. At t = 200 msec, the flow rate increases and the chamber pressure falls somewhat more rapidly.

When the shock wave reaches the surface end of the tunnel, another centered rarefaction wave is formed and moves down the tunnel. When this wave reaches the chamber (t = 310 msec), the chamber pressure decay rate increases. By this time, the chamber pressure was down to approximately 30 psig, and the analysis was arbitrarily stopped.

The chamber pressure variation with time is shown in Figure 5.8 as $P_i$. The peak value is approximately 108 psig. The equivalent location of Gage P1 is shown in the wave diagram (Figure 5.9), and the pressure variation at that point in the tunnel is presented in Figure 5.8 as $P_1$.



CONFIDENTIAL

Comparison of $P_1$ (theoretical) and $P_{1m}$ (observed) can be made directly. However, one must bear in mind that the analysis determines average values over a cross section of the tunnel, while the pressure gage measures the pressure at one point on the floor and is sensitive to local effects. It should also be noted that fairly strong axial gradients existed near the chamber end of the tunnel; thus, small changes in axial position could yield somewhat larger changes in the pressure variation. During the time interval t = 50 to 100 msec, the agreement between $P_1$ and $P_{1m}$ was quite good, noting, of course, the oscillations caused by the bends in the tunnel. During the time interval t = 100 to 140 msec, the agreement was good in form; however, the observed pressure was somewhat greater (note the pressure decay during the latter portion of this interval). After a time t = 140 msec, there was complete disagreement between the observed and computed pressure variation. It is difficult to comment on the observed pressure record other than to say that the recording system apparently did not function properly. The analysis indicated that the flow was still inward into the chamber and the considerably higher pressure in the chamber would eventually be felt in the tunnel itself. The shock wave which moved from the chamber to the surface was definitely expected and was necessary if the inflow were to be stopped in a short period of time. In any event, the continuous decay in pressure (after t = 120 msec) at the gage position P1 could not be justified.

5.3.2 Structure Damage. In view of the instrumentation employed, it was clear from the outset that the only component of the UK 3.7 structure amenable to a structural response analysis was the roof slab of the main chamber. Inasmuch as the slab sustained only slight deflections, it did not provide a suitable basis for establishing the adequacy of existing damage prediction schemes.

## 5.4 CONCLUSIONS

The UK 3.7 underground structure and associated entranceway at ground range of 900 feet was indeed a device to change the exterior pressure wave into an attenuated wave with a lower peak value.

The interior pressure wave preserved the same type of precursor features as the exterior wave, but the peak pressure was reduced to approximately 60 percent of the exterior pressure. The interior rise time was longer than the free-stream rise time because of the choking effect of the entranceway.

The above-observed wave attenuation should lead to reduction in impulses and hence a reduction in translational and rotational damage for items to be stored underground.

The method of analysis must take into consideration the finite length of the entrance tunnel. This parameter was significant in delaying the interior pressure build-up. If loading information was desired in the tunnel or in the chamber near the entranceway, a non-steady analysis was essential; however, if the average pressure build-up in the chamber were desired, a reasonable estimate of the form and of the maximum pressure could be obtained by using the quasi-stationary analysis (Reference 5). The resulting pressure variation would then have to be translated time wise to account for the tunnel length. The bends in the entrance tunnel were apparently not important, inasmuch as they changed only locally, the flow (and pressure) in the channel.



CONFIDENTIAL

# Chapter 6

# BLAST LOADING ON INTERIOR OBSTACLES

The test involving two of the UK 3.5b structures was designed to obtain a confirmation of basic information on the loading in the interior of an empty hollow model and on a solid obstacle located inside the model. This represented the first full-scale attempt to verify existing shock tube data on the loading of interior obstacles. While the test was designed primarily to tie in with existing studies involving the AFSWP-Air Force and Armour Research Foundation 6-foot-diameter and 8-inch-square shock tubes (References 11 and 12), the test structure dimensions were such as to permit correlation with existing Princeton and Michigan shock-tube data, as well as with the Operation Greenhouse full-scale data on empty hollow models. However, new shock-tube data became available after the test (Reference 13), and these data were more suitable for direct comparison with the field data than the data in any of the first-cited sources. Thus, only the latter comparison was carried out.

This test represented a utilization of existing structures for objectives differing radically from those for which the original test was designed.

## 6.1 PROCEDURE

6.1.1 Test Structures. This test utilized the existing UK 3.5b structure at a ground range of 4,200 feet (Plumbbob designation: F-3.4-9024.01 and .02), which consisted of three identical cells originally designed as a supporting structure for a roof-panel test. These cells were of heavy, reinforced-concrete construction and measured approximately 27 feet long, 15 feet wide, and 8 feet high. They had symmetrically placed openings in the front and back walls amounting to approximately 18 percent of the nominal wall area. The roof panels were completely destroyed in the UK 3.5 test.

The two end cells, UK 3.5ba and 3.5bc, were modified in the following manner. A 6-inch, blast-resistant, reinforced-concrete roof slab was built atop both cells and a 2-foot cubical concrete block was rigidly mounted in the center of the floor of the UK 3.5c cell. No obstacle was placed in the other cell. The floors of both cells were leveled, and the surrounding frontal area was cleared. Preshot photographs of the cells are shown in Figures 6.1 and 6.2. The center cell of the structure was utilized by another agency for a roof-panel test.

6.1.2 Instrumentation. Three Wiancko electronic air pressure gages were located in the 2-foot block, one gage each in the center of the front, top, and rear surfaces. Two BRL self-recording pressure gages were mounted flush with the floor of the other cell, one at a point corresponding to the front edge of the block and one at the rear quarter of the cell. Gage locations are shown in Figure 6.3. Free-field blast measurements were determined by means of a BRL self-recording q gage adjacent to the UK 3.5b structure, as shown in Figure 6.3.

## 6.2 RESULTS

Records were obtained from the three electronic pressure gages on the block (Gages P1, P2, and P3, Figure 6.3), from the self-recording pressure gage in the center of the empty cell (P4), and from the self-recording q gage located outside the cells (P6). The remaining self-recording gage, located in the rear of the empty cell (P5), did not operate properly and recorded only a peak pressure. No explanation for the failure of this gage is available, but the recorded peak pressure of 9.2 psi is believed to be meaningful. The pressure-time records are shown in Figures 6.4, 6.5, and 6.6.

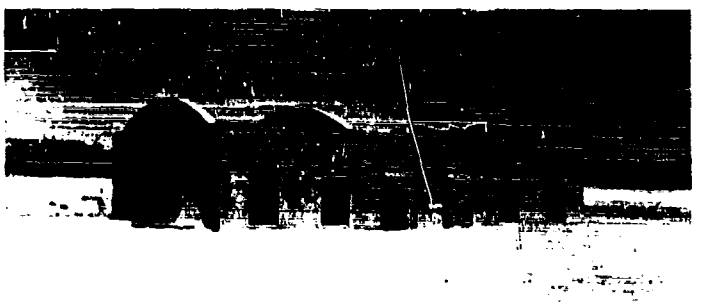

Figure 6.1 Pretest, UK 3.5b structure, front side view, facing northwest.

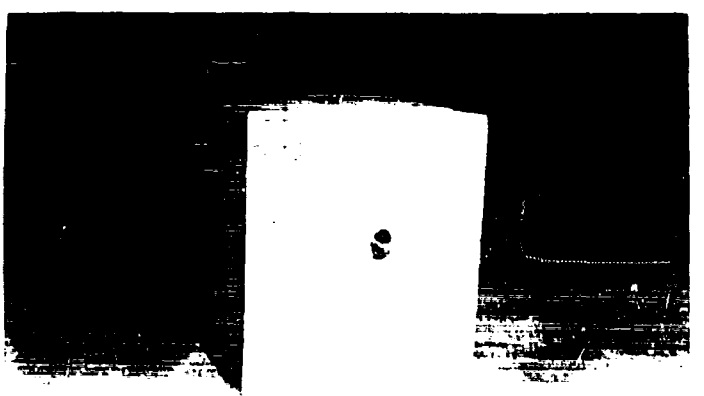

Figure 6.2 Pretest, UK 3.5bc cell, interior front view of 2-foot cubicle, facing west.

6.2.1 Free-Stream Overpressure. A smooth curve approximating the free-stream overpressure obtained from Gage P6 is superposed upon the reading of Gage P1 in Figure 6.4. It can be seen from this figure that the nature of the pressure decay and the positive phase duration indicated by Gages P1 and P6 differed considerably. Although a similar difference in wave decay and duration was observed by comparing the records of the other two electronic Gages P2 and P3 with the static pressure record of Gage P6, the record of Gage P4 located in the center of the floor of the empty cell did not disagree radically with that of Gage P6. The three electronic Gages P1, P2, and P3, mounted on the interior block, showed durations of roughly



CONFIDENTIAL

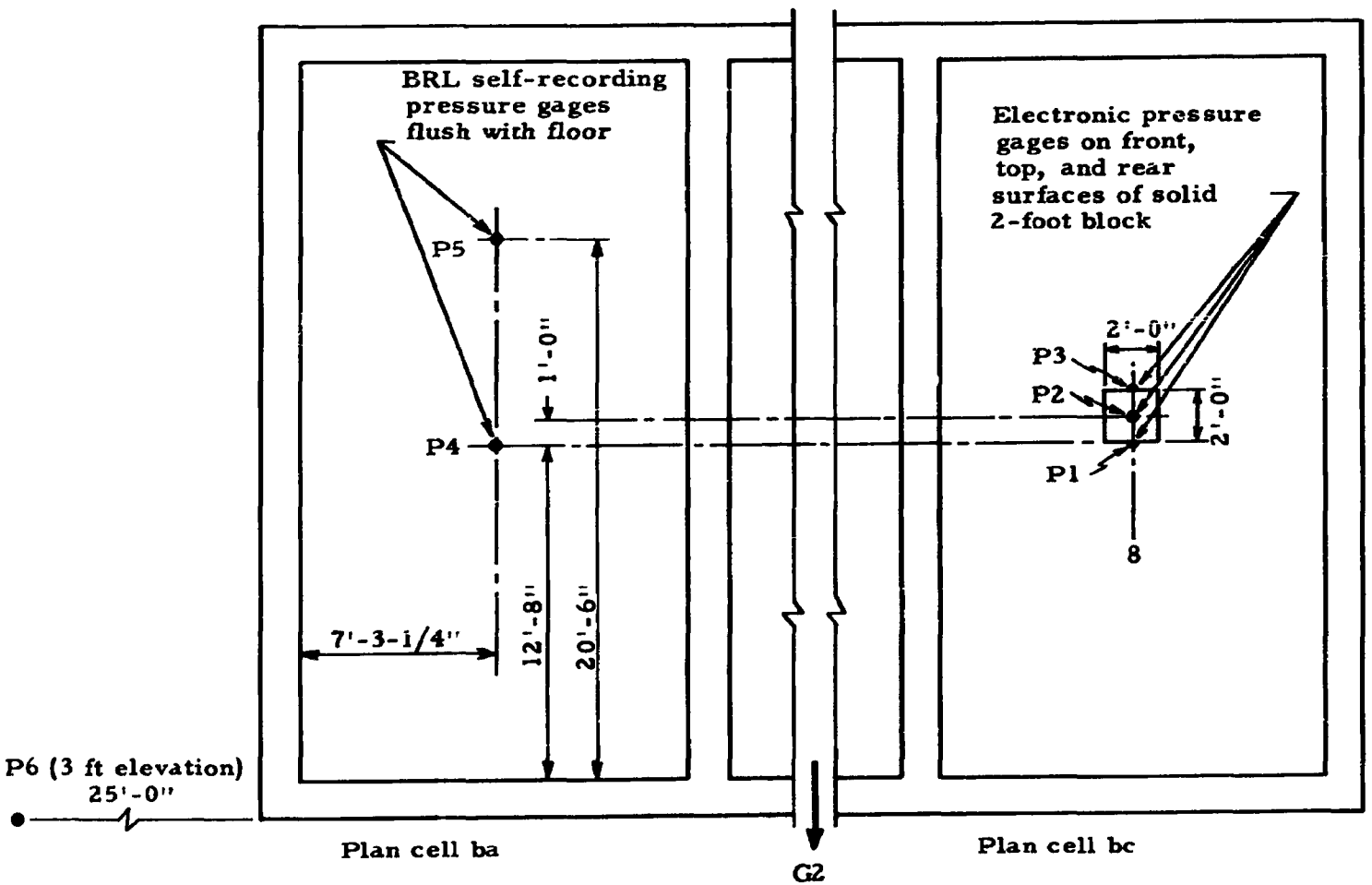


Figure 6.3 Location of pressure gages in UK 3.5ba and bc test cells.



CONFIDENTIAL

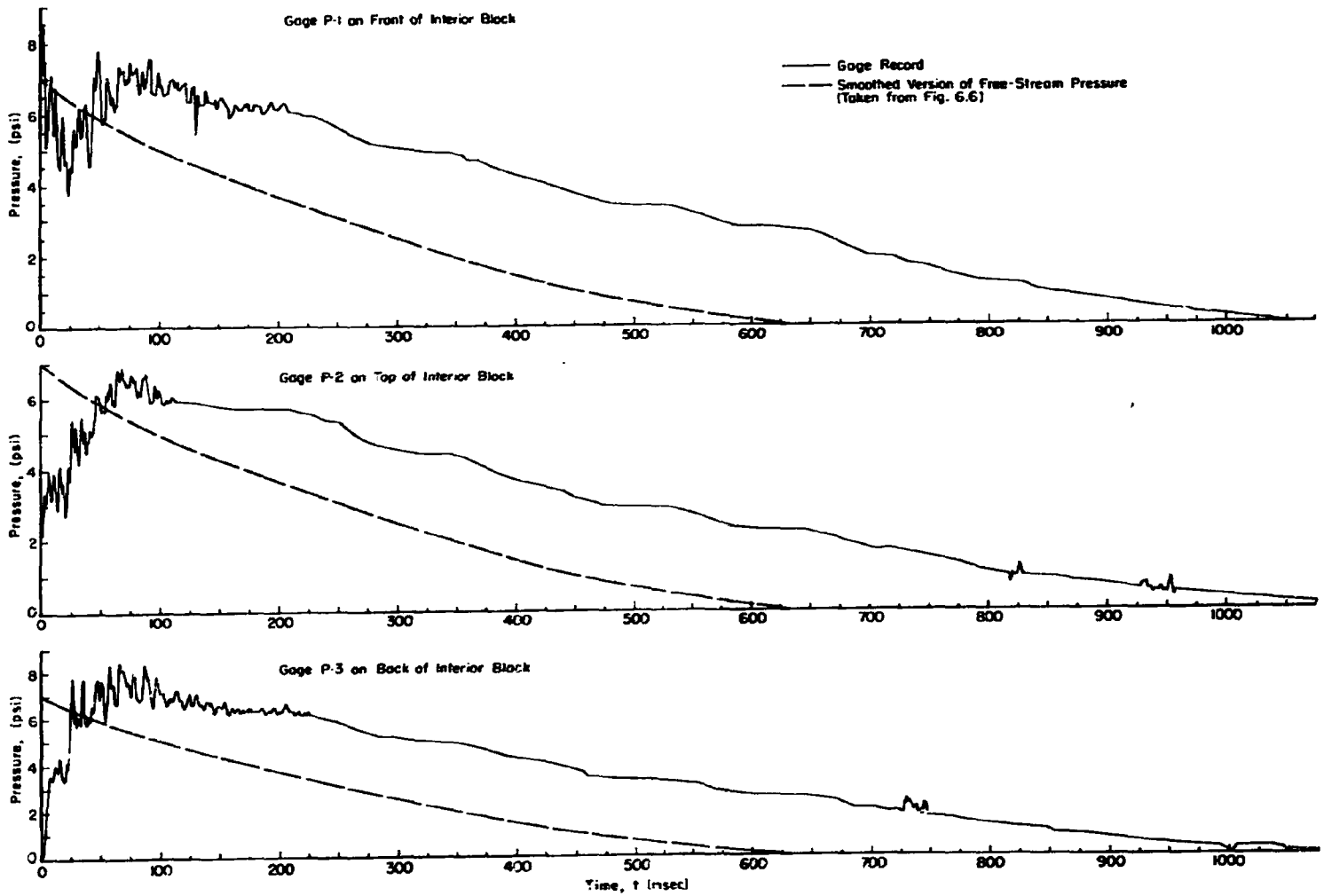


Figure 6.4 Pressure-time records of various gages.



CONFIDENTIAL

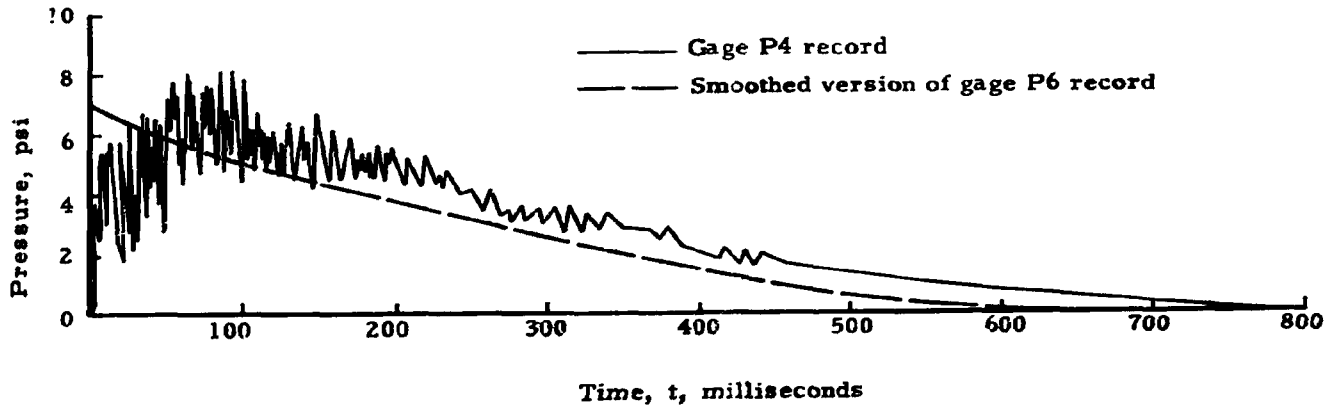


Figure 6.5 Pressure-time record of gage P4 at center of floor in empty cell.

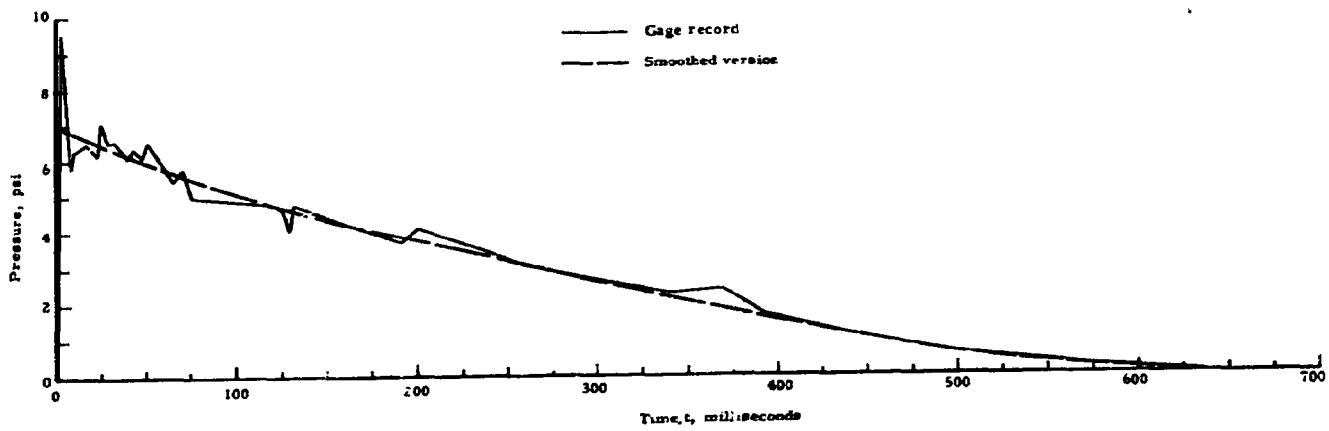


Figure 6.6 Free-stream static pressure record of gage P6.



CONFIDENTIAL

1,000 to 1,100 msec. This was considerably different from the durations of about 650 msec for Gage P6, 850 msec for Gage P4, and about 800 msec for the blast line and other free-stream monitors located at a ground range in the neighborhood of 4,200 feet.

It is immediately evident from Figure 6.4 that no reasonable analysis of the records from Gages P1, P2, and P3 could be carried out unless the wave shape and duration were either elongated for Gage P6 or compressed for Gages P1, P2, and P3, so that the durations become approximately equal. By making this type of equalizing modification of the durations and wave shapes, the records could be analyzed satisfactorily, at least for the first 100 to 200 msec of loading. Since the diffraction phase of the loading was completed by this time, one could conclude that the records supplied satisfactory diffraction information but were inadequate for the drag phase analysis.

The question as to whether the records should respectively be elongated or compressed was not readily answered. Gage P6 was a self-recording-type gage for which the time axis was usually less reliable than that of the electronic gages. On the other hand, while the records of the electronic gages agreed closely in duration, these three gages all recorded on the same tape, and therefore this agreement could easily have resulted from one malfunction of the instrumentation and the records should not be looked upon as independent measurements of the duration. If it were vitally important to this analysis that the duration be determined accurately, quite a dilemma would result. However, for the purpose of analyzing the diffraction phase, the choice of how to modify the durations can be made arbitrarily. In this analysis, it was decided to modify the free-stream durations (Gage P6) to about equal the durations of the electronic Gages P1, P2, and P3. This should in no way be construed as an inference that the durations shown by the blast-line gages were incorrect, since the choice was purely arbitrary.

6.2.2 Linearized Pressure-time Curves. Enlarged plots of the early phase of the loading as measured by Gages P1, P2, P3, and P4 are shown in Figure 6.7. Linearized approximations to each of these gage records and the modified smooth approximation to the outside overpressure are superposed.

6.2.3 Comparison with Shock-Tube Data. The data from this test were compared to shock-tube data from a $1/14$ scale model of the UK 3.5ba and 3.5bc cells; that is, a model with a height-width-length ratio of 8:15:27 and with an inside floor-to-ceiling height of 4 inches. The shock-tube model had 18 percent openings in both the front and back walls and was subjected to a blast wave having an initial overpressure of approximately 7.0 psi, with the wave shape and the ratio of wave-duration-to-model length roughly the same as those used in the field test. This model was tested with and without the interior block present on successive shots.

The shock-tube data were linearized in a form similar to that of Figures 6.6 and 6.7 for the field records. The linearized plots of the early phase of the loading on the field model are compared to those obtained from the shock-tube model in Figure 6.8. In these data comparisons the normalized dimensionless pressures obtained by dividing the values of critical pressures from Gages P1, P2, P3, and P4 by the modified overpressure value at the respective times of occurrence are plotted as ordinates against the abscissas in terms of a dimensionless time L/U, where L is the length of the model and U is the speed of propagation of the shock front.

## 6.3 DISCUSSION

6.3.1 Pressures in the Empty Cell. The pressure-time variation at the center of the floor in the empty cell (UK 3.5ba), shown in Figure 6.5, constituted the interior free-stream wave incident upon the 2-foot cubical located in the other cell (UK 3.5bc). The multiple reflections incident during the initial portion of the gage record probably resulted from the interaction of the shock with beams and pilasters within the test structure. The presence of the initial wave, the reflected wave from the back wall, and the re-reflected wave from the front wall can be observed in Figure 6.7.



CONFIDENTIAL

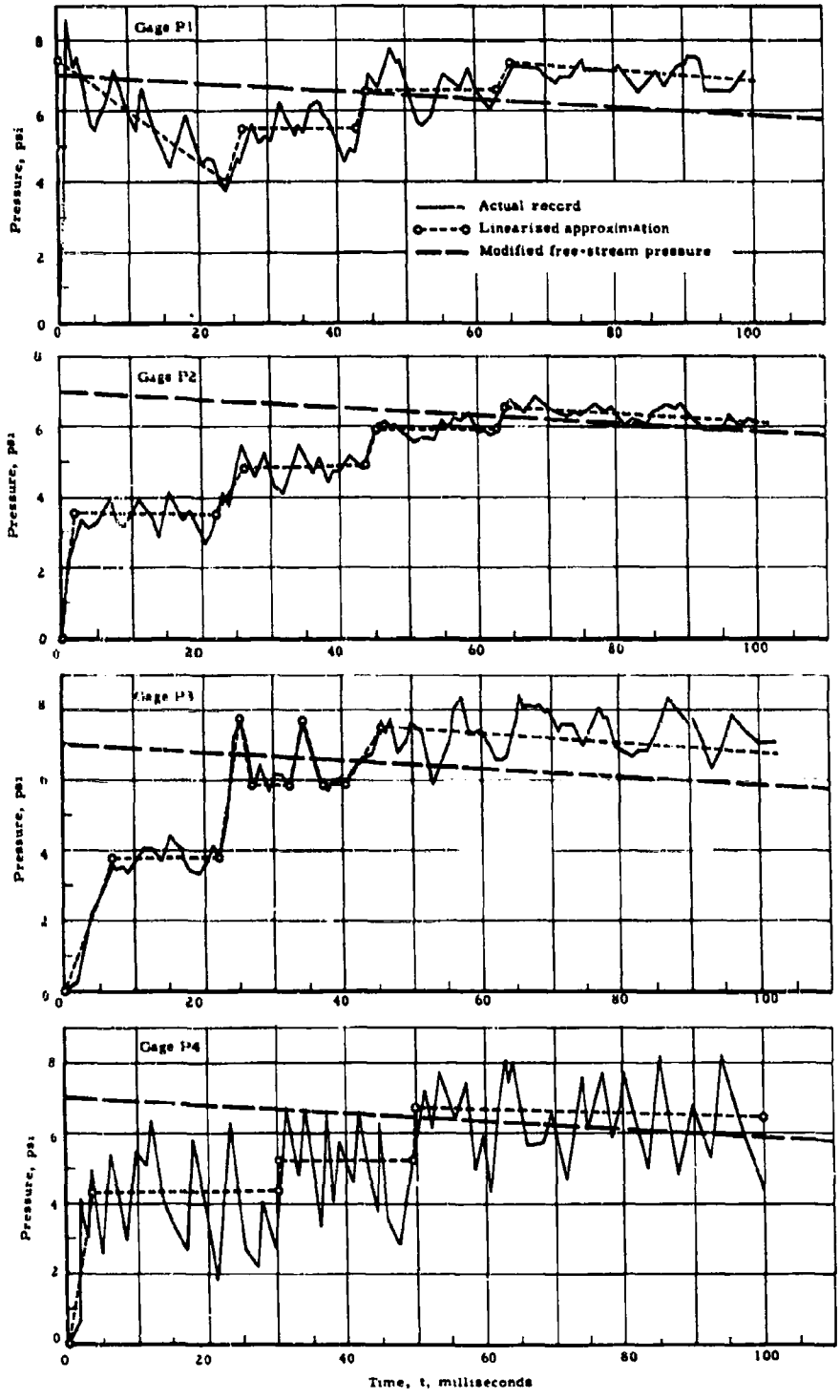


Figure 6.7 Diffraction phase pressure-time records of various gages.



CONFIDENTIAL

Figure 6.8 shows the comparison of linearized shock-tube and field results of the normalized pressure-time variation at the center of the floor of the empty cell. The initial inside pressure (unless otherwise stated, inside pressures refer to the plateau values of the linearized traces; initial inside pressure refers to the first plateau) was of about the same magnitude for the field and shock tube, i.e., about 0.6 and 0.5 psi of side-on pressure, respectively. The shock tube pressure decreased to about 0.32 of outside free-stream overpressure, before rising to the second plateau at t = 1.5 L/U. At later times, the shock-tube and field-data inside pressure ratios were in good agreement. The shock-tube pressure ratio was slightly less than that of Gage P4 in the field structure until the rise to maximum pressure occurred, after which the shock-tube pressure became slightly higher than that in the field structure.

The peak pressure of 9.2 psi reported for Gage P5 (not shown) seems reasonable since the pressure should increase as the measuring-gage position approaches the back wall because of the earlier arrival of the reflected wave. It should be noted that while a peak pressure of about 8.0 psi is indicated for Gage P4 in Figure 6.7, the average maximum pressure in the same time interval is only about 6.7 psi. Thus, the average maximum pressure at Gage P5 would probably be less than the peak of 9.2 psi.

Two quantities which are of interest in an interior loading study of this type are the initial and maximum inside pressure ratios. While the overall pressure-time build-up inside the hollow model is rather complex, a simple graphical relationship between these quantities and the percent of wall openings has been established (Reference 14). The results of a rather detailed shock-tube study indicate that both these quantities are, for all practical purposes, independent of initial outside overpressure in the range of zero to 30 psi. A plot of these two quantities versus percent of wall openings is shown in Figure 6.9. The curves deal with the pressure at the center of the floor in a structure similar to the 3.5ba cell. Also in Figure 6.9, the results obtained from the field test are compared to those of shock-tube tests on a model with equal openings in front and back walls. (Figure 6.8 also shows a comparison with shock-tube data from a model having a height-width-length ratio of 2:3:6 and 30 percent openings in the front and back walls (Reference 14).) The curves are drawn through known end points where the values of the abscissa are equal to zero and 100 percent. Although the shape of the curve for maximum pressure ratio is speculative for openings greater than about 40 percent, it is believed that the initial pressure-ratio curve is reliable for the full range of zero to 100 percent openings.

6.3.2 Pressures on the Interior Block. The linearized diffraction-loading phenomena on the three surfaces of the 2-foot cubical block are more complex than the loading phenomena on the floor. However, the trends in the loading on the block are still recognizable in terms of the loading on the floor. The change in pressure at the time t = 0, 1, 2, and 3 L/U time units (with zero time taken as the time when the shock first reaches the block) are observable in each case. The normalized pressure-time records for the top of the block in the shock-tube and field models compare well (Figure 6.8). The agreement of pressures between field and shock-tube measurements on the front and back of the block are not as good, especially prior to the time t = L/U, i.e., before the reflected wave returning from the back wall reaches the block. This disagreement is probably caused by differences which exist in the inside waves incident upon the center of the floor where the block is located (Figure 6.8). The shock-tube records for the front and back of the block are believed to be more reliable than the field records. The shape of the loading curves for the front and back of the block, as well as the magnitudes of pressure and time, obtained in the shock-tube tests were reproduced in repeated shots under similar conditions.

## 6.4 CONCLUSIONS

Field-test loadings on obstacles located in a hollow model and exposed to clean Mach-wave shapes can be satisfactorily predicted from shock-tube experiments.

For the particular geometry studied, three individual shocks affect the pressure build-up to interior pseudo-steady state on the block and in the hollow model: the interior incidence



CONFIDENTIAL

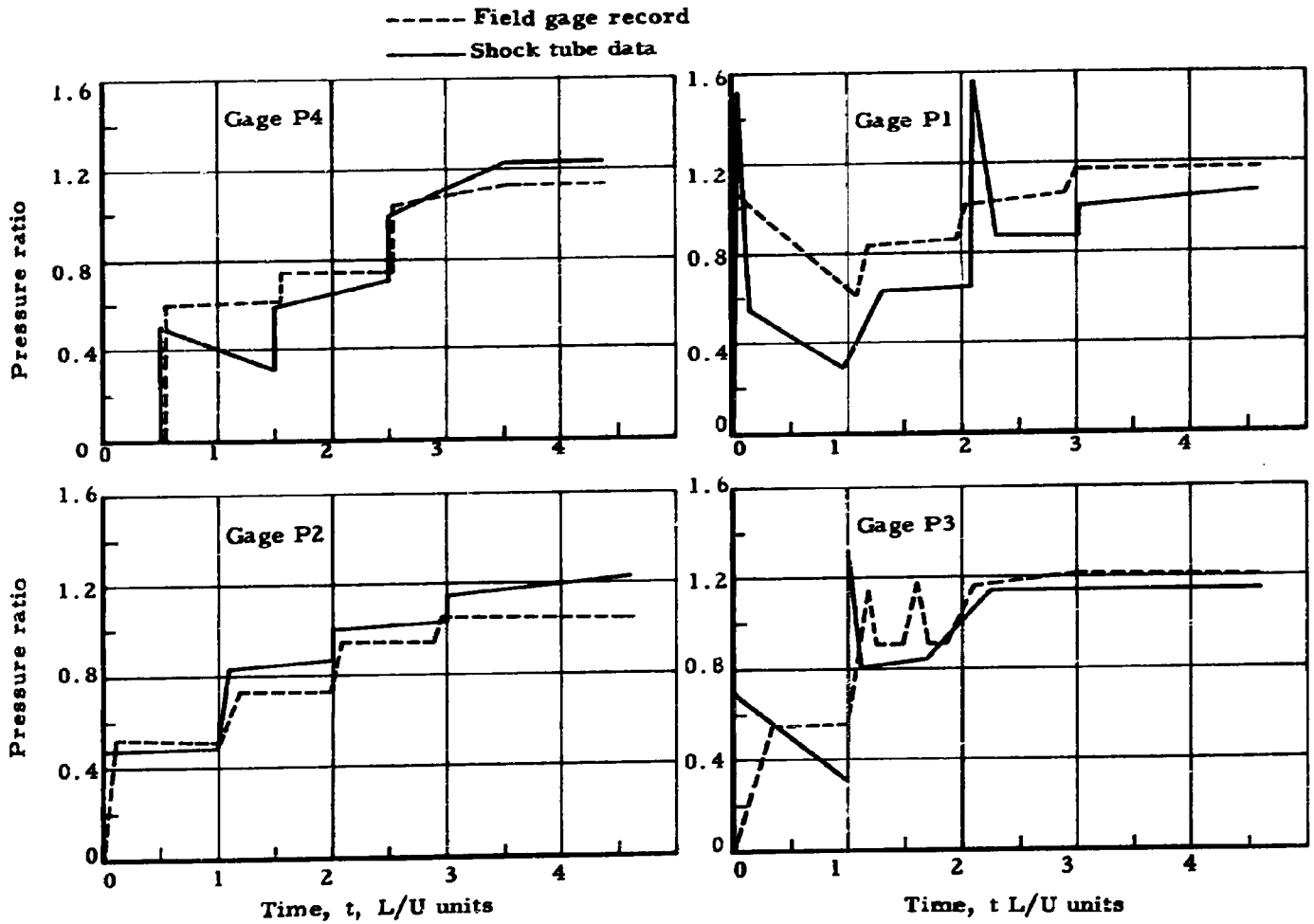


Figure 6.8 Comparison of linearized pressure-time data at various gage locations.



CONFIDENTIAL

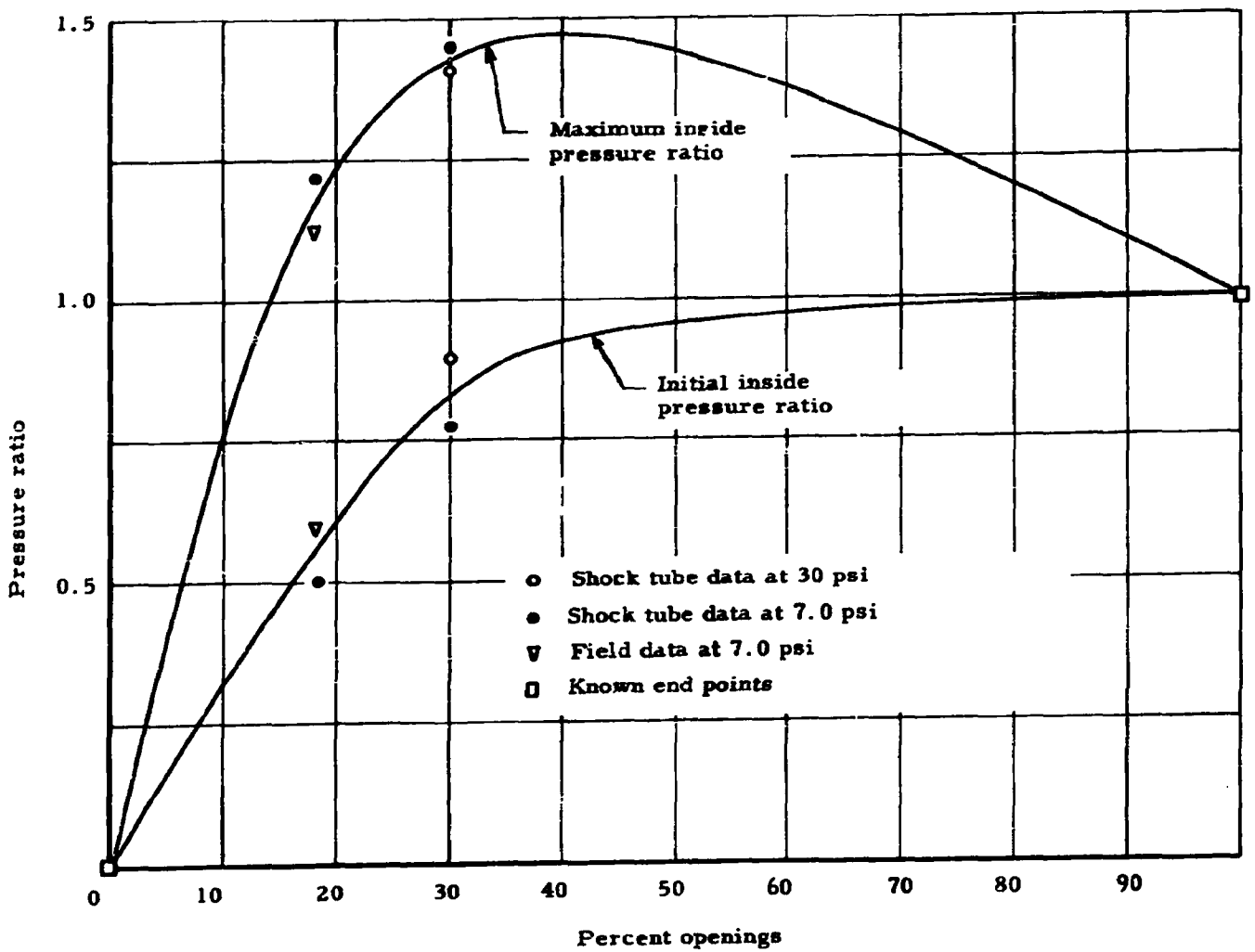


Figure 6.9 Inside initial and maximum pressure ratios versus percent openings.



CONFIDENTIAL

shock, its reflection from the back wall, and its re-reflection from the front wall. The interior pseudo-steady state phase begins roughly after the shock has traversed the length of the test cell three times.

Interior maximum pressures in the cells were up to 20 percent higher than the exterior free-stream pressure for the case of equal openings of 18 percent in the front and back walls with no openings in the sides or roof. However, the maximum pressure could be much higher than this value for other combinations of openings. It is expected that the maximum pressure will not exceed 1.5 times the outside side-on pressure for the case of equal openings in the front and back surfaces, all other surfaces being completely closed.



CONFIDENTIAL

# Chapter 7

# BLAST LOADING BEHIND FAILING WALLS

Existing methods for predicting blast loading on buildings with nearly solid walls (and roofs) are limited to the two extreme conditions where either the walls do not fail, or they fail so early in the loading period that their presence can be neglected from the outset. But just how early is so early is currently a moot question. As part of the UK 3.5 test on wall- and roof-panel response (Reference 15) a pressure gage had been located behind an unreinforced brick masonry panel that failed. While this panel would normally be assumed to fail almost immediately and not appreciably affect the entering blast wave, the pressure record showed the entering wave to be a compression wave with a relatively long rise time. Unfortunately, insufficient quantitative information could be obtained from the one record to justify any change in existing load-prediction methods, even though it was clear that the loading situation was not as simple as imagined. Recently, shock-tube tests have been completed in which the pressure wave behind failing plastic sheets was determined under a variety of conditions (Reference 16). While these results generally conformed to the field data, the obvious limitations of structural scaling require additional full-scale testing in support of a model approach to the problem.

It is believed that the determination of the effect on blast loading because of failing wall (and roof) cover represents one of the more important unsolved problems in the weapon effect field. The present test was felt to be a significant step, but only a step, toward solving this problem.

It should be noted that this test represented another instance in which an existing structure was conveniently adapted for other than its original test design purpose.

## 7.1 PROCEDURE

7.1.1 Test Structures. The test utilized two of the existing UK 3.29c test cells (UK 3.29c-1 and c-15 at a ground range of 4,200 feet, Plumbbob designation: F-3.4-9023.01 and .02, respectively), which were originally designed as supporting structures for a wall-panel test (Reference 17). The cells measured approximately 16 feet long, 16 feet wide, and 10 feet high. The front walls of both cells were destroyed, whereas the rear walls had remained intact during Operation Teapot.

The two cells were modified in the following manner. A wall panel of corrugated asbestos siding (transite) and a panel of 8-inch cinder block were built into the front of Cells c-1 and c-15, respectively. The walls were of conventional construction, and it was intended that they fail under the incident blast loading. The rear wall of each cell was to remain intact, however. The two types of front-wall panels were chosen so as to offer some variation in break time, mechanism of failure, and size and type of debris. Preshot photographs of the walls are shown in Figures 7.1 and 7.2.

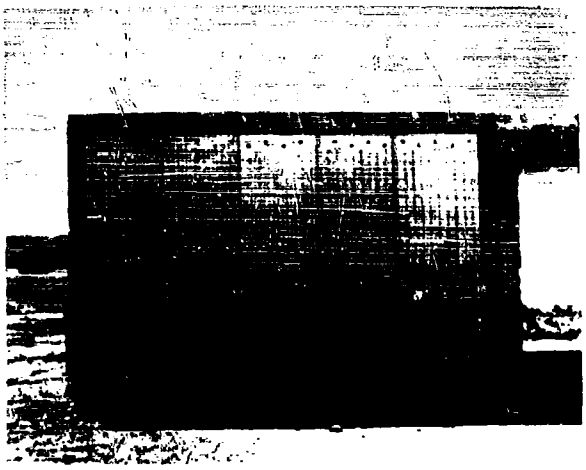

Figure 7.1 Pretest, UK 3.29 c-1, front view of transite wall, facing west.

Figure 7.2 Pretest, UK 3.29 c-15, front view of cinder-block wall, facing west.

Figure 7.3 Pretest, UK 3.29 c, typical installation of pressure gage.



CONFIDENTIAL

7.1.2 Instrumentation. One BRL self-recording gage (air pressure versus time) was installed 18 inches above the floor level, approximately in the center of each cell (Figure 7.3). Free-field blast measurements were obtained from a BRL self-recording q gage installed near the UK 3.5b structure (Figure 1.1).

## 7.2 RESULTS

The test panels were subjected to an incident shock of 7 psi overpressure. As had been expected, both panels failed. The 12-inch brick wall in the rear of Cell c-1 also failed, but not as had been expected (Figure 7.4). The 8-inch reinforced brick wall in the rear of Cell c-15 remained intact, but was displaced outward several inches (Figure 7.5).

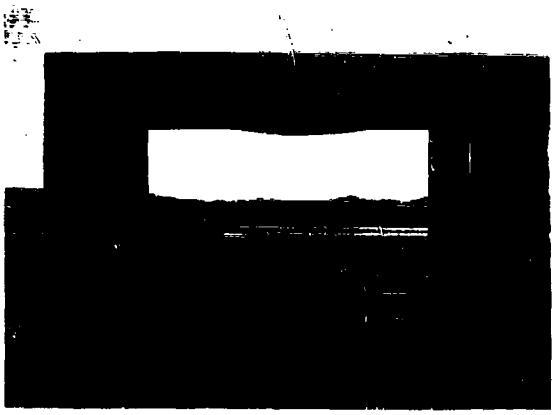

Figure 7.4 Posttest, UK 3.29 c-1, front view of test cell, facing west.

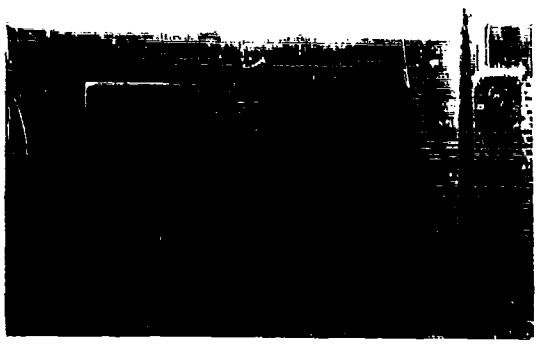

Figure 7.5 Posttest, UK 3.29 c-15, front view of test cell, facing west.

The pressure gage behind the cinder block panel provided a good record for the first 200 msec and then failed (Figure 7.6); fortunately, this covered the complete time range of interest. The gage behind the corrugated asbestos panel recorded a shock of 7 psi peak overpressure, being essentially zero rise time, and then failed immediately after responding to the reflected shock transmitted from the rear wall. The peak pressure recorded at this time was 14 psi. This brief record was not reduced in final form and is not shown.

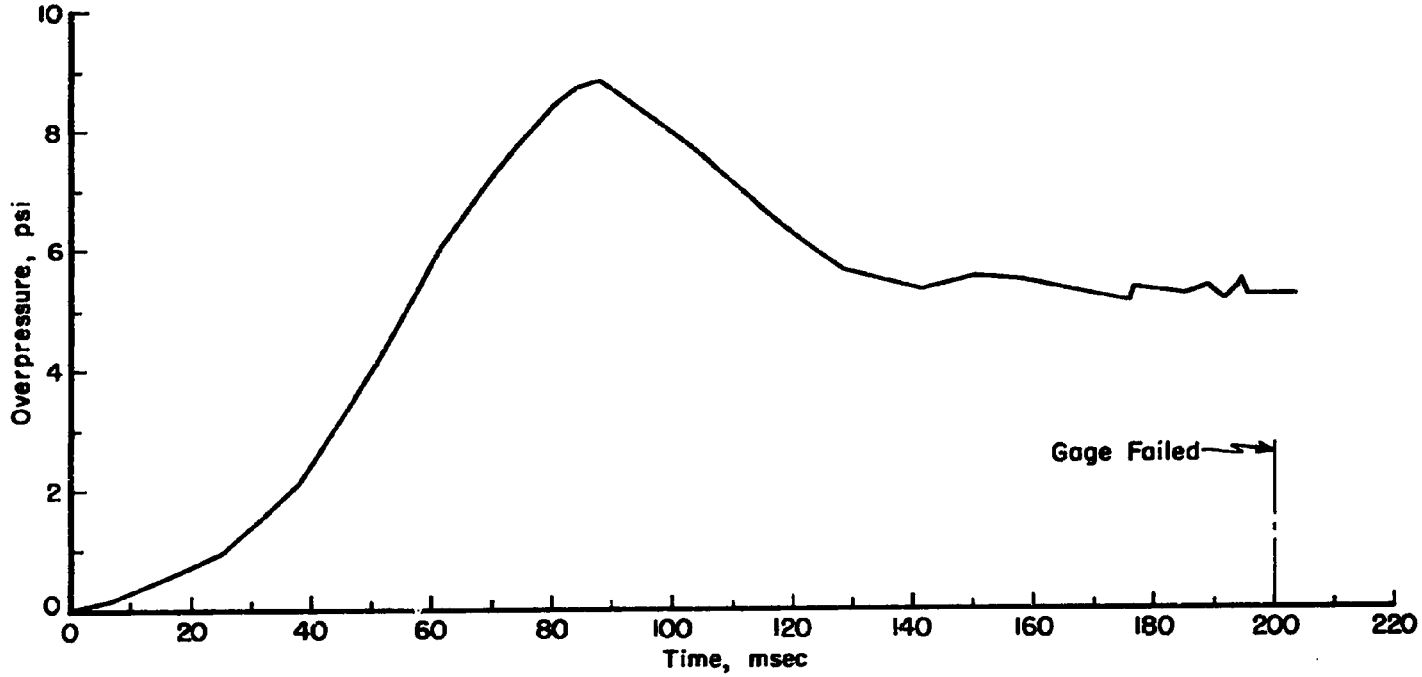


**Figure 7.6 Overpressure versus time variation behind cinder block panel.**



CONFIDENTIAL

The free-stream-pressure wave at the 4,200-foot location of the UK 3.29 structure was obtained from the self-recording q gage located at 3-foot elevation adjacent to the nearby UK 3.5b structure. The pressure record obtained from this gage is shown in Figure 6.6.

## 7.3 DISCUSSION

7.3.1 Pressure Records. Consideration of the pressure data alone served to point up the influence of frangible wall covering on the form of the entering blast wave. The free-field-pressure record shown in Figure 6.6 indicated a clean Mach wave of 7 psi overpressure and 0.63 second duration. The brief record obtained from the gage behind the corrugated asbestos panel indicated a wave with essentially zero rise time and a peak pressure corresponding to the incident exterior wave. The panel failed almost immediately and, insofar as its effect on the interior wave form was concerned, it might as well have been absent entirely. (Actual break times for the test panels may be inferred from the data of Reference 15. For transite, this time appears to be less than about 20 msec, and less than about 30 msec for the cinder block wall.) Thus the rear 12-inch brick wall failed under an incident shock of approximately 7 psi overpressure. However, prior to collapse, the wall was capable of reflecting a shock wave of 14.0 psi overpressure. The failure of this wall, therefore, did not compromise the results of the test. The pressure gage failed at this time, possibly because of being struck by wall debris. Had the rear panel not failed, the reflected pressure from the rear wall would have led to a series of oscillations between reflected and zero overpressure.

The pressure record behind the failing cinder block wall, Figure 7.6, tells quite another story. While the cinder block was structurally a brittle or frangible material, its presence, even in failure, significantly affected the incoming shock. Figure 7.6 shows an interior wave that was evidently a compression wave having a rise time of 93 msec, and a total peak overpressure of 8.9 psi. This peak value already includes the effect of both the incident and reflected waves.

7.3.2 Correlation with Shock Tube Tests. Reference 16 deals with shock-tube tests in which pressures were determined behind frangible plastic sheets. Interior initial maximum overpressure, rise time to this initial maximum, and panel failure time were determined as functions of the incident blast and of structural parameters. The maximum pressures measured in the model tests occurred before interference because of reflections from the rear of the structure reached the gages. Hence, the shock tube results were dependent on the panel characteristics only, and not on the interior geometry of the test cell.

The field test panels had an aspect ratio of 0.625 (height-to-width). This was directly comparable to the 0.6 aspect ratio of the model test panels. The plastic panels exhibited a membrane-type resistance to static loads. This was not too dissimilar to the behavior of the corrugated-asbestos panel, but differed radically from the arch-type resistance of the cinder-block panel (References 15 and 18). However, the model results were presented in such form as to be applicable to many types of resistance functions, at least where rough predictions were desired.

The following analysis concerned only the cinder-block panel inasmuch as the corrugated-asbestos panel represented a situation well beyond the range of the model tests. However, extrapolation of the model data in this instance supported the field-test results in that no distortion of the incident pressure wave was indicated.

According to the theory presented in Reference 18, the resistance of the cinder-block panel to transverse loads was generated by arch-like thrust forces developed at mid-span and at the panel supports. This led to a resistance function (i.e., load-displacement relation) that increased nearly linearly from zero to a maximum value and then decreased to zero. The resistance function for the test cinder-block panel was determined according to the methods of Reference 18 as shown in Figure 7.7.

The shock-tube test data was normalized in terms of a characteristic pressure, $p_f$, and characteristic time, T′, which are given by

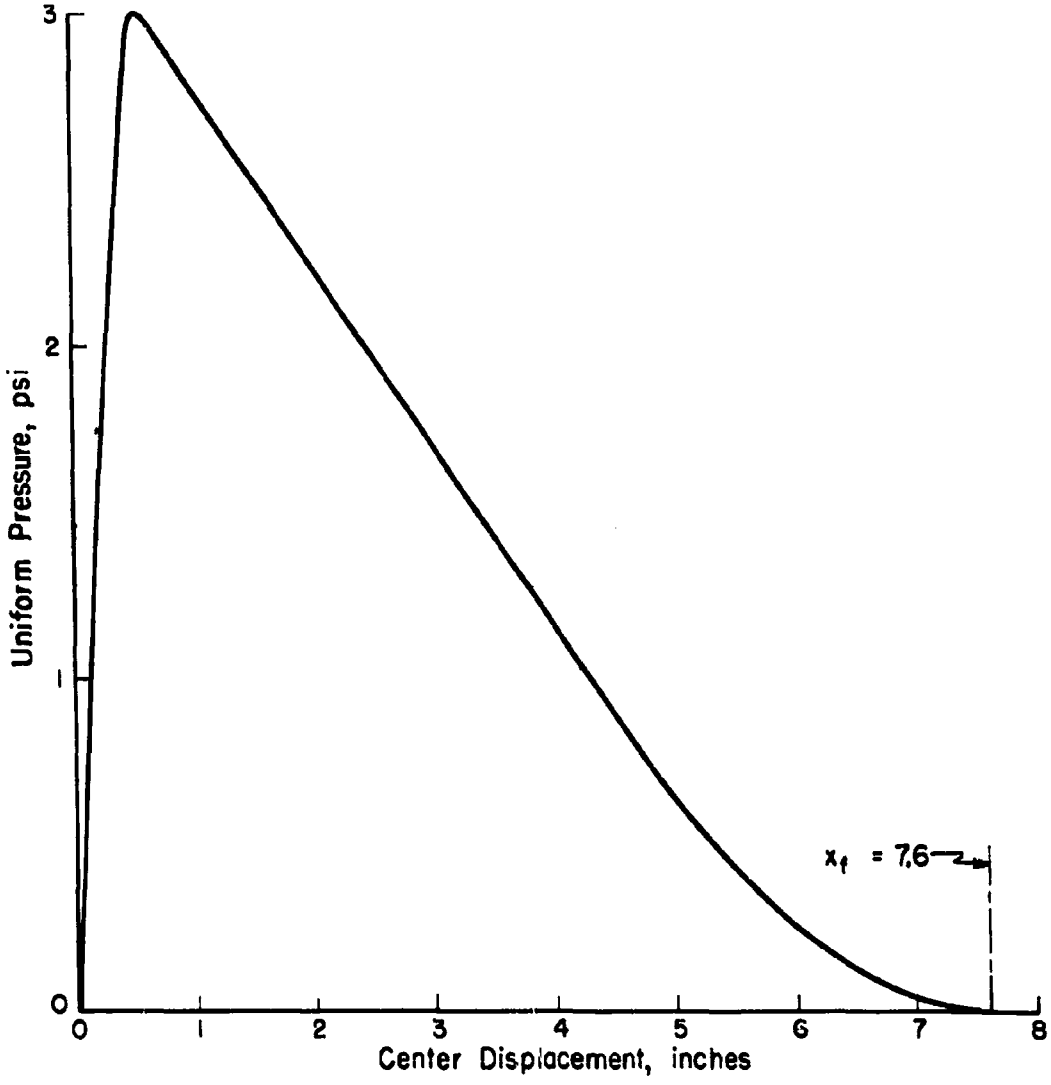


Figure 7.7 Predicted static resistance function for cinder block panel.



CONFIDENTIAL

$$p_f = \frac{2}{t_d} \sqrt{2\, p_{av}\, M\, x_f}$$

$$T' = \sqrt{\frac{2\, M\, x_f}{p_{av}}}$$

where: $t_d$ = diffraction phase clearing time for panel
$M$ = equivalent mass per unit area of panel
$x_f$ = failure center displacement of panel (displacement corresponding to zero resistance
$p_{av}$ = average resistance of panel (average ordinate of load-deflection curve to failure)

The pertinent panel material properties, blast parameters, and normalizing quantities are listed below:

Crushing strain, $e_c = 0.001$
Crushing stress, $s_c = 500$ psi
Mass per unit area, $\rho = 5.66 \times 10^{-4}$ lb-sec$^2$/in.$^3$
Failure center deflection, $x_f = 7.6$ in.
Average resistance, $p_{av} = 1.3$ psi
Equivalent mass, $M = 0.56\,\rho = 3.17 \times 10^{-4}$ lb-sec$^2$/in.$^3$ (Reference 15, Figure 14)
Diffraction clearing time, $t_d = 24$ msec
Characteristic pressure, $p_f = 6.6$ psi
Characteristic time, $T' = 61$ msec

From Reference 16, the predicted maximum interior overpressure corresponding to the field conditions, $p_i$, and the rise time (for the condition of no reflection from the rear wall), $t_r$, were found to be.
$p_i = 5.5$ psi
$t_r = 122$ msec

Now, under the field-test conditions, the time of travel of a pressure signal from the pressure gage to the rear wall and back to the gage was about 29 msec, or about one quarter of the predicted rise time with no rear wall reflection. Thus, the shock-tube tests would predict that reflected signals from the rear wall must reach the gage before the interior pressure builds up to a maximum. This is in accordance with the field data, and the maximum pressure shown in Figure 7.6 was evidently the result of an involved interaction of reflected pressure pulses with the incident pressure wave as modified by the failing cinder-block panel.

Although it was thus not possible to compare the measured maximum pressure and rise time with the shock tube results, a less direct comparison could be made. The pressure records obtained during the shock-tube tests showed the initial pressure build-up to be essentially linear for the condition of no reflection from the rear wall. Thus, the ratio of the predicted quantities, $p_i/t_r$, should be comparable to the initial slope of the pressure record shown in Figure 7.6. The predicted initial slope is

$$p_i/t_r = 4.5 \text{ psi}/100 \text{ msec.}$$

This value compares most favorably with the initial slope of 4.0 psi/100 msec obtained from Figure 7.6.

The above analysis demonstrates an application of shock-tube scale-model data to field predictions in a situation in which the load phenomena are significantly influenced by the response of a structure. Specifically, the analysis indicates that the scale-model results correctly predict a compression wave in the interior of the field test cell, and that maximum pressure will not be reached prior to interference from reflections of compression waves within the structure. Furthermore, the laboratory data predict an initial rate of pressure build-up within 13 percent of that recorded in the field test. This, of course, is not meant as



CONFIDENTIAL

a necessarily realistic estimate of accuracy, in view of general uncertainty regarding the arching theory of panel resistance as well as the numerical values of material properties assumed for the panel.

The quantitative prediction of maximum overpressures in a cavity, such as formed when the front wall fails under conditions where interior reflections occur within the rise time of the incoming compression wave, hinges on a rather elaborate analysis of the wave reflections in the cavity. For a flat-topped shock wave entering the cavity, a series of oscillations between reflected and zero overpressure is predicted and has been observed experimentally; these oscillations have a period of roughly 4L/U, where L is the length of the cavity and U is the speed of shock propagation. For an essentially flat-topped compression wave, the reflection coefficients are virtually the same as for shock waves for overpressures less than 100 psi. A compression wave becomes steeper upon reflection from an infinite wall (Reference 19), and reflection from the closed end of a cavity is identical to reflection from an infinite wall until the reflected wave reaches the open end of the cavity. Even without reflection at a rigid boundary, a compression wave steepens into a shock wave in a finite time, since pressure signals in the interior of the wave are transmitted at higher velocities than are those at the wave front. Hence, where reflections in an open cavity interfere with the incoming pressure build-up, one would expect pressures at any station within the cavity to rise at an increasing rate during the first transit of a reflected pulse from the closed end. This behavior is evidenced in the pressure record of Figure 7.6.

In summary, it may be said that the field-test results provided a reasonable confirmation of the small-scale laboratory data, exhibiting certain characteristics which can be predicted from the small-scale data. In cases where panel failure occurs so early that fragments can be expected to clear before the first reflection of the interior compression wave from the rear wall reaches the newly-open end, it can be assumed that the effect of the frangible panel is solely to deform the incident shock wave into a compression wave. The remainder of the problem is thus the study of a compression wave entering an open cavity. For the corrugated-asbestos panel, it may be supposed that whatever effect the panel has on the entering wave is lost by the time the wave reaches the pressure gage in the center of the cell.

## 7.4 CONCLUSIONS

Corrugated-asbestos (transite) covering that fails under blast loading does not essentially alter the characteristics of the incoming shock.

Cinder-block covering that fails under blast loading markedly influences the characteristics of the incoming shock. For the geometry tested, the exterior shock is converted to a compression wave having a rise time of about 93 msec. A similar behavior was noted in the case of brick walls tested in Project 3.5 of Operation Upshot-Knothole. It may be inferred that a rather wide class of masonry materials utilized in conventional construction (e.g., brick, clay tile, etc.) have a similar effect on interior loading.

Comparison of interior wave shapes and initial rate of pressure build-up with the results of model shock-tube tests on frangible plastic materials indicate the latter to be a feasible method of experimentation, at least with respect to determining the qualitative behavior of blast loading behind failing walls.

## 7.5 RECOMMENDATIONS

Consideration should be given to further shock-tube experimentation utilizing frangible materials which more closely model the resistance properties of masonry materials.

If additional field testing seems desirable, other existing UK 3.29 and UK 3.5 test cells can be utilized for both wall- and roof-panel tests.

Consideration should be given to finding a means of suitably modifying existing blast load prediction schemes for structures containing masonry-curtain walls which are expected to fail under loading.

## Chapter 8

# RESISTANCE OF CONCRETE TO THERMAL RADIATION

Considerable information exists on the structural resistance of concrete structures to the forces resulting from atomic blasts. Designs for protected construction generally utilize conventional working stresses for concrete construction and do not take into account possible deterioration or loss of strength of the material because of heat or other damaging features of nuclear devices.

Little is known about the resistance of structural concretes to high-intensity, short-duration, thermal radiation. Ordinarily, thin coatings that can be applied to concrete have little or no beneficial effect on the resistance of concrete to very high temperatures. A successful coating for this purpose, in addition to being reflective, should be highly refractory, thermal-shock resistant, and insulative. For maximum resistance, it is likely that special concretes containing refractory cement and aggregates must be utilized.

One process, flame ceramics, is a technique for spraying various oxides through the flame of a metallizing gun. Coatings can be sprayed on a great number of materials, including concrete, in thickness up to about 0.02 inch. For example, coatings of alumina can be applied in this manner. Alumina is reflective and will withstand temperatures up to about 3,100F.

Another technique, slurry ceramics, consists of painting a slurry of certain ceramic oxides onto the surface to be coated. Some measure of bond is achieved merely by drying; however, a more tenacious bond results from heating the surface to about 600F. A typical slurry-ceramic coating is stabilized zirconia. This material also will withstand about 3,100F, is reflective and somewhat insulative.

A number of proprietary concrete-curing agents are commercially available. Some of these are reflective and are intended to avoid overheating of the concrete from the sun. Although the composition of these materials and their possible beneficial effect for this application were not known, it was felt that one of these materials should be tested.

It seemed likely that the best resistance to thermal radiation would be obtained from concretes specifically designed for that purpose. For many years, calcium-aluminate-hydraulic cements have been recognized as refractories for low-temperature and medium-temperature applications. A low-purity, calcium-aluminate cement, containing about 20 percent of iron oxides and silica, is manufactured in this country under the trade-name Lumnite. (Made by Universal Atlas Cement Company, Buffington, Indiana.) This product, mixed with suitable refractory aggregrates, can be utilized as a refractory for temperatures up to about 2,700F.

Within the past year, the Aluminum Company of America has introduced a high-purity, calcium-aluminate cement having certain enhanced properties. This cement, when mixed with suitable aggregate, is refractive to temperatures in excess of 3,200F for extended periods. Information on its resistance to higher temperatures for short durations is not available. The thermal-shock resistance of this material is reported to be excellent.

Special aggregates must be used in refractory concrete. Various fire clay, dense, or lightweight grogs can be used for low- or medium-temperature applications. The Aluminum Company of America recommends the use of tabular alumina aggregates with calcium aluminate cements. Other aggregates which seemed worthy of testing because of their resistance to high temperatures and thermal shock were calcined kyanite, topaz, silicon carbide, and high-temperature firebrick.

## 8.1 PROCEDURE

8.1.1 Test Items. Twelve types of special coatings and refractories were tested. These were prepared in the form of 12- by 12- by 2-inch precast panels as follows:

1. Portland-cement concrete, untreated.
2. Flame-sprayed alumina on portland-cement concrete.
3. Flame-sprayed mullite on portland-cement concrete.
4. Slurry ceramic stabilized zirconia on portland-cement concrete.
5. Reflective curing agent on portland-cement concrete.
6. Portland-cement concrete with expanded shale aggregate.
7. Lumnite cement, topaz admixture, firebrick aggregate.
8. Alcoa calcium aluminate cement, kyanite aggregate.
9. Alcoa cement, topaz admixture, firebrick aggregate.
10. Alcoa cement, tabular alumina aggregate.
11. Alcoa cement, silicon carbide aggregate.
12. Alcoa cement, tabular alumina aggregate, flame-sprayed alumina coating.

The 12 types of test panels were exposed at each of three ground-range locations: 60 feet (F-3.4-9059.01), 300 feet (F-3.4-9059.02) and 800 feet (F-3.4-9059.03), as shown in Figure 1.1. Two groups of panels were positioned at the 300-foot location. One set of panels was covered with water the evening prior to the test so that there would be a water film present at shot time to simulate a wash-down system; the other three groups were tested in an air-dry condition.

The panels were cast into a concrete pad 4- by 5- by 1-foot deep and set flush with the ground surface. At the 300-foot location the two pads were poured together, one being depressed about 1 inch. This set of panels was covered with water. Figures 8.1 and 8.3 are preshot photographs of two of the test panels in place. The panels are numbered in these figures in accordance with the above listing.

8.1.2 Instrumentation. No recording instrumentation of any type was utilized. It was believed that careful visual examination and such techniques as tapping with a hammer and picking with a knife by an experienced concrete engineer would provide a sufficiently accurate estimation of the relative merit of each of the test materials at the various locations.

In addition pretest and posttest readings were taken of all test panels with a portable concrete-testing device. (Concrete Test Hammer—Model II, supplied by Soiltest, Incorporated, Chicago, Illinois.)

## 8.2 RESULTS

The panels were first observed 6 days after the test. All panels were covered with soil, those at the 60-foot ground range were buried under nearly 4 inches of soil. For the purpose of the posttest photographs (Figures 8.2, 8.4, and 8.5), the panels were cleaned and watered.

Panels 2, 3 and 4 showed a deterioration of the special coatings. The degree of deterioration was somewhat less severe with increasing distance from ground zero. Several of the other panels showed slight scaling around the edges, but otherwise there was no discernible damage to any of the panels. The restraining concrete pad and grout fill between the test panels showed no indication of damage.

At the 300-foot location, the appearance of the watered panels was no different than that of the dry panels. A series of wet runs was performed with an extra panel prior to the test in



CONFIDENTIAL

Figure 6.1 Pretest view of concrete panels at 60-foot ground range, facing ground zero.

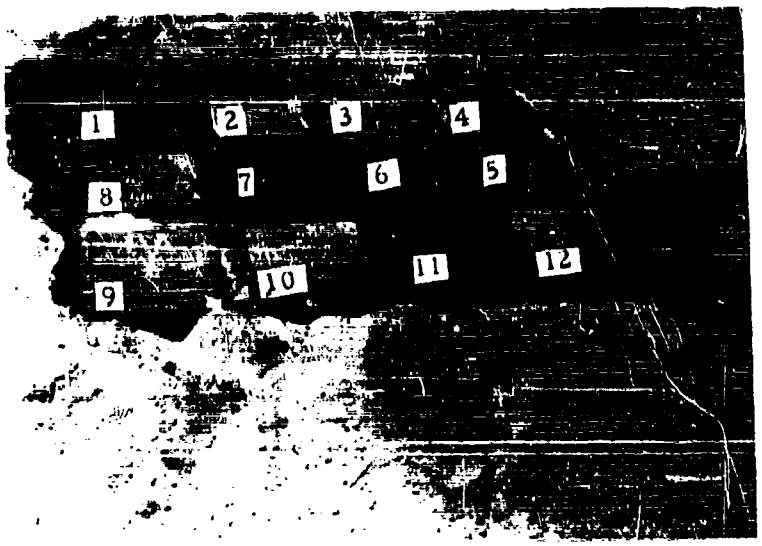


Figure 6.2 Posttest view of concrete panels at 60-foot ground range, facing ground zero.



CONFIDENTIAL

Figure 8.3 Pretest view of concrete panels at 300-foot ground range, facing ground zero.

Figure 8.4 Posttest view of concrete panels at 300-foot ground range, facing ground zero.

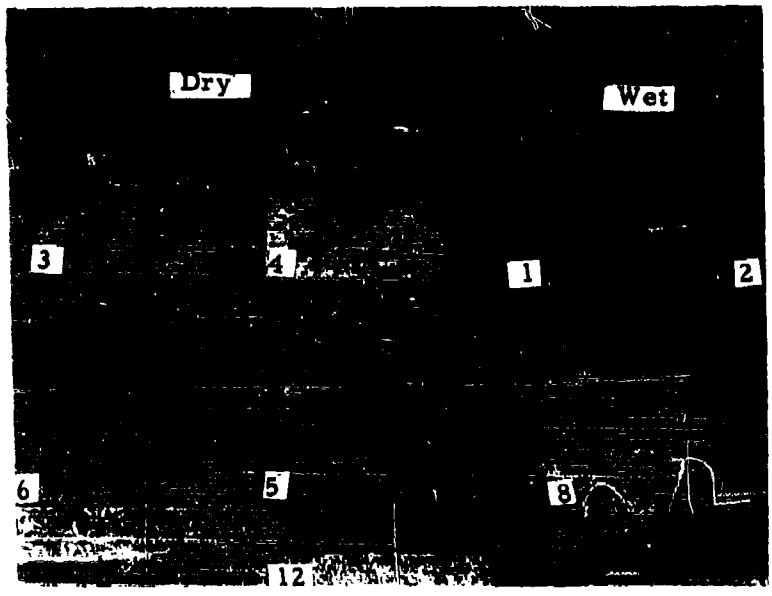


Figure 8.5 Posttest view of damaged concrete panels at 300-foot ground range, facing ground zero.

order to establish the amount of water present on the panels at shot time. From these results it was estimated that the panels at the 300-foot location were covered with about $^1/_{16}$ inch of water at shot time.

Pretest and posttest readings were taken of each panel and the grout fill with a portable concrete tester. The pretest readings were obtained 4 days before the test, 7 days after the panels were cast in place, and posttest readings were taken 11 days after the test. The majority of the panels yielded higher readings (greater compressive stress) after the test, probably indicating the result of additional curing. Exceptions to this were Panels 7 and 11 at the 60-foot and 300-foot locations, which gave significantly lower readings. It was found that the reading of the tester was dependent on the degree of fixity of the item being tested. Thus, the lower readings noted above could be indicative of the fact that the panels became loose in the foundation pad.

## 8.3 DISCUSSION

This test was intended to determine the comparative behavior of concretes and special coatings when exposed to close-in thermal radiation from an atomic detonation. The selection of test materials designed for conventional high-temperature application was considered reasonable in view of the almost total lack of pertinent information available prior to the test.

It is now clear, however, that even untreated portland-cement concrete is capable of withstanding thermal inputs comparable to those obtained at a 700-foot slant range for Shot Priscilla. In fact, both the portland-cement-concrete-panel (Panel 1) and the portland-cement grout between panels stood up as well as or better than some of the special concretes and coatings. This is also confirmed by the completely undamaged condition of the finished concrete work belonging to the balloon installation within the immediate ground-zero area.

The scaling of certain of the special coatings (Figure 8.5) was probably due more to the inadequacy of the bonding technique than to actual deterioration of the coating material.



CONFIDENTIAL

Computation of transient surface temperatures of the various panels was considered but not attempted in view of serious uncertainties concerning the magnitude and time details of the heat input at the close-in positions, and the thermodynamic properties of the panels.

## 8.4 CONCLUSIONS

On the basis of the comparative behavior of the test panels and other concrete structures within the immediate ground-zero area, it can be concluded that untreated portland-cement concrete is unaffected by thermal radiation comparable to that which was obtained at a 700-foot slant range from Shot Priscilla.

## 8.5 RECOMMENDATIONS

No further testing of this type should be conducted unless there is need for similar information corresponding to a thermal input considerably greater than that obtained during Shot Priscilla.

# Chapter 9

# MISCELLANEOUS STRUCTURES

The objective of this test was to record preshot and postshot conditions of virtually all test-site structures which were exposed to a shot and which were not included in the test plans of other agencies. This was to be accomplished by visual inspection, still photography, and where necessary by on-the-spot measurements. The purpose was to obtain as much bonus information as possible on the response of structures. A secondary purpose was to maintain a permanent record of the existing conditions of structures at the test site. No quantitative interpretation of data obtained was intended as part of this project.

Although the primary effort of the test was concentrated in photography of existing structures in Frenchman Flat exposed to Shot Priscilla, additional photography was accomplished in Area 1 of Yucca Flat where existing FCDA structures were exposed to Shot Galileo.

## 9.1 PROCEDURE

9.1.1 Test Structures. The structures inspected in the Frenchman Flat Area included:

1. UK 3.4a, b, c, and e (Open-framed sections)
2. UK 3.5c (Wall and roof panel test cell)
3. UK 3.11a and b (Steel warehouses)
4. UK 3.12a, (Brick building with precast panels)
5. UK 3.13b, (Precast gable shelter)
6. UK 3.14 (Precast warehouse)
7. UK 3.15 (Steel arch shelter with earth cover)
8. UK 3.16a, b, and c (Prefabricated wood paneled structures)
9. UK 3.29a, b, c, and d (Wall panels).

The structures inspected in Area 1 of Yucca Flat included:

1. TP 31.1a2 (Two-story brick house)
2. TP 31.1b2 (Two-story frame house)
3. TP 31.1c2 (One-story frame rambler)
4. TP 31.1e1, e2 (One-story precast concrete house)
5. TP 31.1f1 (One-story reinforced concrete block house)
6. TP 31.2e1 (Union carbide building)
7. TP 34.1j, m (Masonry shelter)
8. TP 34.1i, e (Reinforced concrete shelter)
9. TP 34.1h, k (Precast reinforced concrete shelter).

For convenience, a description of these structures is combined with the record of pretest and posttest damage in Section 9.2.

9.1.2 Instrumentation. A limited field survey was performed for several structures, but generally only visual inspection and photographic coverage were employed in connection with this test. It was the intent that free-stream pressures be ascertained from nearby blast line gages, where possible, or by suitable predictions.

## 9.2 RESULTS

A number of the structures sustained additional damage as a result of this test. Table 9.1 lists the incident pressures which occurred in this and past tests, together with brief comments regarding the increased damage to the Frenchman Flat Structures. Similar information concerning the Yucca Flat Structure is contained in Table 9.2. A more detailed description of the structures and the nature of the damage is contained in the sections which follow.

TABLE 9.1 SUMMARY OF LOADING AND DAMAGE TO UK STRUCTURES IN FRENCHMAN FLAT

| Structure | Ground Range, ft | Peak Overpressure, psi | | | Plumbbob Damage |
|---|---|---|---|---|---|
| | | UK-9 | Teapot-12 | Plumbbob | |
| UK 3.4 a, b, c, e* | 2,000 | 11.6 | 18.0 | 22.2 | Three items destroyed |
| UK 3.5 c | 1,700 | 12.0 | 27.0 | 35.0 | Center portion of structure destroyed |
| UK 3.11 a | 12,000 | 1.6 | | | Significant additional damage to roof and frame |
| UK 3.11 b | 20,000 | 1.0 | | | Minor additional Damage to roof and frame |
| UK 3.12 a | 4,900 | 6.4 | 4.0 | 6.0 | Slight additional damage to roof |
| UK 3.13 b | 4,900 | 6.4 | 4.0 | 6.0 | No additional damage |
| UK 3.14 | 6,500 | 4.4 | 3.0 | 2.6 | Rear wall partially collapsed front wall suffered large deflections |
| UK 3.15 | 2,700 | 10.8 | 7.5 | 10.3 | Damage to arch and collapse of portions of end walls |
| UK 3.16 a | 7,600 | 3.4 | | | Negligible additional damage |
| UK 3.16 b | 12,000 | 1.6 | | | No additional damage |
| UK 3.16 c | 20,000 | 1.0 | | | No additional damage |
| UK 3.29 a, b | 6,500 | 4.4 | 3.0 | 2.6 | Significant damage to some wall panels. (see Table 9.5 through 9.8) |

*These drag-type structures were subjected to the following peak dynamic pressures: UK-10, 12 psi; TP-12, 50 psi; Plumbbob, 55 psi (3-foot elevation), 107 psi (10-foot elevation).

9.2.1 UK 3.4, 3.4a, b, c, and e Truss Sections—Description. These were four of a series of five open-framed structures originally tested in UK 3.4 for the purpose of determining the air-blast loading on open-framed structures. (The fifth structure was destroyed during Operation Teapot). The basic open-framed structure was a duplicate of the center section of a through-type, open-deck, single-track truss bridge (UK 3.4a). A duplicate of the top chord assembly (UK 3.4b), the bottom chord assembly (UK 3.4c), and a single I beam from the latter section (UK 3.4e) were also tested. Pretest photographs are shown in Figures 9.1 and 9.5.

Each of the bridge structures was mounted on steel sensor bars 4½ inches square in cross section by approximately 3 feet long; on the UK 3.4e beam the sensors were steel bars 1½ inches square and approximately 15 inches long. Four pairs of the large sensors, one at each corner, supported each bridge section; two pairs of the smaller bars, one at each end, supported the beam.

The beam was filled with concrete and re-tested in Operation Teapot as item TP 3.2e.

**Pretest Damage:** There was no significant damage to the UK 3.4b and c structures as a result of previous tests. All but the lower chord of the UK 3.4a structure was destroyed in the original test. Thus, the UK 3.4a and c structures were essentially identical prior to this test.

**Posttest Damage:** The UK 3.4a bridge section stayed on its foundation with no apparent damage to the sensor bars. The floor stringers were bowed laterally approximately 40 inches at the center (Figure 9.2). The stringer-to-floor beam connections at the north end of the section failed in the roots of the connecting angles. At the other end of the stringers, only the angles on the ground zero side failed. Although the stiffeners between these stringers were severely bent and twisted, their connections to the stringers were intact.

TABLE 9.2 SUMMARY OF LOADING AND DAMAGE TO FCDA STRUCTURES IN YUCCA FLAT

| Structure | Ground Range, ft | Peak Overpressure, psi | | Plumbbob Damage |
|---|---|---|---|---|
| | | Teapot | Plumbbob | |
| 31.1a-2 | 10,500 | 1.7 | 1.3* | Significant damage to roof and second-story interior partitions, basement shelters undamaged |
| 31.1b-2 | 7,800 | 2.6 | 1.9* | Some roof damage second-story interior partitions damaged, some first floor joists broken, basement shelters undamaged |
| 31.1c-2 | 10,500 | 1.7 | 1.3* | Additional damage to roof trusses, bathroom shelter undamaged |
| 31.1e-1 | 4,700 | 5.1 | 4.3† | Cracks and spalling of concrete in ceiling and wall panels, some movement of interior partitions |
| 31.1e-2 | 10,500 | 1.7 | 1.3* | Negligible additional damage |
| 31.1f-1 | 4,700 | 5.1 | 4.3[1] | Slight additional damage cracks in front wall |
| 31.1f-2 | 10,500 | 1.7 | 1.3[2] | No additional damage |
| 31.2e-1 | 5,500 | 4 | 3.9‡ | Minor plaster cracks, some spalling of concrete on exterior walls |
| 34.1-h, i, j | 2,750 | 9.7 | 8.6† | Not inspected |
| 34.1-k, l, m | 3,750 | 7.9 | 5.5† | Not inspected |

* From data of past tests scaled to 1 kt
† From data of ITR 1481 Shot Galileo
‡ Extrapolated from data of ITR 1481

The UK 3.4b upper chord section was blown from the foundation and dismembered. A portion of this section came to rest approximately 1,000 feet behind the foundations. The remainder of the section was scattered over a wide area. The mode of failure was somewhat unusual in that the northwest and southeast sensors failed, whereas the northeast and southwest supports failed at the posts of the truss section. This is shown in Figure 9.3. The sensors at these supports, although noticeably bent, appeared to be intact.

The UK 3.4c lower chord section was knocked off its foundation and fell about 30 feet to the rear. The whole section was rotated 180 degrees so that the stringers were now bowed toward ground zero. Why this occurred is not known. The damage to the stringers was almost



CONFIDENTIAL

identical to that of the UK 3.4a structure (Figure 9.4), except that the stringers-to-floor beam connections failed at the end of the section. The northwest sensor base anchor was pulled from the foundation, with the failure occurring in the anchor bolts. Failure of the supports for this structure evidently occurred in the sensor bars.

It should be noted that the UK 3.4a and c structures became presumably identical sections following the original damage to the former. The fact that one section was blown off its supports while the other remained in place is attributed to variations in strength of the sensor welds. The similarity in damage to the section proper supports this view.

The UK 3.4e beam sensors failed at one end, allowing the beam to rotate approximately 35 degrees about the other support. (Figure 9.6). The forward sensor bar at this end was cracked almost all the way across the section and appeared to be on the verge of failing. There was no measurable permanent set in the beam itself. The fact that there was no spalling of the concrete fill in the beam indicates that it probably did not sustain an appreciable maximum deflection.

9.2.2 UK 3.5c Structure-Description. This structure was designed as a nonresponding supporting frame for tests of wall panels and roof sections in the UK 3.5 test. (A pretest photograph of the structure is shown in Figure 9.7.) The center cells each measured approximately 16 feet wide, 10 feet high, and 7 feet deep. The rear and side walls of the cell were approximately 16 inches thick, and the frontal area facing ground zero was left open to accommodate the test panels. The test cells that supported roof panels were each 15 feet wide, 10 feet high, and 30 feet deep. The front and rear walls of the end cells each had two openings measuring 3 feet by 4 feet. The walls and sides of the test cells were 16 inches thick and were reinforced by pilasters every 7½ feet. In addition, horizontal bracing was placed at the top and bottom of the walls. No wall or roof panels were installed in this structure for the present test.

Pretest Damage: The UK 3.5c structure sustained no damage during Operation Upshot-Knothole; minor damage to the center portion of the roof was incurred during Operation Teapot. However, the framework appeared to be without damage prior to this test.

Posttest Damage: This structure suffered severe damage in this test (Figures 9.8 and 9.9). The grade beam at the front side of the structure was pulled up out of the ground about 4 feet, with failures occurring at the one-third points of the center cell. The back walls and roof of the center cells were completely destroyed, one portion coming to rest approximately 300 feet behind the structure. The cell on the south side of the structure appeared to be essentially undamaged, whereas the cell on the opposite side was damaged. A slab of concrete approximately 6 inches deep by 3 feet wide was pulled away from the end wall of the north cell and was supported only by the reinforcing steel. Figure 9.8 shows also a large horizontal crack in the front wall of this cell.

9.2.3 UK 3.11a and b Structures-Description. The UK 3.11 structures were steel warehouses measuring 40 feet by 100 feet by approximately 20 feet in height. (Pretest photographs of the buildings are shown in Figures 9.10, 9.12, and 9.14). Structure 3.11a was of light steel construction comprising 21 wedge-beam, gable type bents spaced 5 feet on centers with corrugated metal roofing and siding attached to the bents through purlins and girts. The eave height was 14 feet, and the ridge was 19 feet 6 inches above the finished floor. The bents were formed of wedge-beam framing elements consisting of two vertical columns and two sloping beams. Each element was made of $^3/_{16}$-inch plate shaped in the form of a channel with variable web and flange widths. The beams were connected to the column at the eave ends by means of twenty $^3/_4$-inch bolts through the webs. At the ridge the beams were connected to each other by a single ½-inch bolt placed longitudinally through a connection plate welded to the ends of the members. Purlins and girts were of 16-gage metal in the form of hat sections 4 inches deep by 7 inches wide at the base and 2 feet 3 inches on center. Roofing and siding were 24-gage galvanized sheet metal. The 3.11b structure was identical to 3.11a, except that the bent spacing was 10 feet, the purlin spacing was 4 feet, and the girt spacing was 4 feet 6 inches.

Pretest Damage: Both structures were damaged somewhat as a result of previous tests (Figure 9.10). The entire frame of the UK 3.11a structure was leaning away from ground zero, with permanent deflections up to 5 inches at the crown. The forward rafters were buck-



CONFIDENTIAL

led along the length of the building (Figure 9.12) but were not broken at the crown. The steel sheeting was deformed between girts and purlins on the front, sides, and roof of the building. Both side doors had been blown out. The UK 3.11b structure sustained much lesser roof damage but more noticeable deformation of the front siding because of the wider spacing of girts. The side doors were intact and were left open for the present test. A detailed damage survey following the original UK 3.11 test can be found in Reference 20. Only slight additional damage occurred as a result of the Operation Teapot tests.

Posttest Damage: The damage to the UK 3.11 structures was mainly an accentuation of that incurred in previous tests (Figures 9.11, 9.13, and 9.15). In the UK 3.11a structure further buckling was noticeable in both the horizontal and vertical members of the supporting frame especially on the ground zero side of the roofs. All the bents failed at the ridge of the roof with the exception of the north-end bent and two bents at the south end. Separation of the bents at the ridge occurred because of failure of the connecting bolts (Figure 9.13). Noticeable buckling occurred in the horizontal members of the side of the structure away from ground zero at a section where a weld splice was made. Although the structure did not collapse, its usability is marginal.

The UK 3.11b structure suffered considerably less damage, although some buckling of the frames was evident. This structure would still be usable if some siding were replaced.

9.2.4 UK 3.12a Structure-Description. This structure was a one-story brick building with a timber roof which was completely covered with precast reinforced-concrete panels (Figure 9.16). These panels were welded to each other and bolted to the building. The building was rectangular in plan and elevation, having a length of 44 feet, a width of 21 feet 4 inches, and a height of 11 feet 6 inches above grade. Brick walls 12 inches thick extended 1 foot 6 inches below grade and were supported on a continuous footing pad 2 feet 8 inches wide and 1 foot thick. The roof of the structure consisted of 1-inch diagonal sheathing supported by joists 3 by 12 inches spaced 16 inches on centers and spanning the short direction of the brick walls. The roof was covered by four precast roof panels, each 10 feet $7\frac{7}{8}$ inches wide. Both the wall and roof panels were bolted to the primary structure.

Pretest Damage: The structure incurred some damage as a result of previous tests. The inside wall nearest ground zero had a few courses of brick completely removed from the wall. This occurred at approximately the mid-height of the wall and extended about a third of the length of the wall, starting at the center and running south toward the door. The inside of the roof showed considerable splitting of roof joists throughout the length of the building. Sheathing had failed in the south center quarter of the roof where the roof panels were either supported on the sheathing or struck the sheathing in a previous test (Figure 9.17). Pretest deflections of the roof are shown in Table 9.3. The door to the structure was closed prior to the present test.

Posttest Damage: There was little additional damage to the UK 3.12a structure as a result of this test, although, as indicated in Table 9.3, there was some additional deflection of the roof slabs. Since no pretest survey of the walls was made, it is not known quantitatively what additional deflections these panels suffered. There did appear to be more cracking of the panels but none of these cracks would seriously affect the use of the structure. Additional damage was inflicted in the timber joists and sheathing of the roof. Some portions of the precast roof slabs were pushed through the sheathing as shown in Figure 9.18.

9.2.5 UK 3.13b Structure-Description. This structure was a small shelter having inside plan dimensions of 22 feet by 48 feet (A posttest photograph of the structure is shown in Figure 9.19). The interior of the structure was subdivided into three main sections by means of two precast concrete partitions. The main framing consisted of 12 pairs of precast panels 2 inches thick with wedge-shaped edge beams. The panels were bolted together along the edge beams at the crown of the building and, also, to the foundation. They had a nominal width of 4 feet, and each pair formed a gable type bent in cross-sectional outline with a crown height of 13 feet 7 inches from the finished floor.

Pretest Damage: No significant damage was inflicted on the exterior of the structure in previous tests, although some small cracks were visible in the walls and roof. Heavy dam-



CONFIDENTIAL

age to the interior partitions occurred in the original UK 3.13 test, apparently caused by the blast wave entering the structure. The doors to the structure were closed prior to the present test.

**Posttest Damage:** There was no visible additional damage to this structure as a result of this test.

9.2.6 UK 3.14 Structure–Description. This structure was a rectangular precast concrete building measuring 122 feet 7 inches by 41 feet 4 inches in plan with a height of 11 feet. (Pretest photographs of the structure are shown in Figures 9.20 and 9.21.) Seven bents, spaced 20 feet on centers, supported the precast roof and wall panels. The seven bents used in this structure were identical and were composed of four component framing members. These members comprised two identical end columns, which included a short horizontal section, a center

TABLE 9.3 RESULTS OF PRETEST AND POSTTEST SURVEY OF UK 3.12a ROOF

| Point* | Pre-Test Deflection, inch | Post-Test Deflection, inch | Deflection Increment, inch |
|---|---|---|---|
| A | 1 1/8 | 1 1/2 | 3/8 |
| B | 2 | 4 1/4 | 2 1/4 |
| C | 1 5/8 | 3 1/4 | 1 5/8 |
| D | 3/4 | 1 3/4 | 1 |
| E | 2 1/2 | 5 | 2 1/2 |
| F | 2 1/4 | 3 3/4 | 1 1/2 |
| G | 1 1/8 | 1 7/8 | 3/4 |
| H | 2 5/8 | 5 | 2 3/8 |
| I | 2 1/4 | 3 3/4 | 1 5/8 |
| J | 1 1/8 | 1 7/8 | 3/4 |
| K | 2 | 4 1/4 | 2 1/4 |
| L | 1 3/4 | 3 5/8 | 1 7/8 |
| M | 7/8 | 1 7/8 | 1 |
| N | 5/8 | 2 1/2 | 1 7/8 |
| O | 9/16 | 2 1/2 | 1 15/16 |
| P | 1/2 | 1 1/2 | 1 |
| Q | 1 1/4 | 2 5/8 | 1 3/8 |
| R | 5/8 | 1 1/8 | 1/2 |

*See Figure 9.28 for location of survey points.

column of uniform section, and a center beam haunched over the center column and connected to the end columns. Each member, except for the center column, was composed of two channel-shaped elements welded together by means of insert plates to form a hollow box section 1 foot 3 inches wide. The center column, 1 foot 3 inches square in section with an 8-inch diameter hole in the center, was cast in one piece. Precast concrete struts were provided between bents at the column locations. These struts were 12 inches deep by 10 inches wide and had a 6-inch-diameter hole throughout. They were connected to the bents by the welding together of the insert plates. There were 16 thin-shell ribbed panels 19 feet 11 3/4 inches by 9 feet 11 3/4 inches in plan, having a 2-inch-thick shell supported by edge beams and intermediate beams. The wall panels were 19 feet 11 3/4 inches by 11 feet high.

**Pretest Damage:** As a result of previous tests, the roof panels were severely damaged and the front walls were dished in slightly (Figure 9.21). No pretest measurements were made of the actual deflections of any portion of this structure.

**Posttest Damage:** The UK 3.14 structure sustained significant additional damage in this test. The rear wall panels, which were standing prior to the test, were severely damaged.



CONFIDENTIAL

Four of these panels were lying on the ground, one other panel was on the verge of falling, and the last panel was badly broken at mid-height as can be seen in Figure 9.22. The failure of the rear-wall panels apparently occurred in the welded fasteners ataching these panels to the supporting frame. The front-wall panels exhibited pronounced deflections. These deflections varied from practically zero at the bottom edge of the panels to a maximum at the upper edge. Mid-span deflections of the panels at the top edge of the slabs were as shown in Table 9.4. The slabs were numbered consecutively from the north end of the structure.

TABLE 9.4 MID-SPAN DEFLECTIONS OF UK 3.14 WALL PANELS

| Panel Number | 1 | 2 | 3 | 4 | 5 | 6 |
|---|---|---|---|---|---|---|
| Deflection, inch | 8 | 20½ | 16 | 9 | 8 | 4½ |

9.2.7 UK 3.15 Structure—Description. This structure was a 25- by 48-foot steel-arch personnel shelter covered by an earth berm. (Pretest photographs of the structure are shown in Figures 9.23 and 9.25.) The shelter was manufactured by Armco Drainage and Metal Products, Inc. The barrel of this structure was an Armco Multi-Plate arch composed of curved corrugated and punched sheets bolted together to form a semicircular arch roof, the edges of the arch bearing on and being bolted to longitudinal base channels. All plates were of the same radius of curvature, but of two different widths to effect a staggered longitudinal seam. The end walls were built up of corrugated sections or panels. The loads from the panels were transferred to the foundation by means of a base angle. An Armco Multi-Plate pipe, 84 inches in diameter, was bolted to the front wall of the structure to form an entrance tunnel. Originally, the tunnel was T-shaped to form a baffle against an impinging shock wave. However, the T portion was removed prior to Operation Teapot.

Pretest Damage: As a result of previous tests some slight shifting of the earth cover took place (Figure 9.23), but no damage to the shelter itself could be observed, except that the steel plates around the door were bowed in and had pulled loose at the base connection. The door was sandbagged shut prior to the present test.

Posttest Damage: The UK 3.15 structure showed visible additional damage as a result of this test. Additional shifting of the earth cover took place (Figure 9.24), and the door was found ajar. Five or six panels comprising the north wall at the side away from ground zero pulled loose from the retaining channel fastened to the arch shell, thereby allowing fill material to enter. Similar action took place at the south end of the structure where six or seven panels failed (Figure 9.26). Apparently the structure was pushed away from ground zero causing the rear-ward portion of the arch shell to rise, thus loosening the end restraint on the end walls in this area. Those panels which failed showed no evidence of buckling. The front side of the arch shell has been dished in approximately 2 feet at a line about 50 degrees up from the foundation. The structure has been made serviceable with repairs to the end walls.

9.2.8 UK 3.16a, b, c Structures—Description. The three UK 3.16 structures were of wood frame and panel construction with windows in all exterior walls and a skylight in the roof (Figure 9.27). Each building was composed of seven cubicles approximately 8- by 8- by 10-feet high and was constructed of panels of ¾-inch plywood glued and nailed to 2- by 4-inch frames in the b and c structures and to 2- by 6-inch frames in the a structure. The frame timbers were set approximately 16 inches on centers. These structures were originally designed to test windows, glazing, screens, inside curtains, and outside blast resistance shields.

Pretest Damage: Most of the glazing in these structures was destroyed in previous tests except that in the rear of structures UK 3.16b and c. Only minor structural damage to the buildings occurred. No glazing was installed for the present test.

Posttest Damage: The only structure of this group which experienced any visible additional damage was UK 3.16a. The front face of this structure was severely scorched because



CONFIDENTIAL

of thermal radiation. The jalousie at the north side of the building was blown off and some additional damage to the glazing was evident.

9.2.9 UK 3.29a, b, c, and d Structures—Description. The UK 3.29a and c structures were used for tests of solid curtain walls. The structures were of reinforced concrete construction and divided lengthwise into 16 cells, 14 of which had an inside width of 16 feet, one of 12 feet, and one of 20 feet; the inside height of all cells was 10 feet, and the depth was 16 feet. The UK 3.29b and d structures were used for tests of windowed curtain walls and interior partitions. These structures were similar to the above, except that the width of only one of the cells was 20 feet and the depth of all cells was 20 feet.

The floor slab of all structures was 12 inches thick (8 inches of which was below grade), the roof slab was 10 inches thick, and the cell walls were 10 inches thick. The nature of various test panels is indicated in Tables 9.5 through 9.8.

Pretest Damage: The structures themselves were undamaged as a result of previous tests. The pretest condition of the various test panels is indicated briefly in Tables 9.5 through 9.8. A comprehensive documentation of the damage incurred in the original UK 3.29 test is given in Reference 6. Negligible additional damage occurred during Operation Teapot. In general, all interior portions and exterior glazing were destroyed in the UK 3.29b and d structures. As indicated in Tables 9.5 through 9.8, certain of the test cells were re-used by other agencies.

Posttest Damage: The additional damage incurred by UK 3.29 wall panels in this test is summarized in Tables 9.5 through 9.8. No damage was observed to the test structures themselves. Pretest and posttest photographs of several of the wall panels are shown in Figures 9.29 through 9.38.

9.2.10 TP 31.1a-2 Structure—Description. This structure was a two-story brick house with basement, of conventional design and construction. Lean-to and corner room personnel shelters (designated as TP 3.41a items) were built in the basement. Pretest photographs are shown in Figures 9.39 and 9.41.

Pretest Damage: The structure was completely intact. The exterior of the building showed no evidence of cracks or other structural damage (Figures 9.39 and 9.41). The windows and doors were boarded shut, and it was not possible to inspect the interior of the building.

Posttest Damage: All door and window coverings were destroyed, and the window frames were broken (Figures 9.40 and 9.42). The roof panel on the ground-zero side was caved in (Figure 9.40) and had separated at the ridge. The interior partitions were extensively damaged, and portions of the second-story ceiling were destroyed (Figure 9.43). The plaster was cracked and broken out in places throughout the first story. The basement walls, floors, and shelters were undamaged.

9.2.11 TP 31.1b-2 Structure—Description. This structure was a two-story frame house, with basement, strengthened somewhat in excess of conventional construction. Personnel shelters of lean-to, corner room, and reinforced concrete construction (designated as TP 3.41a items) were built in the basement. Pretest photographs of the building are shown in Figures 9.44 and 9.46.

Pretest Damage: The structure was completely intact. The only evidence of damage to the exterior was slight cracks in the front siding and some peeling of roofing paper (Figures 9.44 and 9.46). The windows and doors were boarded shut, and it was not possible to inspect the interior of the building.

Posttest Damage: Virtually all the window and door covering was blown away. The exterior frame appeared intact, but the roof had deflected inward somewhat. Numerous shingles were blown off the roof (Figures 9.45 and 9.47).

The second-story interior partitions showed some evidence of motion, and several ceiling sections had been removed (Figures 9.48 and 9.49). The first-story interior walls were essentially undamaged except in the vicinity of some of the window frames. These frames were splintered and pushed inward.

TABLE 9.5 SUMMARY OF DAMAGE TO UK 3.29a WALL PANELS*

| Panel† | Material | Pretest Condition | Posttest Condition |
|---|---|---|---|
| 3.29a-1f | 12-inch brick | Good | Same |
| 1r | 12-inch brick | Good | Same |
| 2f | - | Out | - |
| 2r | - | Out | - |
| 3f | 8-inch block and 4-inch brick | Good | Same |
| 3r | 8-inch block and 4-inch brick | Good | Out |
| 4f | 8-inch block and 4-inch brick | Good | Same |
| 4r | 8-inch block and 4-inch brick | Good | Same |
| 5f | - | Out | Same |
| 5r | 4-inch brick and 4-inch concrete block | Brick wall out, center top portion of concrete block out | Out |
| 6f | 8-inch brick | Good | Same |
| 6r | 8-inch brick | Good | Same |
| 7f | - | Out | - |
| 7r | - | Out | - |
| 8f | - | Out | - |
| 8r | - | Out | - |
| 9f | - | Out | - |
| 9r | 4-inch brick and 8-inch concrete | Top portion of brick wall out, concrete block wall badly cracked in same area | Out |
| 10f | 8-inch block and 4-inch brick | Good | Slight cracking |
| 10r | 8-inch block and 4-inch brick | Good | Same |
| 11f | - | NC‡ | - |
| 11r | - | NC | - |
| 12f | - | NC | - |
| 12r | - | NC | - |
| 13f | - | NC | - |
| 13r | - | NC | - |
| 14f | 8-inch reinforced concrete | Two large holes in right hand portion of wall | Same |
| 14r | 8-inch reinforced concrete | Two small holes in left side of wall | Same |
| 15f | - | Out | - |
| 15r | 8-inch reinforced brick | Two large holes in left side of wall | Same |
| 16f | - | Out NC | - |
| 16r | 22-gage corrugated metal | Dished in | Minor tearing |
| 17f | - | NC | - |
| 17r | - | Out | - |
| 18f | - | NC | - |
| 18r | - | NC | - |

* Panels were at 6,500-foot ground range and were exposed to estimated 2.6-psi peak overpressure.
† f indicates front panel (i.e., facing ground zero). r indicates rear panel. All panels were solid.
‡ NC indicates new construction by another agency.



CONFIDENTIAL

TABLE 9.6 SUMMARY OF DAMAGE TO UK 3.29b WALL PANELS*

| Panel† | Material | Pretest Condition | Posttest Condition |
|---|---|---|---|
| 3.29b-1f | 4-inch brick and 8-inch block | Wall and sash good | Same |
| 1r | 4-inch brick and 8-inch block | Good | Same |
| 2f | 4-inch brick and 8-inch block | Good | Same |
| 2r | 4-inch brick and 8-inch block | Out | |
| 3f | 4-inch brick and 8-inch block | Wall and sash good | Some slight cracking |
| 3r | 4-inch brick and 8-inch block | Good | Some cracking |
| 4f | 4-inch brick and 8-inch block | Wall and sash good | Same |
| 4r | 4-inch brick and 8-inch block | Good | Same |
| 5f | 4-inch brick and 8-inch block | Wall and sash good | Same |
| 5r | 4-inch brick and 8-inch block | Five courses of brick missing at upper right corner | One-fourth of brick and some block out in upper right corner |
| 6f | 4-inch brick and 8-inch block | Good | Same |
| 6r | 4-inch brick and 8-inch block | Good | Same |
| 7f | 4-inch brick and 8-inch block | Wall and sash good | Same |
| 7r | 4-inch brick and 8-inch block | Good | Some cracks |
| 8f | 4-inch brick and 8-inch block | Wall and sash good | Same |
| 8r | 4-inch brick and 8-inch block | Good | Same |
| 9f | 4-inch brick and 8-inch block | Wall and sash good | Same |
| 9r | 4-inch brick and 8-inch block | Good | Wall out |
| 10f | 4-inch brick and 8-inch block | Good | Large hole in upper center portion Extensive cracking |
| 10r | 4-inch brick and 8-inch block | Good | Same |
| 11f | 4-inch brick and 8-inch block | Wall and sash good | Same |
| 11r | 4-inch brick and 8-inch block | Good | Same |
| 12f | 4-inch brick and 8-inch block | Wall and sash good | Same |
| 12r | 4-inch brick and 8-inch block | Good | Same |
| 13f | 4-inch brick and 8-inch block | Wall and sash good | Same |
| 13r | 4-inch brick and 8-inch block | Good | Same |
| 14f | 4-inch brick and 8-inch block | Wall and sash good | Same |
| 14r | 4-inch brick and 8-inch block | Good | Same |
| 15f | 4-inch brick and 8-inch block | Sash pushed in, walls intact | Same |
| 15r | 4-inch brick and 8-inch block | Six courses of brick at top center missing, cracks | Two-thirds of brick and one-half of block out |
| 16f | 4-inch brick and 8-inch block | Wall and sash good | Same |
| 16r | 4-inch brick and 8-inch block | Few small cracks | Same |

* Panels were at 6,500-foot ground range and were exposed to estimated 2.6-psi peak overpressure.

† f indicates front panel (i.e., facing ground zero). r indicates rear panel. All front panels had window openings except 10f which was solid; all rear panels were solid.



CONFIDENTIAL

TABLE 9.7 SUMMARY OF DAMAGE TO UK 3.29c WALL PANELS*

| Panel† | Material | Pretest Condition | Posttest Condition |
|---|---|---|---|
| 3.29c-1f | Corrugated asbestos | Good (NC)‡ | Out |
| 1r | 12-inch brick | Good | Out |
| 2f | 8-inch block | Out | - |
| 2r | | Out | - |
| 3f | 4-inch brick and 8-inch block | Out | - |
| 3r | 4-inch brick and 8-inch block | Out | - |
| 4f | 4-inch brick and 8-inch block | Out | - |
| 4r | 4-inch brick and 8-inch block | Out | - |
| 5f | 4-inch brick and 4-inch block | Out | - |
| 5r | 4-inch brick and 4-inch block | Out | - |
| 6f | 8-inch brick | Out | - |
| 6r | 8-inch brick | Out | - |
| 7f | 12-inch block | Out | - |
| 7r | 12-inch block | Out | - |
| 8f | 4-inch brick and 4-inch block | Out | - |
| 8r | 4-inch brick and 4-inch block | Out | - |
| 9f | 4-inch brick and 8-inch block | Out | - |
| 9r | 4-inch brick and 8-inch block | Out | - |
| 10f | 4-inch brick and 8-inch block | Out | - |
| 10r | 4-inch brick and 8-inch block | Out | - |
| 11f | 4-inch brick and 4-inch block | NC | - |
| 11r | 4-inch brick and 4-inch block | NC | - |
| 12f | 4-inch brick and 8-inch block | NC | - |
| 12r | 4-inch brick and 8-inch block | NC | - |
| 13f | 4-inch brick and 4-inch file | NC | - |
| 13r | 4-inch brick and 4-inch file | NC | - |
| 14f | 8-inch reinforced concrete | 2 small holes in right side of wall | Same |
| 14r | 8-inch reinforced concrete | 2 small holes in left side of wall | Same |
| 15f | 8-inch concrete block | Good (NC) | Out |
| 15r | 8-inch reinforced brick | Good | Large vertical cracks at top of wall, top edge pushed out 2-inches to 10-inches |
| 16f | - | NC | - |
| 16r | 22-gage corrugated metal | Out | - |
| 17f | - | NC | - |
| 17r | Corrugated asbestos | Out | - |
| 18f | - | NC | - |
| 18r | Precast reinforced concrete | Out | - |

* Panels were at 4,200-foot ground range and were exposed to 7.5-psi peak overpressure.
† f indicates front panel (i.e., facing ground zero). r indicates rear panel. All panels were solid.
‡ NC indicates new construction by another agency.



CONFIDENTIAL

TABLE 9.8 SUMMARY OF DAMAGE TO UK 3.29d WALL PANELS*

| Panel† | Material | Pretest Condition | Posttest Condition |
|---|---|---|---|
| 3.29d-1f | 4-inch brick and 8-inch block | Sash bent, wall cracked and a few bricks missing | Center section of wall and sash out, additional dishing and cracking of side wall sections |
| 1r | 4-inch brick and 8-inch block | Upper right quarter of brick wall out, block wall intact | Out |
| 2f | 4-inch brick and 8-inch block | Out | Out |
| 2r | 4-inch brick and 8-inch block | Out | |
| 3f | 4-inch brick and 8-inch block | Sash out, top center portion of panel out | Same |
| 3r | 4-inch brick and 8-inch block | Out | - |
| 4f | 4-inch brick and 8-inch block | Sash partially missing, center section of wall outside of wall sections | Top center of wall out, portion of bottom center wall out, additional cracking of side wall sections |
| 4r | 4-inch brick and 8-inch block | Out | |
| 5f | 4-inch brick and 8-inch block | Out | Sash out, top and bottom center portions of wall out |
| 5r | 4-inch brick and 8-inch block | Out | |
| 6f | 4-inch brick and 8-inch block | Sash partially missing, center section of wall out, side wall sections pushed in and cracked, some brick and blocks missing at top center | Top center of wall out, additional cracking and dishing of side wall sections |
| 6r | 4-inch brick and 8-inch block | Out | |
| 7f | 4-inch brick and 8-inch block | Sash partially missing, center section of wall out side wall sections pushed in and cracked, some brick and block missing at top center | Sash and top center of wall out, additional cracking and dishing of side wall sections |
| 7r | 4-inch brick and 8-inch block | Out | |
| 8f | 4-inch brick and 8-inch block | Sash partially missing, center section of wall out, side wall sections pushed in and cracked, portion of wall out at top center | Sash and top center of wall out, additional cracking and dishing of side wall sections |
| 8r | 4-inch brick and 8-inch block | Out | |
| 9f | 4-inch brick and 8-inch block | Sash bent, wall pushed in and cracked, portion at upper left corner missing | Sash, top, and center section of wall out, additional cracking and dishing of side wall sections |
| 9r | 4-inch brick and 8-inch block | Upper left quarter of brick wall out, portion of block wall out in upper left corner, some cracks in remainder of wall | Almost entire wall out |
| 10f | 4-inch brick and 8-inch block | Out | |
| 10r | 4-inch brick and 8-inch block | Out | |
| 11f | 4-inch brick and 8-inch block | Sash partially miss[illegible] center section of wall ou[illegible] ie wall sections pushed in and cracked | Sash and top center of wall out, additional dishing and cracking of side wall sections |
| 11r | 4-inch brick and 8-inch block | Some cracking, a few bricks missing in top course | Out |
| 12f | 4-inch brick and 8-inch block | Out | Top center of wall out, cracking of remainder |



CONFIDENTIAL

TABLE 9.8 SUMMARY OF DAMAGE TO UK 3.29d WALL PANELS* (Continued)

| Panel† | Material | Pretest Condition | Posttest Condition |
|---|---|---|---|
| 12r | 4-inch brick and 8-inch block | Out | |
| 13f | 4-inch brick and 8-inch block | Sash partially missing, center section of wall out, side wall sections pushed in and cracked, some brick and block missing at center | Top and center of wall out, portion of bottom center wall out, additional cracking and dishing of side wall sections |
| 13r | 4-inch brick and 8-inch block | Out | |
| 14f | 4-inch brick and 8-inch block | Sash partially missing, center section of wall out, side wall sections pushed in and cracked, some brick and block missing at center | Top center of wall out, portion of bottom center wall out, additional cracking and dishing of side wall sections |
| 14r | 4-inch brick and 8-inch block | Some cracking | Out |
| 15f | 4-inch brick and 8-inch block | Sash out, center sections of wall out, some cracking of side wall sections | Top and bottom center of wall out, additional cracks in side wall sections |
| 15r | 4-inch brick and 8-inch block | Out | |
| 16f | 4-inch brick and 8-inch block | Sash bent, slight cracking of walls | Top center of wall out, additional cracks in side wall sections |
| 16r | 4-inch brick and 8-inch block | Out | |

* Panels were at 4,200-foot ground range and are exposed to 7.5-psi peak overpressure.

† f indicates front panel (i.e., facing ground zero). r indicates rear panel. All front panels had window openings except 10f which was solid; all rear panels were solid.

The basement walls and floors and interior personnel shelters showed no evidence of damage. Several of the first-floor joists were broken, however.

9.2.12 TP 31.1c-2 Structure—Description. This structure was a one-story house of conventional design and construction. A personnel shelter of reinforced concrete construction (designated as TP 34.1a item) was built in the bathroom of the house. Pretest photographs of the building are shown in Figures 9.50 and 9.51.

Pretest Damage: The building was intact. Some splitting of the front siding was evident (Figures 9.50 and 9.51). The lower side of the roof over the entrance was lifted up along one edge but was still in place. There was some damage to the roof covering. In the interior of the building, the ceiling (dry wall construction) was depressed throughout and torn down in some places. The front wall was torn in places and pushed inward. The sashes were intact and some windows were boarded. The concrete floor slab was not cracked. The bathroom shelter was undamaged.

Posttest Damage: There was but slight additional damage to the building. The rear-window boarding was blown off, and one of the sashes was splintered (Figure 9.52). The plywood cover on the front-porch eave was lifted up. Six ceiling joists were broken (Figure 9.53).

9.2.13 TP 31.1e-1 Structure—Description. This structure was a one-story house with attached garage, of precast reinforced concrete construction. Photographs of the building are shown in Figures 9.54 and 9.55.

Pretest Damage: The building frame was intact. The front door, garage door, side and rear windows were boarded. The front glazing was out, and the rear door was open. Some cracks were evident on the inside of the front walls along the length of the building. Much junk and debris was found in several of the rooms (Figure 9.56). It is believed that some of this was removed prior to the test.



CONFIDENTIAL

**Posttest Damage:** There was some additional damage to the building. There was evidence of spalling of concrete from the ceiling panels at the joints and from the top of wall panels (Figures 9.57 and 9.58). Numerous radial cracks occurred around the window openings. There was some evidence that the interior partitions facing open windows had shifted slightly.

9.2.14 TP 31.1e-2 Structure—Description. This structure was a one-story house with attached garage, of precast reinforced concrete construction, identical to the TP 31.1e-1 structure (Figures 9.54 and 9.55).

**Pretest Damage:** The house was essentially undamaged. The wooden cover on the doors and windows showed some cracking which might have been caused by a shot following the original Operation Teapot test.

**Posttest Damage:** With the exception of slight cracks in the wall panels at the joints, there was no evidence of additional damage to the building.

9.2.15 TP 31.1f-1 Structure—Description. This structure was a one-story house of reinforced concrete block construction. Pretest photographs of the building are shown in Figures 9.59 and 9.62.

**Pretest Damage:** The building had sustained only slight damage. Minor cracks were evident on the outside of the front wall below the picture window (Figure 9.59). Several blocks had been removed from this area and the opening boarded shut (Figure 9.60). Most of the door and window openings were boarded shut (Figure 9.64). Some cracks and minor spalling were evident in the ceiling and walls.

**Posttest Damage:** The building sustained slight additional damage (Figure 9.63). Some large cracks occurred in the front wall near the corners (Figure 9.61) and around the window openings. The front wall below the picture window was strengthened on the inside with heavy wood members (Figure 9.65), and no additional damage was noted.

9.2.16 TP 31.1b-2 Structure—Description. This structure was a one-story house of reinforced concrete block construction, identical to the TP 31.1f-1 structure (Figures 9.59 and 9.62).

**Pretest Damage:** At the time of the pretest inspection the building was in use for high explosive storage, and, although it was not possible to inspect the interior, the building appeared to be undamaged.

**Posttest Damage:** Most of the window and door cover was broken, but the building was otherwise undamaged.

9.2.17 TP 31.2e-1 Structure—Description. This structure, referred to as the Union Carbide Building, was a control-room building designed to be blast resistant and having reinforced gypsum walls and roof integral with a steel frame. Pretest photographs are shown in Figures 9.66, 9.67, and 9.68.

**Pretest Damage:** The structure was intact and appeared to be in good condition. The front and side plastic glazing was out; the rear glazing was essentially intact. Prior to the test all openings were boarded shut (not shown in pretest photographs). The roof beams appeared undamaged.

**Posttest Damage:** The exterior panels showed additional cracking and some spalling. Otherwise the structure was intact (Figure 9.69).

9.2.18 TP 34.1-h, i, j, k, l, m Structures—Description. These structures were aboveground personnel shelters. All shelters were of identical geometry, and access was through a heavy timber door. Shelters 34.1h and k were of precast reinforced-concrete construction; Shelters 34.1i and l were of reinforced-concrete construction poured in place; Structures 34.1j and m were of masonry-block construction. Representative pretest photographs are shown in Figures 9.70, 9.71, and 9.72.

**Pretest Damage:** All shelters were intact and showed no evidence of cracks or other structural damage. The heavy wooden doors on all shelters were closed at the time of the pretest inspection.



CONFIDENTIAL

**Posttest Damage:** No posttest damage inspection was performed. All structures were observed from a distance, and, inasmuch as the reported pressures were below those of the original Operation Teapot test (Table 9.2), it is presumed that the shelters sustained no additional damage.

Figure 9.1 Pretest, UK 3.4a, b, and c structures, front side view, facing southwest.

Figure 9.2 Posttest, UK 3.4a structure, side view, facing south.

Figure 9.3 Posttest, UK 3.4b foundation, front side view, facing southwest.



CONFIDENTIAL

Figure 9.4 Posttest, UK 3.4c structure, rear view, facing east.

Figure 9.5 Preshot, UK 3.4c beam, front side view, facing northwest.

Figure 9.6 Posttest, UK 3.4c beam, front side view, facing southwest.

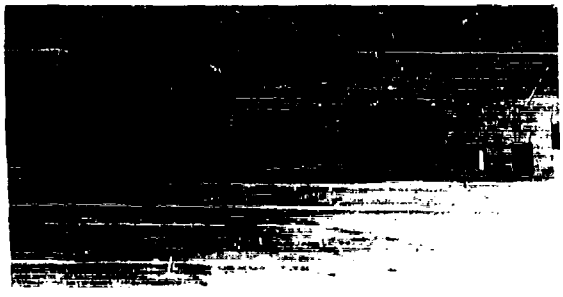

Figure 9.7 Pretest, UK 3.5c structure, front view, facing west.

Figure 9.8 Posttest, UK 3.5c structure, front view, facing west.

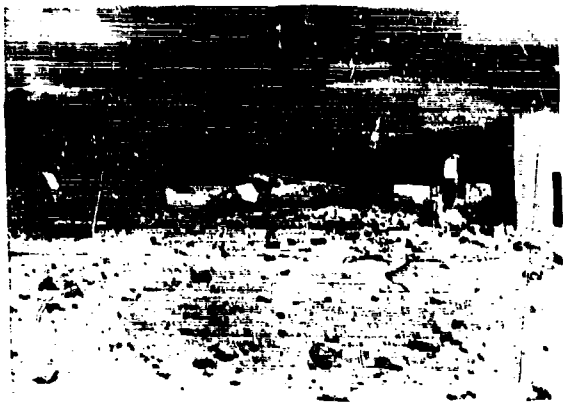

Figure 9.9 Posttest, UK 3.5c structure, rear view, facing east.



CONFIDENTIAL

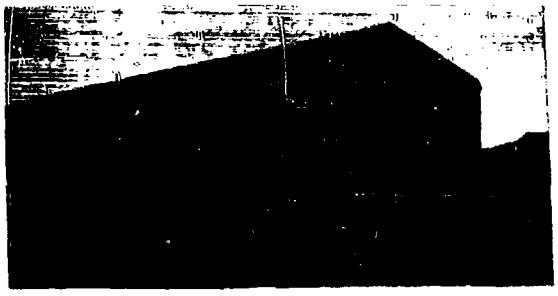

Figure 9.10 Pretest, UK 3.11a structure, front side view, facing southwest.

Figure 9.11 Posttest, UK 3.11a structure, front side view, facing southwest.

Figure 9.12 Pretest, UK 3.11a structure, interior of roof, facing southwest.

Figure 9.13 Posttest, UK 3.11a structure, interior of roof, facing south.

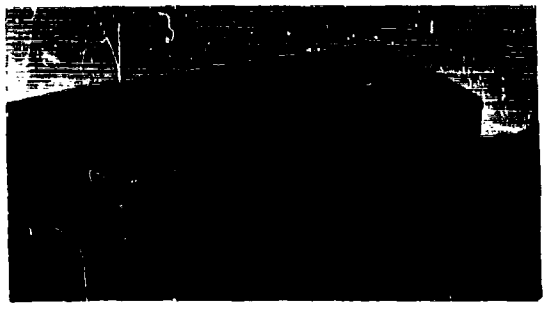

Figure 9.14 Pretest, UK 3.11 b structure, front side view, facing southwest.

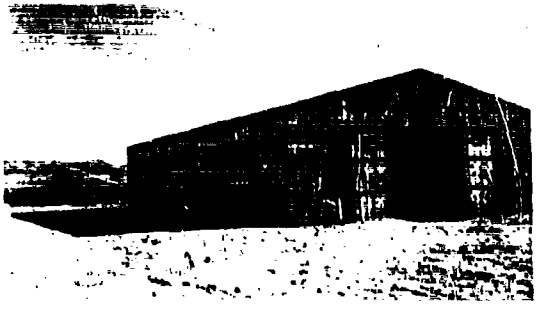

Figure 9.15 Posttest, UK 3.11 b structure, front side view, facing southwest.



CONFIDENTIAL

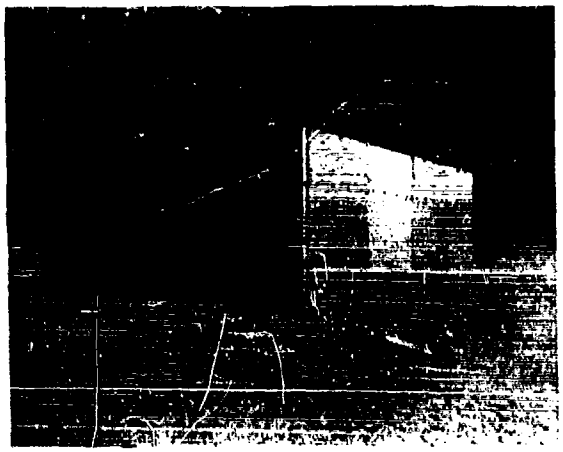

Figure 9.16 Posttest, UK 3.12 a structure, rear side view, facing southeast.

Figure 9.17 Pretest, UK 3.12 a structure, interior of roof, facing west.

Figure 9.18 Posttest, UK 3.12 a structure, interior of roof, facing west.

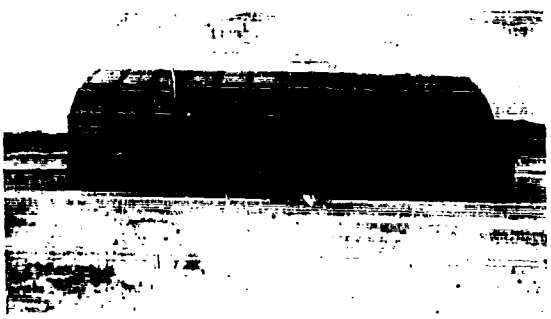

Figure 9.19 Posttest, UK 3.13 b structure, front view, facing west.

Figure 9.20 Pretest, UK 3.14 structure, facing northeast.

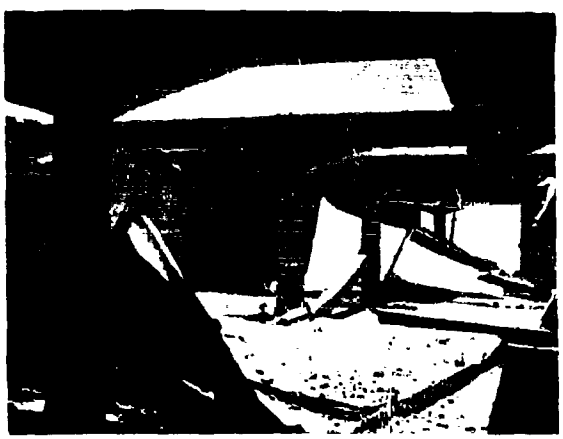

Figure 9.21 Pretest, UK 3.14 structure, interior side view, facing southeast.



CONFIDENTIAL

Figure 9.22 Posttest, UK 3.14 structure, rear side view, facing northeast.

Figure 9.23 Pretest, UK 3.15 structure, front side view, facing southwest.

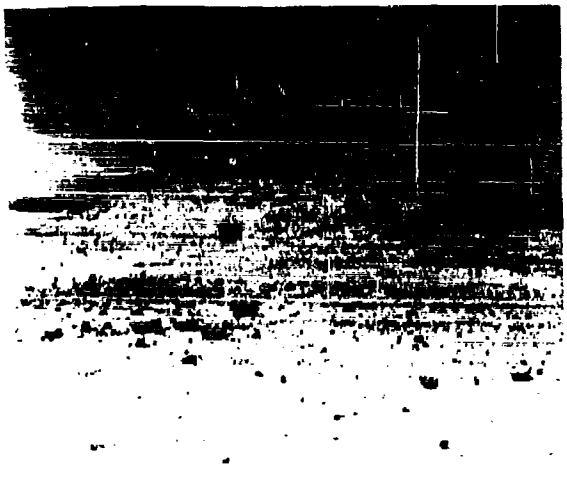

Figure 9.24 Posttest, UK 3.15 structure, front side view, facing southwest.

Figure 9.25 Pretest, UK 3.15 structure, interior side view, facing southeast.

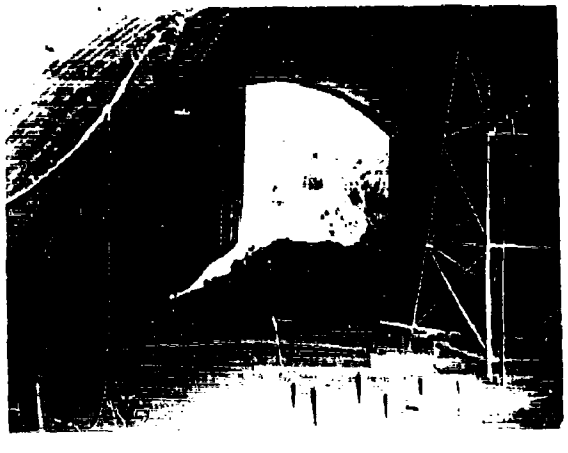

Figure 9.26 Posttest, UK 3.15 structure, interior side view, facing southeast.

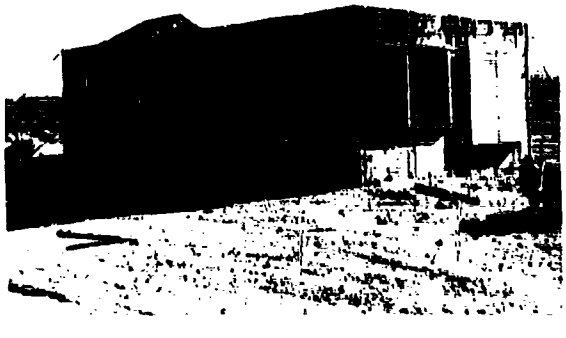

Figure 9.27 Posttest, UK 3.16c, front side view, facing southwest.

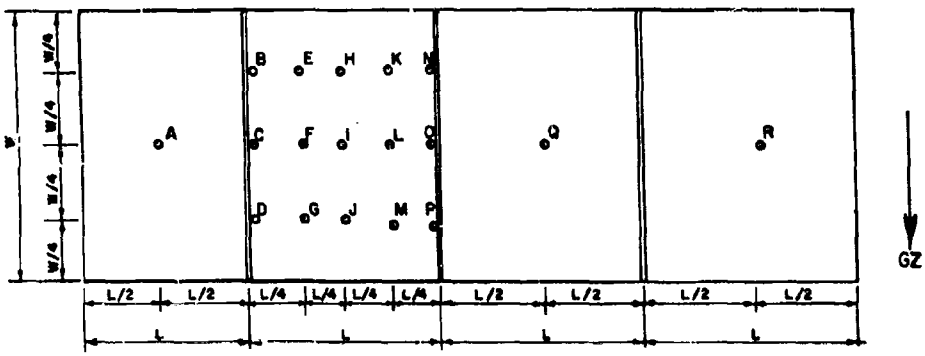


Figure 9.28 Location of survey points on roof of UK 3.12a structure.

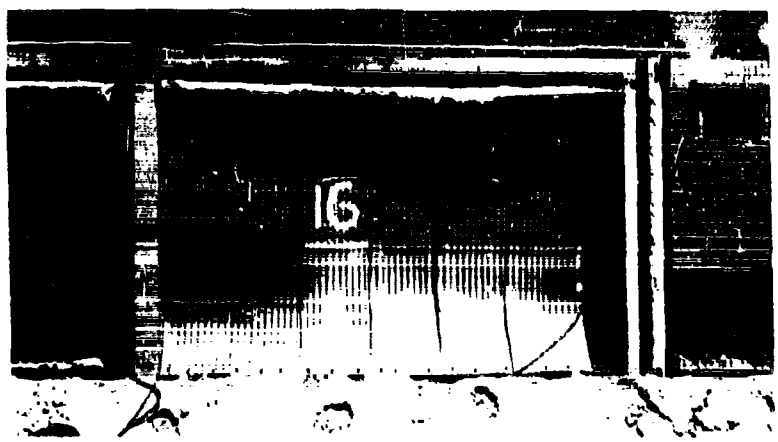

Figure 9.29 Pretest, UK 3.29 a-16, rear panel (22 gage corrugated metal).

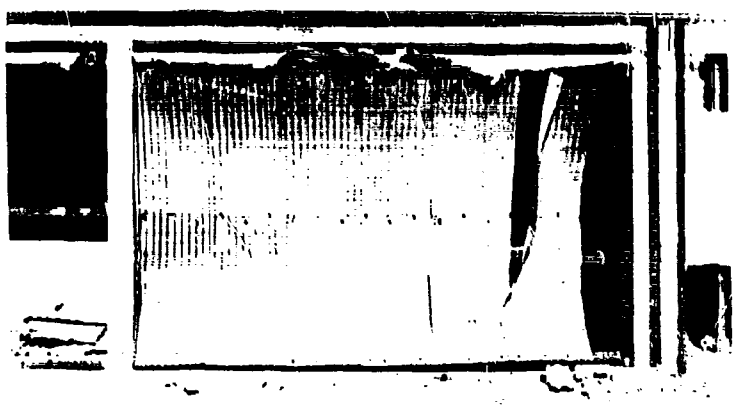

Figure 9.30 Posttest, UK 3.29 a-16, rear panel (22 gage corrugated metal).



CONFIDENTIAL

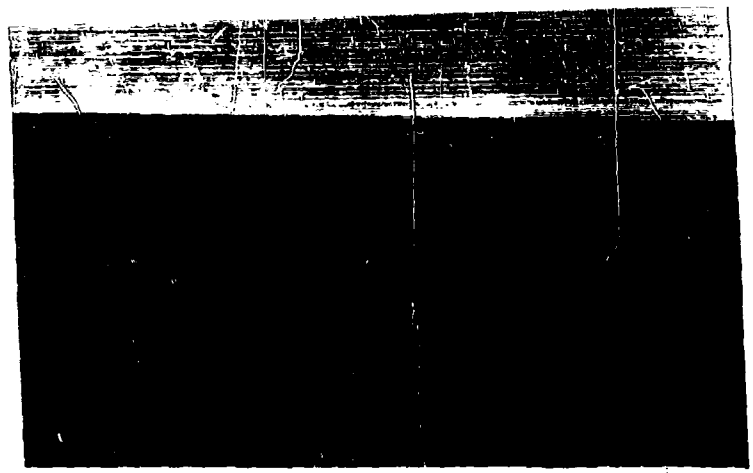

Figure 9.31 Pretest, UK 3.29 b-10, front panel (4-inch brick and 8-inch block).

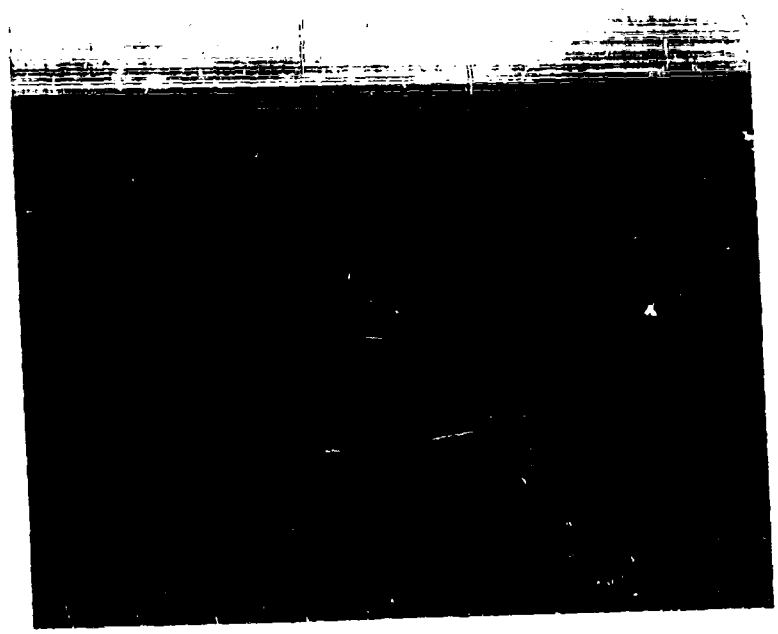

Figure 9.32 Posttest, UK 3.29 b-10, front panel (4-inch brick and 8-inch block).



CONFIDENTIAL

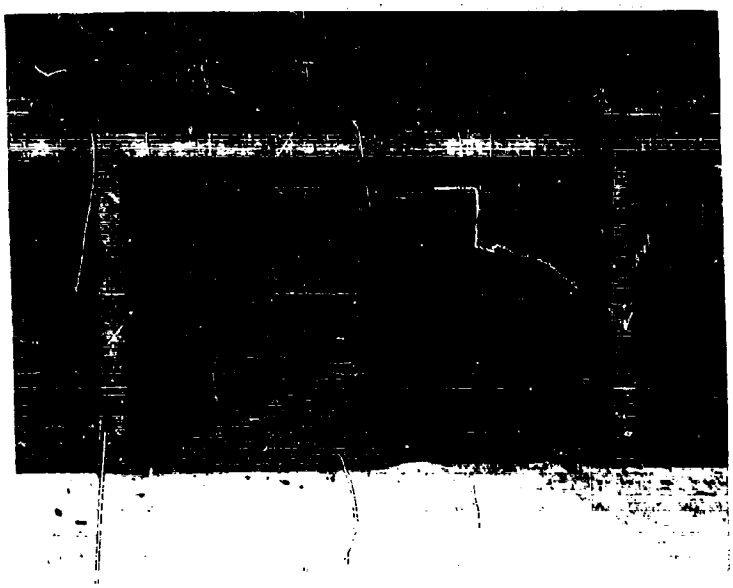

Figure 9.33 Pretest, UK 3.29 b-15, rear panel (4-inch brick and 8-inch block).

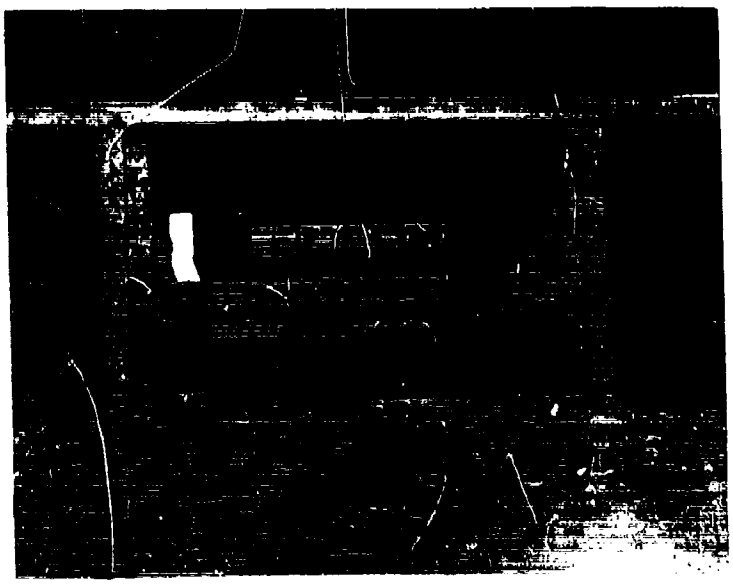

Figure 9.34 Posttest, UK 3.29 b-15, rear panel (4-inch brick and 8-inch block).

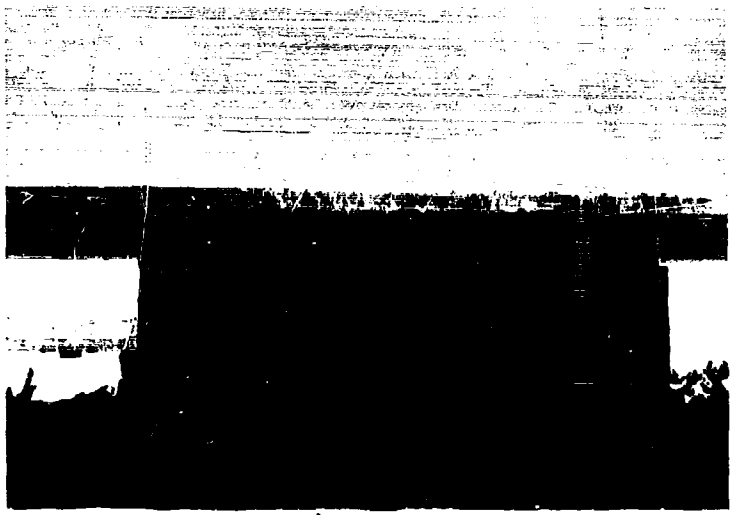

Figure 9.35 Pretest, UK 3.29 d-11, front panel (4-inch brick and 8-inch block).

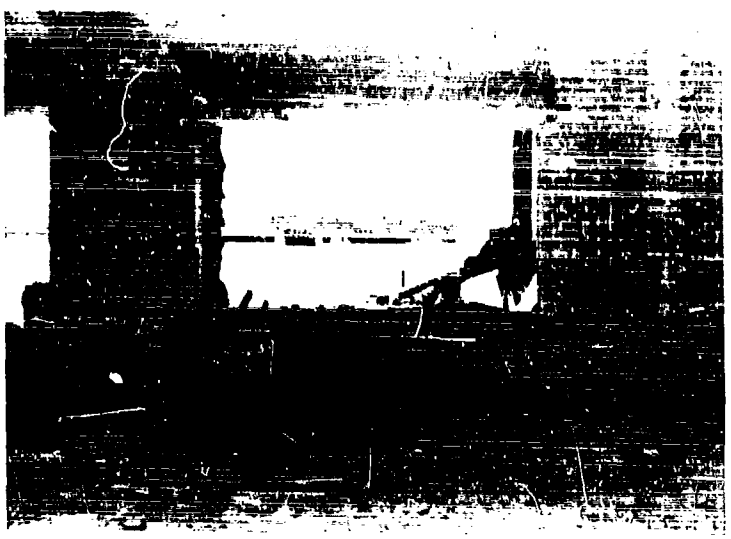

Figure 9.36 Posttest, 3.29 d-11, front panel (4-inch brick and 8-inch block).

Figure 9.37 Pretest, UK 3.29 d-1, rear panel (4-inch brick and 8-inch block).

Figure 9.38 Posttest, UK 3.29 d-1, rear panel (4-inch brick and 8-inch block).



CONFIDENTIAL

Figure 9.39 Pretest, TP 31.1 a-2, side view of building, facing southeast.

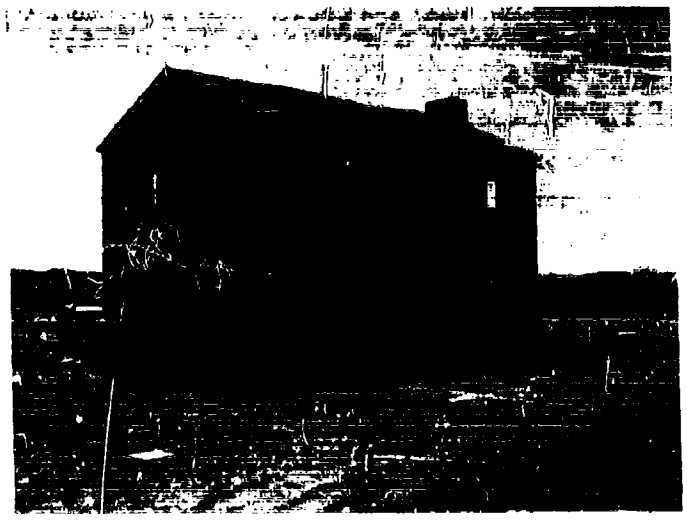

Figure 9.40 Posttest, TP 31.1 a-2, side view of building, facing southeast.



CONFIDENTIAL

Figure 9.41 Pretest, TP 31.1 a-2, side view of building, facing northwest.

Figure 9.42 Posttest, TP 31.1 a-2, side view of building, facing northwest.



CONFIDENTIAL

Figure 9.43 Posttest TP 31.1 a-2, second floor interior.

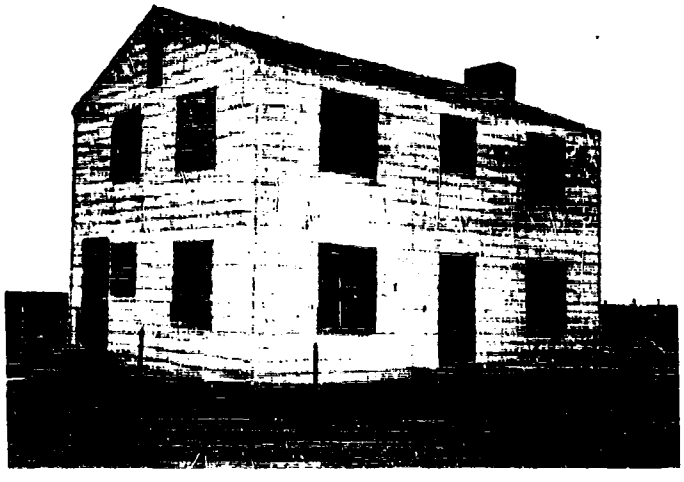

Figure 9.44 Pretest, TP 31.1 b-2, side view of building, facing southeast.

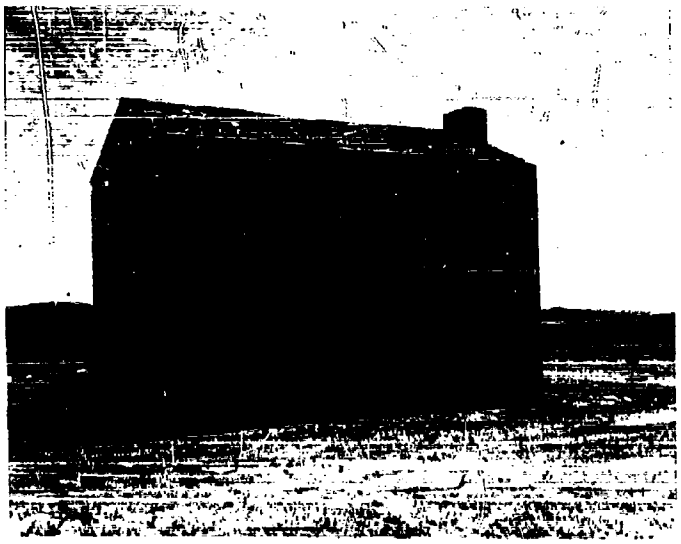

Figure 9.45 Posttest, TP 31.1 b-2, side view of building, facing southeast.

Figure 9.46 Pretest, TP 31.1 b-2, side view of building, facing northwest.

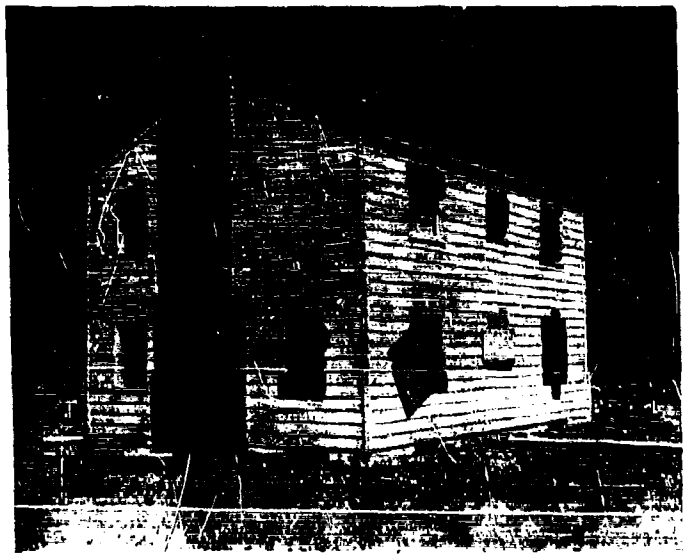

Figure 9.47 Posttest, TP 31.1 b-2, side view of building, facing northwest.

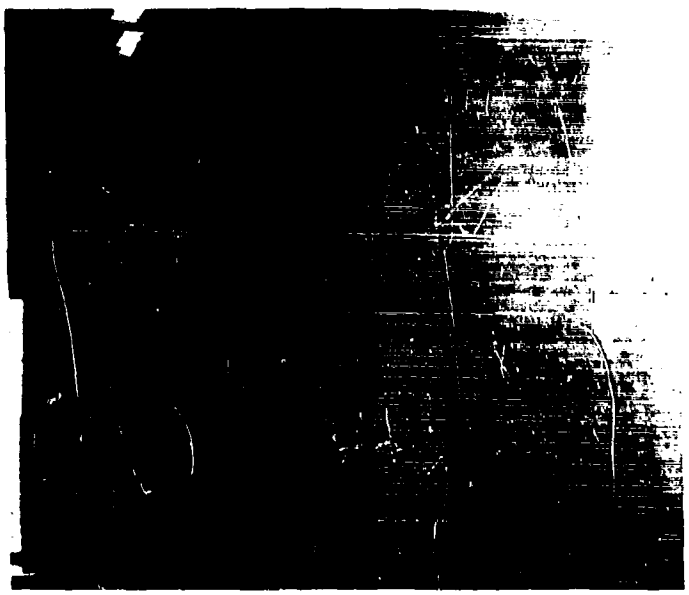

Figure 9.48 Posttest, TP 31.1 b-2, interior of second story.



CONFIDENTIAL

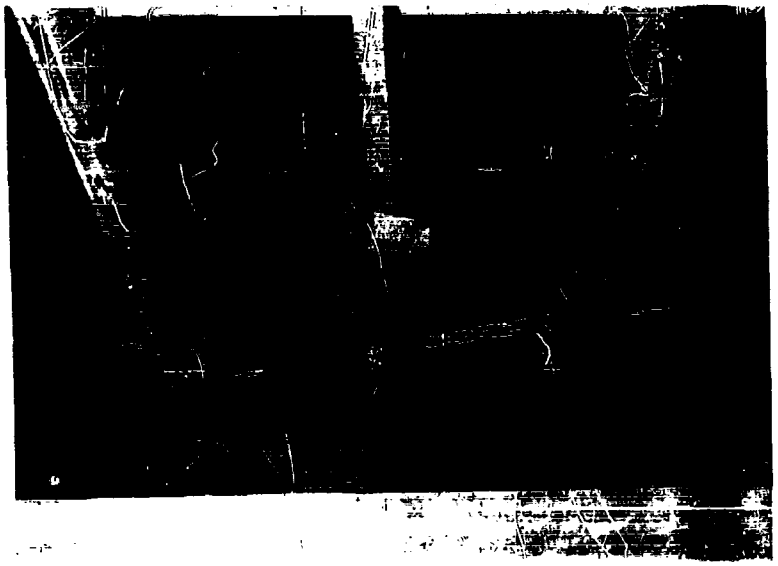

Figure 9.49 Posttest, TP 31.1 b-2, interior of second story.

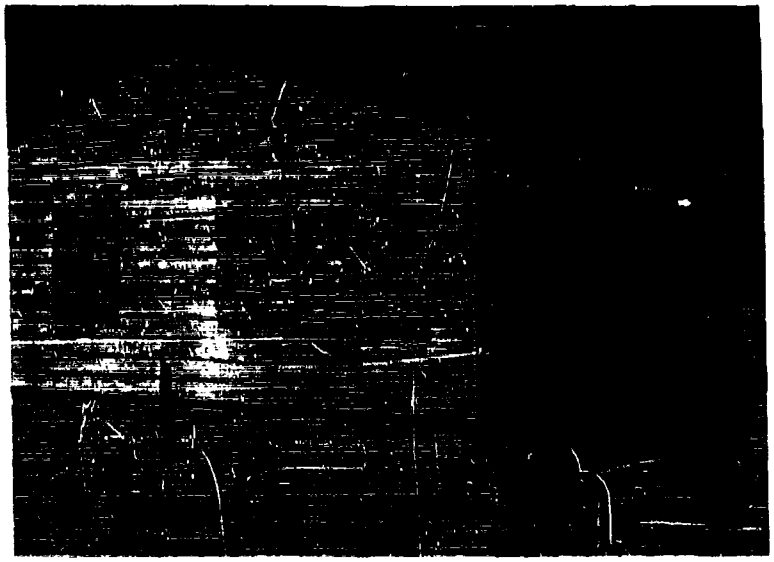

Figure 9.50 Pretest, TP 31.1 c-2, side view of building, facing southwest.



CONFIDENTIAL

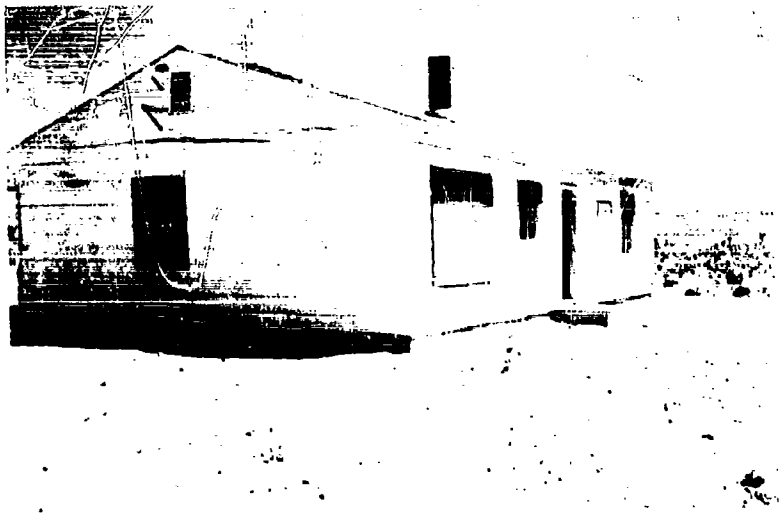

Figure 9.51 Pretest, TP 31.1 c-2, side view of building, facing northeast.

Figure 9.52 Posttest, TP 31.1 c-2, side view of building, facing northeast.



CONFIDENTIAL

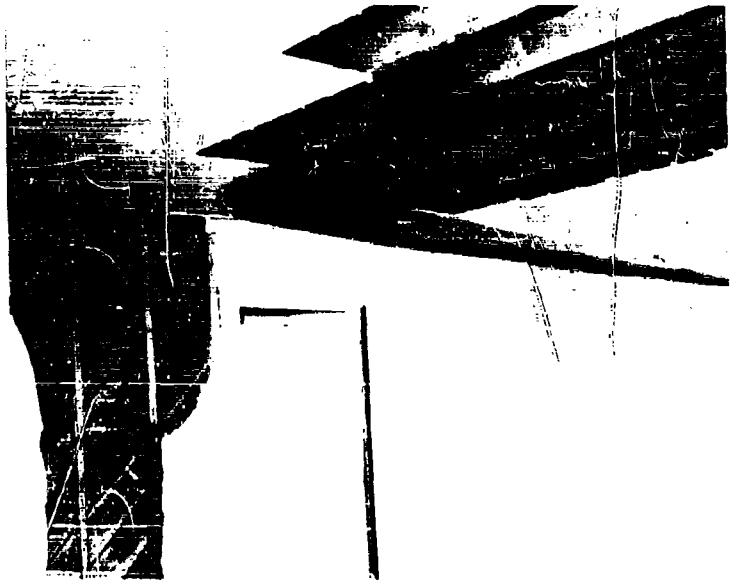

Figure 9.53 Posttest, TP 31.1 c-2, interior of building.

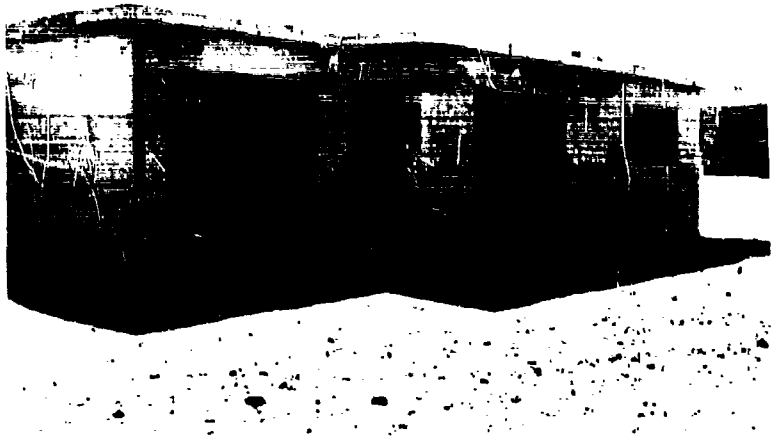

Figure 9.54 Posttest, TP 31.1 e-1, side view of building, facing southwest.



CONFIDENTIAL

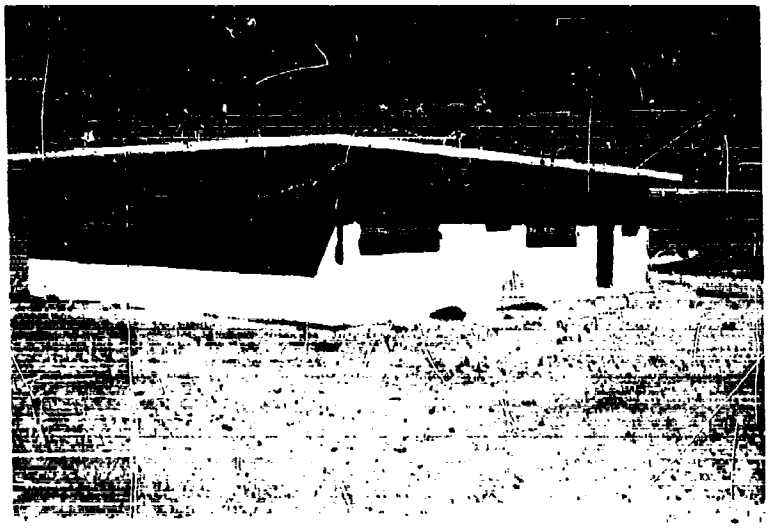

Figure 9.55 Posttest TP 31.1 e-1, side view of building, facing northeast.

Figure 9.56 Pretest, TP 31.1 e-1, interior of living room, facing northwest.



CONFIDENTIAL

Figure 9.57 Posttest, TP 31.1 e-1, interior of living room, facing northwest.

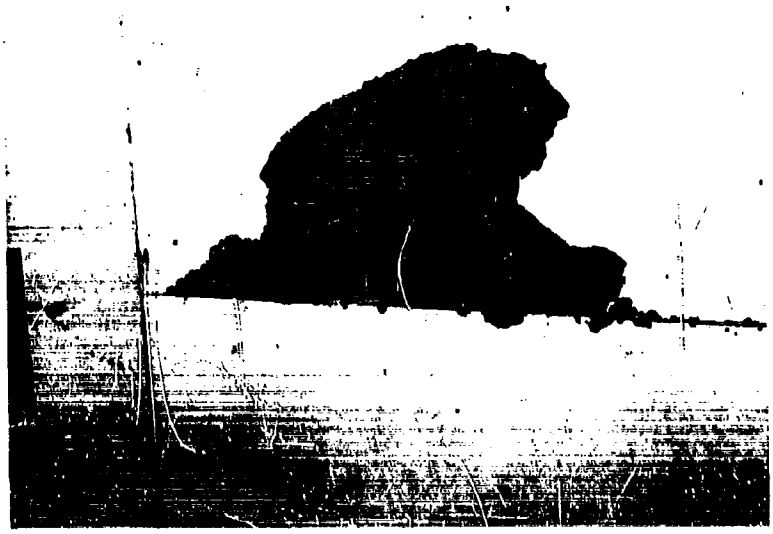

Figure 9.58 Posttest, TP 31.1 e-1, interior of ceiling, facing northwest.



CONFIDENTIAL

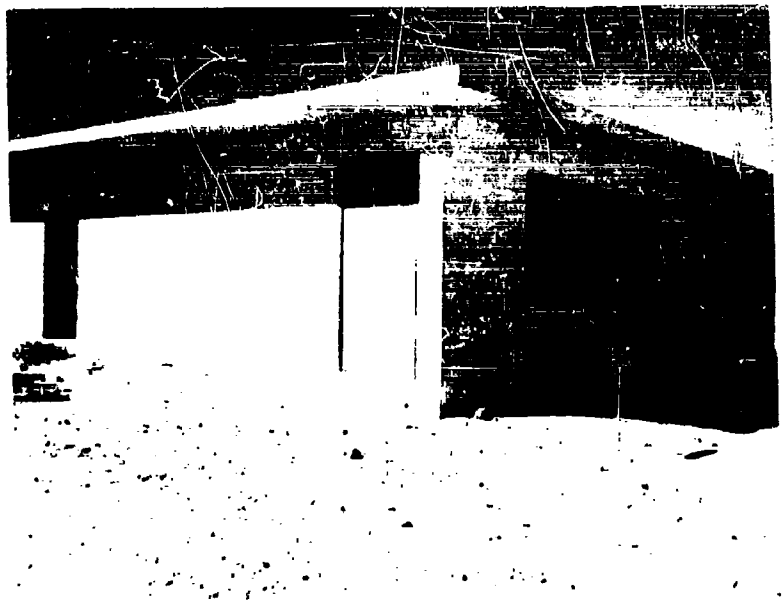

Figure 9.59 Pretest, TP 31.1 f-1, side view of building, facing southwest.

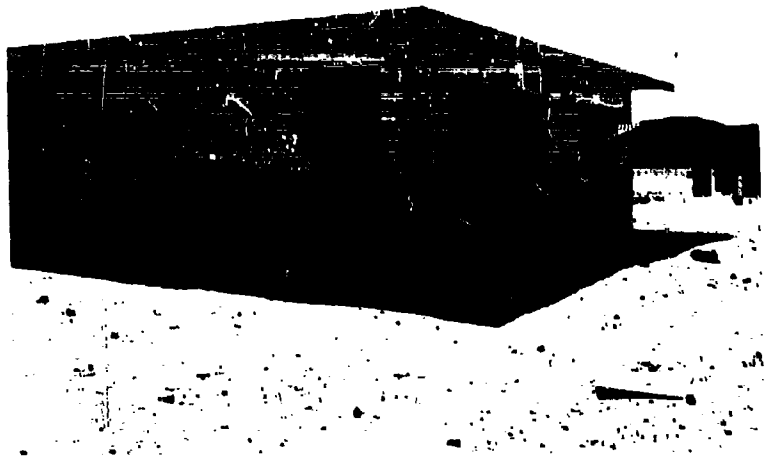

Figure 9.60 Posttest, TP 31.1 f-1, side view of building, facing southwest.

Figure 9.61 Posttest, TP 31.1 f-1, front view of building, facing south.



CONFIDENTIAL

Figure 9.62 Pretest, TP 31.1 f-1, side view of building, facing northeast.

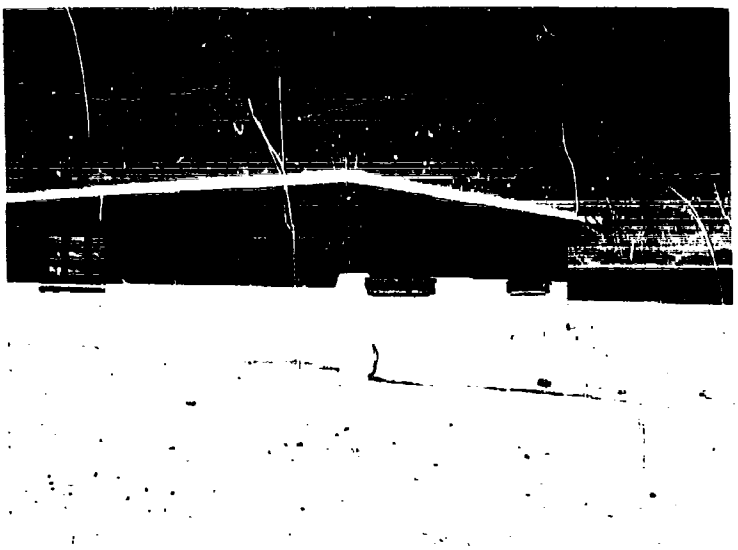

Figure 9.63 Posttest, TP 31.1 f-1, side view of building, facing northeast.

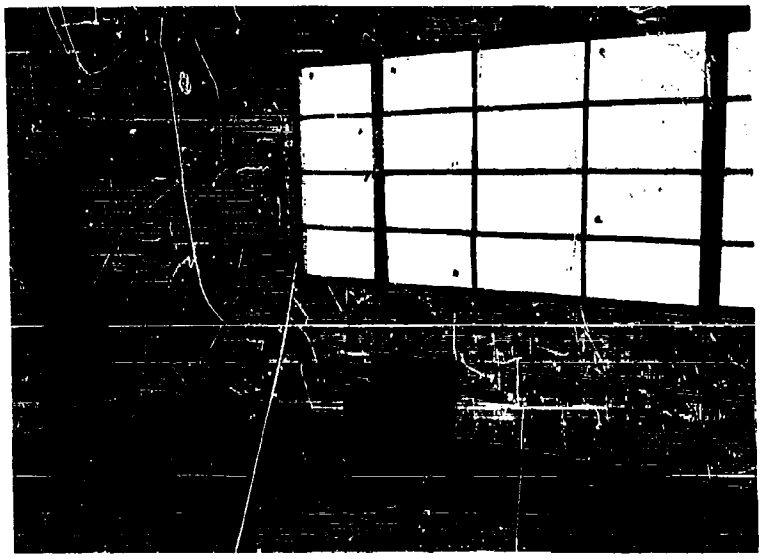

Figure 9.64 Pretest, TP 31.1 f-1, interior of living room, facing northwest.

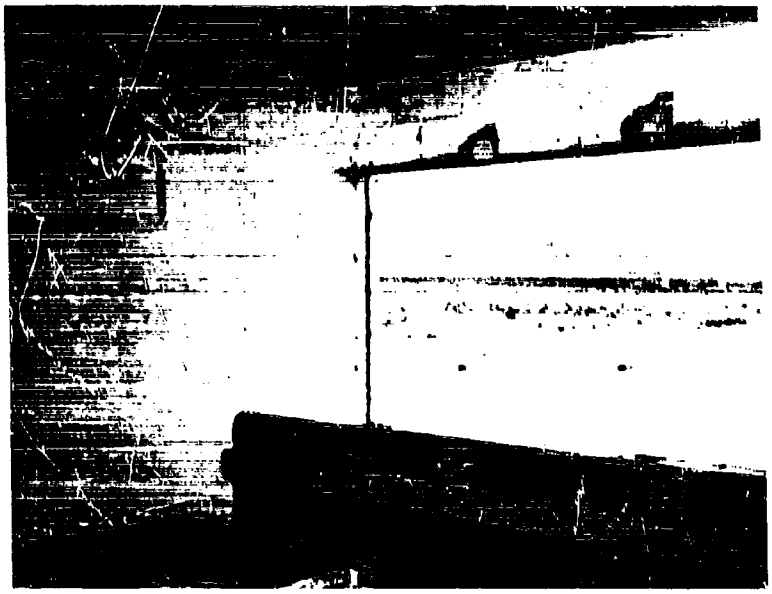

Figure 9.65 Posttest, TP 31.1 f-1, interior of living room, facing northwest.



CONFIDENTIAL

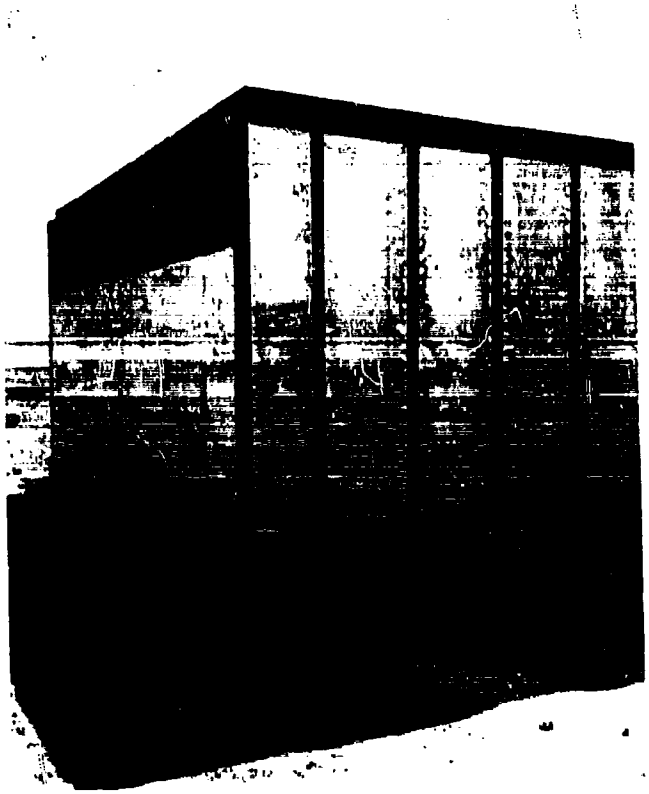

Figure 9.66 Pretest, TP 31.2 e-1, side view of building, facing southeast.

Figure 9.67 Pretest, TP 31.2 e-1, side view of building, facing northwest.

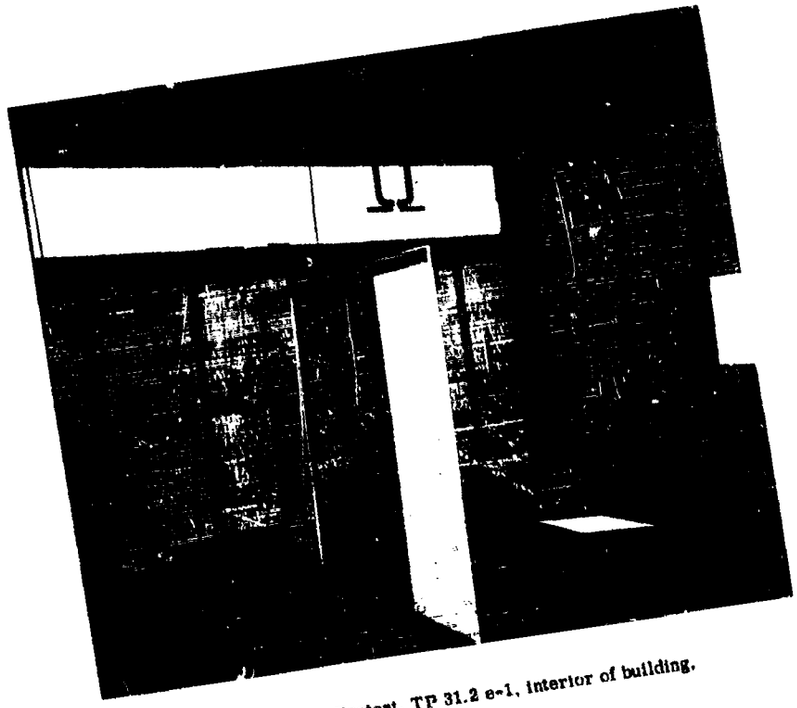

Figure 9.68 Pretest, TP 31.2 e-1, interior of building, facing north.



CONFIDENTIAL

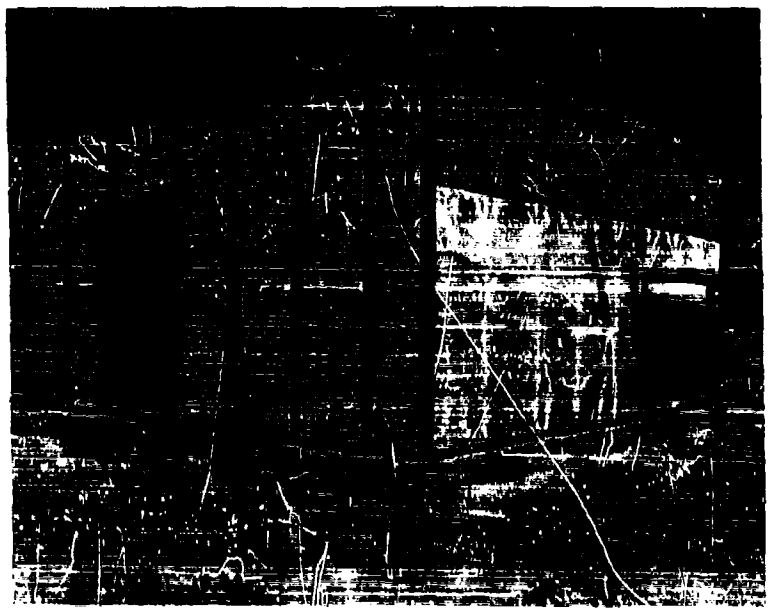

Figure 9.69 Posttest, TP 31.2 e-1, side view of building, facing northeast.



CONFIDENTIAL

Figure 9.70 Pretest, TP 34.1k, side view of shelter, facing southeast.

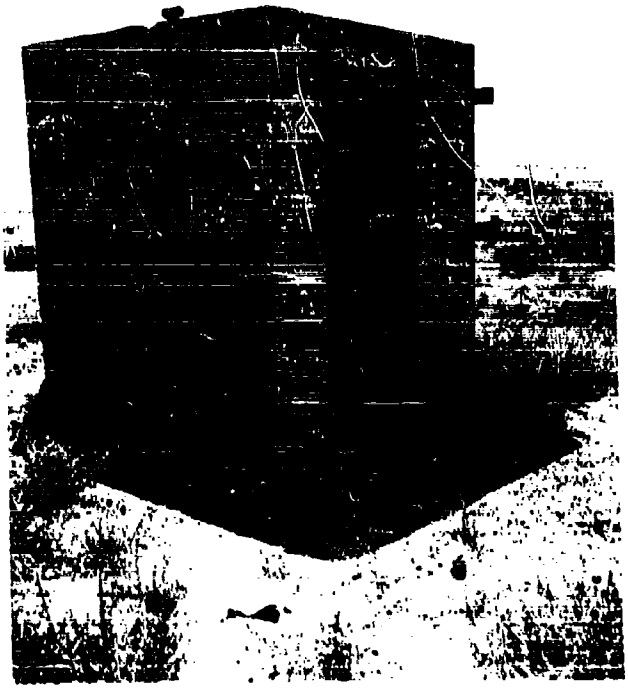

Figure 9.71 Pretest, TP 34.11, side view of shelter, facing southeast.



CONFIDENTIAL

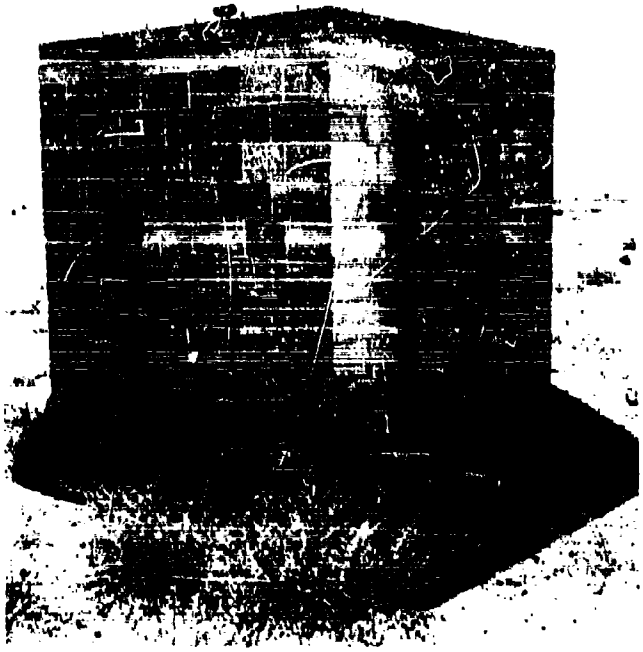

Figure 9.72 Pretest, TP 34.1j, side view of shelter, facing southeast.



CONFIDENTIAL

# REFERENCES


1. G. K. Sinnamon and others; "Effect of Positive Phase Length of Blast on Drag Type Industrial Buildings"; Project 3.7, Operation Teapot, ITR-1129, May 1955; University of Illinois; Secret Restricted Data.
2. J. P. Allgood, W. A. Shaw, and L. D. Mills; "Test Concrete Panels"; Project 3.8, Operation Teapot, ITR-1130, May 1955; Bureau of Yards and Docks; Secret Restricted Data.
3. N. M. Newmark and G. K. Sinnamon; "Air Blast Effects on Underground Structures"; Project 3.8, Operation Upshot-Knothole, WT-727, January 1954; University of Illinois; Confidential Restricted Data.
4. G. K. Sinnamon; "Air Blast Effects on Underground Structures"; Project 3.4, Operation Teapot, ITR-1127, May 1955; University of Illinois; Confidential Restricted Data.
5. G. K. Sinnamon, W. J. Austin, and N. M. Newmark; "Air Blast Effects on Entrances and Air Intakes of Underground Installations"; Project 3.7, Operation Upshot-Knothole, WT-726, February 1955; University of Illinois; Confidential Restricted Data.
6. Letter dated 4 February 1957 (FCWT1 960.3AG); Confidential Restricted Data.
7. W. A. Shaw and J. R. Allgood; "An Atomic Blast Simulator"; Technical Paper, U. S. Naval Civil Engineering Laboratory.
8. Hetenyi; "Handbook of Experimental Stress Analysis."
9. A. H. Shapiro; "The Dynamics and Thermodynamics of Compressible Fluid Flow"; Vols. I and II, 1953.
10. H. H. Korst; "Analysis of Some Thermodynamic Processes by the Method of Characteristics for Non-Steady One-Dimensional Flow; Proceedings of the Midwestern Conference on Fluid Dynamics, 1950.
11. T. H. Schiffman and A. Wiedermann; "Experimental Observations of Interior Pressures in Hollow Models"; Final Test Reports No. 7, July 1956, Air Force Contract No. AF33(616)-2644; Armour Research Foundation; Confidential.
12. J. P. King and T. H. Schiffman; "Two-Dimensional Shock Tube Interior Loading Studies"; Ad Hoc Analytical Services for Physical Vulnerability Division, USAF, Report No. 3, Call V, Phase I, June 1956; Air Force Contract No. AF33(600)-27802; Armour Research Foundation; Confidential.
13. Armour Research Foundation; "Interior Loading in Hollow Models, Part IV"; Report No. 8 of Contract No. AF29(601)-796, (Preliminary Test Report No. 3), ARF Project No. D144, 8 April 1958; Unclassified.
14. E. V. Gallagher; "Interior Air Blast Loading in Hollow Model Structures"; ARF Project No. D144, AFSWC, TN-58-27; Armour Research Foundation; Unclassified.
15. E. Sevin; "Tests on the Response of Wall and Roof Panels and the Transmission of Load to Supporting Structure"; Project 3.5, Operation Upshot-Knothole, WT-724, May 1955; Armour Research Foundation; Secret Restricted Data.
16. T. A. Zaker; "Effect on Wall Panel Failure of Shock Parameters"; Final Test Report No. 8, July 1956; Air Force Contract No. AF33(616)-2644; Armour Research Foundation; Unclassified.
17. B. C. Taylor; "Blast Effects of Atomic Weapons Upon Curtain Walls and Partitions of Masonry and Other Materials"; Project 3.29, Operation Upshot-Knothole, WT-741; Federal Civil Defense Administration; Confidential Restricted Data.

18. K. E. McKee; "Dynamic Characteristics of Structural Clay Masonry Walls"; Armour Research Foundation Phase Report No. IV, ARF No. K576, October 1956; Unclassified.
19. T. H. Schiffman; "Numerical Solution for the Reflection of a Compression Wave from a Rigid Wall"; Proceedings of the First Shock Tube Symposium (SWR-TM-57-2), Cambridge, Massachusetts, February 1957.
20. R. M. Langmire and L. D. Mills; "Navy Structures"; Projects 3.11–3.16, Operation Upshot-Knothole, WT-729, Bureau of Yards and Docks; Confidential Restricted Data.



CONFIDENTIAL

# DISTRIBUTION

*Military Distribution Category 32*

ARMY ACTIVITIES

1 Deputy Chief of Staff for Military Operations, D/A, Washington 25, D.C. ATTN: Dir. of R&D
2 Chief of Research and Development, D/A, Washington 25, D.C. ATTN: Atomic Div.
3 Chief of Engineers, D/A, Washington 25, D.C. ATTN: ENONB
4 Chief of Engineers, D/A, Washington 25, D.C. ATTN: ENOEB
5 Chief of Engineers, D/A, Washington 25, D.C. ATTN: ENOTB
6- 7 Office, Chief of Ordnance, D/A, Washington 25, D.C. ATTN: ORDTN
8 Chief of Transportation, D/A, Office of Planning and Int., Washington 25, D.C.
9- 11 Commanding General, U.S. Continental Army Command, Ft. Monroe, Va.
12 Director of Special Weapons Development Office, Headquarters CONARC, Ft. Bliss, Tex. ATTN: Capt. Chester I. Peterson
13 President, U.S. Army Artillery Board, Ft. Sill, Okla.
14 President, U.S. Army Air Defense Board, Ft. Bliss, Tex.
15 Commandant, U.S. Army Command & General Staff College, Ft. Leavenworth, Kansas. ATTN: ARCHIVES
16 Commandant, U.S. Army Air Defense School, Ft. Bliss, Tex. ATTN: Command & Staff Dept.
17 Commandant, U.S. Army Armored School, Ft. Knox, Ky.
18 Commandant, U.S. Army Artillery and Missile School, Ft. Sill, Okla. ATTN: Combat Development Department
19 Commandant, U.S. Army Aviation School, Ft. Rucker, Ala.
20 Commandant, U.S. Army Infantry School, Ft. Benning, Ga. ATTN: C.D.S.
21 Commanding General, Chemical Corps Training Comd., Ft. McClellan, Ala.
22 Commandant, USA Transport School, Ft. Eustis, Va. ATTN: Security and Info. Off.
23 Commanding General, The Engineer Center, Ft. Belvoir, Va. ATTN: Asst. Cmdt, Engr. School
24 Director, Armed Forces Institute of Pathology, Walter Reed Army Med. Center, 625 16th St., NW, Washington 25, D.C.
25 Commanding Officer, Army Medical Research Lab., Ft. Knox, Ky.
26 Commandant, Walter Reed Army Inst. of Res., Walter Reed Army Medical Center, Washington 25, D.C.
27- 28 Commanding Officer, Chemical Warfare Lab., Army Chemical Center, Md. ATTN: Tech. Library
29 Commanding General, Engineer Research and Dev. Lab., Ft. Belvoir, Va. ATTN: Chief, Tech. Support Branch
30 Director, Waterways Experiment Station, P.O. Box 631, Vicksburg, Miss. ATTN: Library
31- 32 Commanding General, Aberdeen Proving Grounds, Md. ATTN: Director, Ballistics Research Laboratory
33 Commanding General, Ordnance Ammunition Command, Joliet, Ill.
34 Director, Operations Research Office, Johns Hopkins University, 6935 Arlington Rd., Bethesda 14, Md.
35 Commander-in-Chief, U.S. Army Europe, APO 403, New York, N.Y. ATTN: Opot. Div., Weapons Br.

NAVY ACTIVITIES

36 Chief of Naval Operations, D/N, Washington 25, D.C. ATTN: OP-03EG
37 Chief of Naval Operations, D/N, Washington 25, D.C. ATTN: OP-75
38- 39 Chief of Naval Research, D/N, Washington 25, D.C. ATTN: Code 811
40 Chief, Bureau of Ordnance, D/N, Washington 25, D.C.
41 Chief, Bureau of Ships, D/N, Washington 25, D.C. ATTN: Code 423
42 Chief, Bureau of Yards and Docks, D/N, Washington 25, D.C. ATTN: D-440
43 Director, U.S. Naval Research Laboratory, Washington 25, D.C. ATTN: Mrs. Katherine H. Cass
44- 45 Commander, U.S. Naval Ordnance Laboratory, White Oak, Silver Spring 19, Md.
46- 47 Commanding Officer, U.S. Naval Radiological Defense Laboratory, San Francisco, Calif. ATTN: Tech. Info. Div.
48- 50 Commanding Officer and Director, U.S. Naval Civil Engineering Laboratory, Port Hueneme, Calif. ATTN: Code L31
51 Commanding Officer, U.S. Naval Schools Command, U.S. Naval Station, Treasure Island, San Francisco, Calif.
52 Superintendent, U.S. Naval Postgraduate School, Monterey, Calif.
53 Officer-in-Charge, U. S. Naval School, CEC Officers, U.S. Naval Construction Bn. Center, Port Hueneme, Calif.
54 Commanding Officer, Nuclear Weapons Training Center, Atlantic, U.S. Naval Base, Norfolk 11, Va. ATTN: Nuclear Warfare Dept.
55 Commanding Officer, Nuclear Weapons Training Center, Pacific, Naval Station, San Diego, Calif.
56 Commanding Officer, U.S. Naval Damage Control Tng. Center, Naval Base, Philadelphia 12, Pa. ATTN: ABC Defense Course
57 Commanding Officer, U.S. Naval Medical Research Institute, National Naval Medical Center, Bethesda, Md.
58 Commanding Officer and Director, David W. Taylor Model Basin, Washington 7, D.C. ATTN: Library
59 Officer-in-Charge, U.S. Naval Supply Research and Development Facility, Naval Supply Center, Bayonne, N.J.
60 Commander, Norfolk Naval Shipyard, Portsmouth, Va. ATTN: Underwater Explosions Research Division
61 Commandant, U.S. Marine Corps, Washington 25, D.C. ATTN: Code AO3H
62 Director, Marine Corps Landing Force, Development Center, MCS, Quantico, Va.
63 Commanding Officer, U.S. Naval CIC School, U.S. Naval Air Station, Glynco, Brunswick, Ga.

AIR FORCE ACTIVITIES

64 Assistant for Atomic Energy, HQ, USAF, Washington 25, D.C. ATTN: DCS/O
65 Hq. USAF, ATTN: Operations Analysis Office, Office, Vice Chief of Staff, Washington 25, D. C.
66 Director of Civil Engineering, HQ. USAF, Washington 25, D.C. ATTN: AFOCE
67- 68 Air Force Intelligence Center, HQ. USAF, ACS/I (ATTN-3V1) Washington 25, D.C.
69 Director of Research and Development, DCS/D, HQ. USAF, Washington 25, D.C. ATTN: Guidance and Weapons Div.
70 The Surgeon General, HQ. USAF, Washington 25, D.C. ATTN: Bio.-Def. Pre. Med. Division
71 Commander, Tactical Air Command, Langley AFB, Va. ATTN: Doc. Security Branch
72 Commander, Air Defense Command, Ent AFB, Colorado. ATTN. Assistant for Atomic Energy, ADLDC-A
73 Commander, Hq. Air Research and Development Command, Andrews AFB, Washington 25, D.C. ATTN: RDRWA
74 Commander, Air Force Ballistic Missile Div. HQ. ARDC, Air Force Unit Post Office, Los Angeles 45, Calif. ATTN: WDSOT
75- 76 Commander, AF Cambridge Research Center, L. G. Hanscom Field, Bedford, Mass. ATTN: CRQST-2
77- 81 Commander, Air Force Special Weapons Center, Kirtland AFB, Albuquerque, N. Mex. ATTN: Tech. Info. & Intel. Div.
82- 83 Director, Air University Library, Maxwell AFB, Ala.
84 Commander, Lowry Technical Training Center (TW), Lowry AFB, Denver, Colorado.
85 Commandant, School of Aviation Medicine, USAF, Randolph AFB, Tex. ATTN: Research Secretariat



CONFIDENTIAL

UNCLASSIFIED CANCELED CONFIDENTIAL

86 Commander, 1009th Sp. Wpns. Squadron, HQ. USAF, Washington 25, D.C.

87- 89 Commander, Wright Air Development Center, Wright-Patterson AFB, Dayton, Ohio. ATTN: WCOSI

90- 91 Director, USAF Project RAND, VIA: USAF Liaison Office, The RAND Corp., 1700 Main St., Santa Monica, Calif.

92 Commander, Rome Air Development Center, ARDC, Griffiss AFB, N.Y. ATTN: Documents Library, RCSSL-1

93 Commander, Air Technical Intelligence Center, USAF, Wright-Patterson AFB, Ohio. ATTN: APCIN-4B1a, Library

94 Assistant Chief of Staff, Intelligence, HQ. USAFE, APO 633, New York, N.Y. ATTN: Directorate of Air Targets

95 Commander-in-Chief, Pacific Air Forces, APO 953, San Francisco, Calif. ATTN: PACIE-M3, Base Recovery

OTHER DEPARTMENT OF DEFENSE ACTIVITIES

96 Director of Defense Research and Engineering, Washington 25, D.C. ATTN: Tech. Library

97 Chairman, Armed Services Explosives Safety Board, DOD, Building T-7, Gravelly Point, Washington 25, D.C.

98 Director, Weapons Systems Evaluation Group, Room 1E880, The Pentagon, Washington 25, D.C.

99-102 Chief, Defense Atomic Support Agency, Washington 25, D.C. ATTN: Document Library

103 Commander, Field Command, DASA, Sandia Base, Albuquerque, N. Mex.

104 Commander, Field Command, DASA, Sandia Base, Albuquerque, N. Mex. ATTN: FCTG

105-109 Commander, Field Command, DASA, Sandia Base, Albuquerque, N. Mex. ATTN: FCWT

110 Administrator, National Aeronautics and Space Administration, 1520 H St., N.W., Washington 25, D.C. ATTN: Mr. R. V.

111 Commander-in-Chief, Strategic Air Command, Offutt AFB, Neb. ATTN: [illegible]

112 Commander-in-Chief, EUCOM, APO 128, New York, N.Y.

ATOMIC ENERGY COMMISSION ACTIVITIES

113-115 U.S. Atomic Energy Commission, Technical Library, Washington [illegible] For DMA

116-117 Los Alamos Scientific Laboratory, Report Library, P.O. Box 1663, Los Alamos, N. Mex. ATTN: Helen Redman

118-122 Sandia Corporation, Classified Document Division, Sandia Base, Albuquerque, N. Mex. ATTN: H. J. Smyth, Jr.

123-125 University of California Lawrence Radiation Laboratory, P.O. Box 808, Livermore, Calif. ATTN: Clovis G. Craig

126 Essential Operating Records, Division of Information Services for Storage at ERC-E. ATTN: John E. Hans, Chief, Headquarters Records and Mail Service Branch, U.S. AEC, Washington 25, D.C.

127 Weapon Data Section, Technical Information Service Extension, Oak Ridge, Tenn.

128-160 Technical Information Service Extension, Oak Ridge, Tenn. (Surplus)

UNCLASSIFIED



CONFIDENTIAL CANCELED